NASA CR- 122371

STAR

Report _____

# IMPROVED PLAQUE MATERIALS FOR AEROSPACE NICKEL-CADMIUM CELLS

E. Luksha and D.J. Gordy — Approved by C.J. Menard

Gould Inc., Gould Laboratories
Energy Technology
1110 Highway 110
Mendota Heights, Mn 55118

June 1971

Final Report


Prepared For

Goddard Space Flight Center
Greenbelt, Maryland 20771

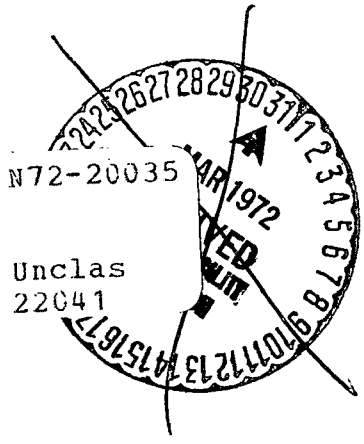




84 P.

| 1. Report No. | 2. Government Accession No. | 3. Recipient's Catalog No. |
|---|---|---|
| 4. Title and Subtitle<br>Improved Plaque Materials For Aerospace Nickel-Cadmium Cells | | 5. Report Date<br>June 1971<br>6. Performing Organization Code |
| 7. Author(s) E. Luksha & D.J. Gordy<br>Approved by C.J. Menard | | 8. Performing Organization Report No.<br>712-091 |
| 9. Performing Organization Name and Address<br>Gould Inc., Gould Laboratories<br>Energy Technology<br>1110 Highway 110<br>Mendota Heights, Mn 55118 | | 10. Work Unit No.<br>11. Contract or Grant No.<br>NAS 5-21097 |
| 12. Sponsoring Agency Name and Address<br>Goddard Space Flight Center<br>Greenbelt Maryland 20771<br>J. Sherfey, Technical Monitor | | 13. Type of Report & Period Covered<br>Final Report<br>11-17-69 Thru 5-31-71<br>14. Sponsoring Agency Code |

15. Supplementary Notes Early results of study presented at the Sixth Advances in Battery Technology Symposium, Southern California – Nevada Section of the Electrochemical Society

16. Abstract

Improved cadmium electrode substrates with precisely controlled microstructures for possible use in aerospace nickel-cadmium cells were prepared. The preparative technique was a powder metallurgical process in which a fugitive pore-former and a nickel powder were blended, then isostatically compacted, and subsequently sintered. Cadmium electrodes prepared from such substrates were cycle tested using an accelerated tortuous test regime. It was discovered that plaques of 60% or 80% porosity prepared with a 25$\mu$ pore-former were better than state-of-the-art electrodes in terms of efficiency and/or mechanical strength. The 60% structures were particularly outstanding in this respect in that they had efficiencies only 5-10 percentage points lower than state-of-the-art electrodes and vastly superior mechanical properties. This added strength was observed to eliminate cracking and physical degradation of the electrodes during processing and cycling. The cadmium electrodes prepared from the 80% porous substrates proved to be the best electrodes made during the course of the work from the point of view of highest efficiency. These were also somewhat stronger than conventional plaques and had better uniformity.

Three-point bend tests were used to measure mechanical properties of the plaques produced and also as a general characterization tool. In addition, the BET surface areas of selected specimens was determined in order to help along toward this end.

The SEM was used for judging microscopic uniformity and quantitatively determining the induced pore size and various other fine structures in the substrates.

The technique of X-ray radiography was used to follow the bulk uniformity of the above-mentioned substrates at various stages of their processing into cadmium electrodes and cycle testing.

| 17. Key Words | 18. Distribution Statement |
|---|---|
| Electrode substrates<br>Nickel Plaques<br>Nickel-cadmium cells | |

| 19. Security Classif. (of this report) | 20. Security Classif. (of this page) | 21. No. of Pages | 22. Price |
|---|---|---|---|
| Unclassified | Unclassified | | |

# PREFACE

This report summarizes exploratory work conducted at the Gould Energy Technology Laboratories on a novel process for the preparation of improved cadmium electrode plaques with precisely controlled pore size and porosity for use in aerospace nickel-cadmium cells. The requirements for these aerospace components include far better uniformity, reproducibility, and life than is currently available with conventional materials. The key features of the work was preparation of plaques via a powder metallurgical technique which consisted of isostatically compacting a blend of a nickel powder with a fugitive pore-former and subsequently sintering the "green" compact. Cadmium electrodes were prepared from these materials and cycle tested in negative limited cells using an accelerated, tortuous test regime. Results were obtained which showed the new structures yielded electrodes that were superior to the conventional structures in mechanical properties and performance. BET surface areas, SEM photomicrographs, X-ray radiographs, and mechanical strengths using a three-point bend test were used to help in the thorough characterization of the electrodes and the components prepared. The improved properties and performance of cadmium electrode prepared from isostatically compacted plaques suggests further studies for optimizing their structure.

# TABLE OF CONTENTS

## LIST OF ILLUSTRATIONS

## LIST OF ILLUSTRATIONS (Cont'd)

## LIST OF TABLES

# I. INTRODUCTION

There is currently a need for very long lived highly reliable secondary batteries for use in space vehicles. Nickel-cadmium batteries of the sealed type are uniquely suited for such application mainly because of their long lives if employed under the proper set of operating conditions. Under tortuous conditions the utility of nickel-cadmium batteries becomes severely limited because cells can fail due to any number of factors, a very common one being cell rupture due to hydrogen generation on overcharge. This is a result of aging effects on both electrodes and especially capacity degradation on the cadmium electrode under very tortuous operating conditions.

Such failures have been blamed on lack of uniformity and reproducibility of the battery components. This is reasonable, for if components are not uniform and reproducible, it is not possible to effectively over-design for the short-comings of the system.

Past efforts to produce uniform materials for aerospace cells have been concerned with bulk or macroscopic uniformity. That is, special attention was given to produce, for example, plaques and electrodes of thickness, loading, porosity, etc. within tighter limits. In spite of this, electrodes that were apparently uniform on a bulk basis have shown widely differing aging characteristics indicating that perhaps not all key variables have been considered.

Rather than concentrating on macroscopic uniformity, in the work discussed herein the uniformity on the microscopic scale was controlled, and its role on the life and aging characteristics were evaluated by testing highly porous plaques of very closely controlled porosity, pore-size, and pore distribution. Since this exploratory program was for the purpose of studying microscopic uniformity, minimum effort was made to produce structures of very high degree of bulk uniformity other than to show that uniform structure could be made by the technique used and assure that results were not confounded by these parameters. Nevertheless, materials with very good but not optimum uniformity were produced. It was felt that the ultimate in uniformity should be pursued after the merit of the process was established.

To this end a powder metallurgical technique was chosen to prepare uniform plaques because these are the most versatile and direct processes for the fabrication of porous materials suitable for practical electrode components. A pore-former type process was selected as holding forth the most promise. With the use of a pore-former, one can precisely control both induced and interstitial porosity to tailor-make a structure to meet a specific application.

This paper distinguishes between two types of porosity. Interstitial porosity is the naturally occurring void volume between neighboring particles in a more or less close packed aggregate. Induced porosity, on the other hand, is formed by the addition of a fugitive pore-former to the unconsolidated powder. An interconnected void volume is subsequently formed by the removal of the added powder.

In the packing of powder particles, particularly in the case of fine or irregularly shaped powders, a form of gross packing imperfection called bridging will occur. Bridging is the formation of an arch or bridge of powder particles producing larger voids within the aggregate and, it is, in part, the cause of the low packing densities of uncompacted high surface area powders. The void volumes, or pore, formed by a bridge may have a vastly greater number of particles surrounding it than in the case of an interstitial pore, and the pore diameter is not directly related to particle diameter.

Induced porosity is caused by the bridging of powder particles caused by the introduction of the pore-forming agent to the powder. The powder is packed about the particles of pore-former, which is subsequently removed by decomposition, solution, or vaporization. As a result, the character of induced porosity is a function of the particle size distribution, volume percent, and surface area of pore-former added to the powder. The pore-former diameter may be orders of magnitude larger than the metal particle diameter and the porosity can exceed 90 %, depending upon the size and strength of the powder particle bridges. It should be appreciated, however, the interstitial porosity between the particles in a bridge or wall surrounding an induced pore can be maintained, and the porosity of an induced pore retains some interstitial character. For example, the large induced pores may be interconnected by means of the fine interstitial pores in the pore wall or bridge, and the total surface area of the compact may include the interstitial pore area. The large pores may also be mutually interconnected for greater permeability.

To prepare an induced-pore electrode plaque, a nickel powder previously screened to yield an average particle diameter of the desired size, and a powdered pore-former of the proper particle size to form pores of the necessary diameter was blended with the nickel powder. The blended powder mixture was then compacted to cold-sinter the nickel particles. The pore-former was removed from the compact leaving a structure that was subsequently sintered at the desired time and temperatures. The following features of the resulting sintered plaque which are illustrated in Figure 1 were especially significant:

- The pore diameter can be any size, some 100 times larger than the metal particle size if required
- The pore size is uniform, reflecting the size distribution of the pore-former
- The pore wall contains any level of interstitial porosity so that all the particle surface is available to the large pores

Pressure can be applied to the powder by means of a number of techniques. For example, uniaxially in a die, isostatically in a flexible mold in a pressurized fluid, or in a rolling mill. Because a powder does not behave in an ideal hydrodynamic manner under pressure, a consequence of interparticles and die wall friction, die pressing usually results in variations in microstructure throughout the compact. These variations are particularly severe in extremely thin compacts. Uniform microstructures can best be achieved by isostatic pressing.

In ordinary die pressing, the friction between powder particles and between powder particles and die walls prevents uniform compaction. The powder becomes highly compacted in areas adjacent to the die and punch surfaces and is somewhat less dense toward the interior of the compacted part. Further, in die compaction the microscopic high points after the powder is struck-off reflect themselves as areas of high densities.

The primary objective of the program was the exploration of isostatic compaction techniques to product thin, polyporous nickel plaque materials for cadmium electrodes of nickel-cadmium batteries for aerospace applications. However, in the early phase of the program plaques were prepared using die compaction techniques*. Thin plaques produced by the die compaction method were not as uniform as commercial material and further work along this line of approach was discontinued in order to devote the entire effort on isostatic compaction.

The isostatic compaction process used was the so-called wet-bag process. The process is illustrated in outline form in Figure 2. In the work reported herein, parts were compacted, via pressurized liquid against rubber diaphragms, from two directions. A detailed description of the process is given in the Experimental Section.

---

*Subcontract to North American Rockwell Corp., Rocketdyne Division

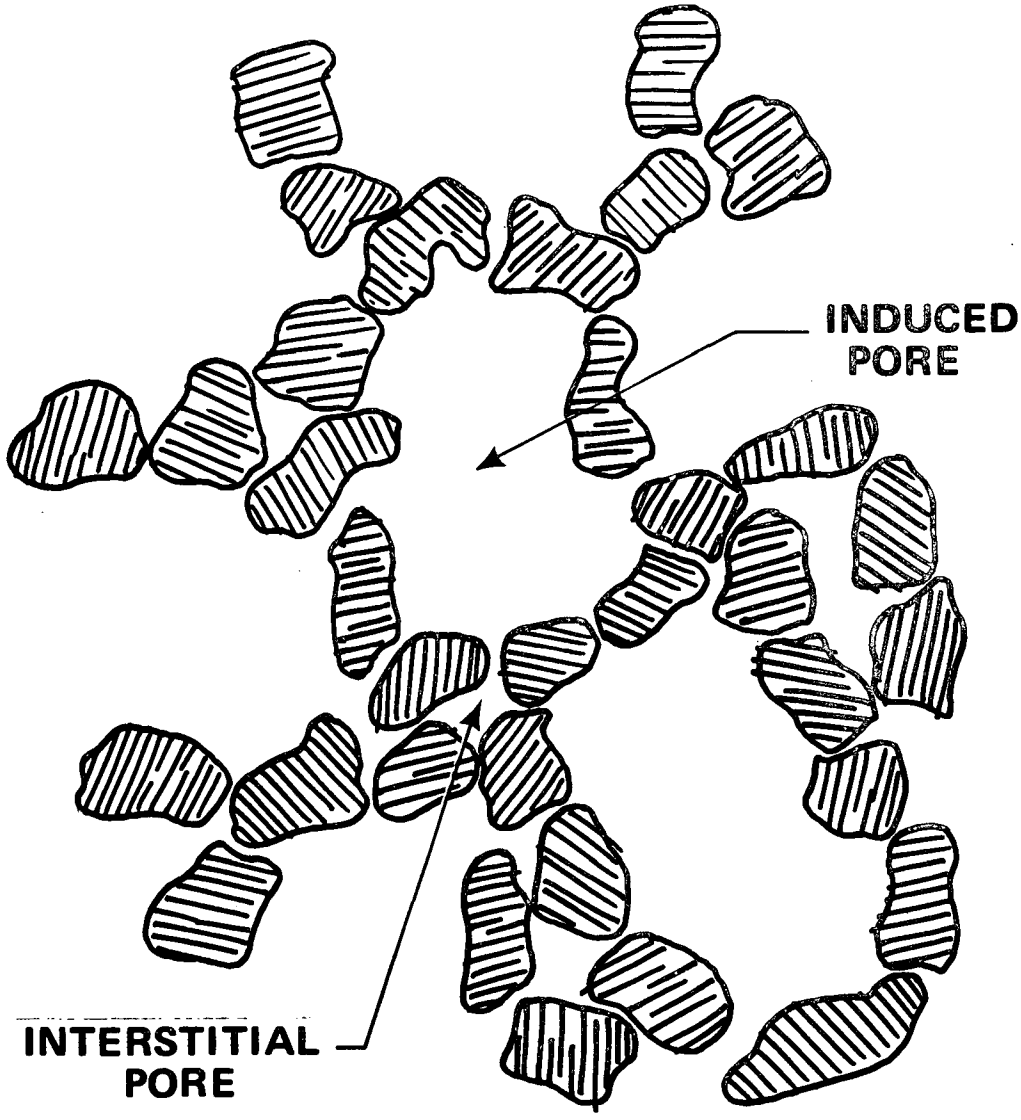


FIGURE 1. INDUCED POROSITY NICKEL SUBSTRATE

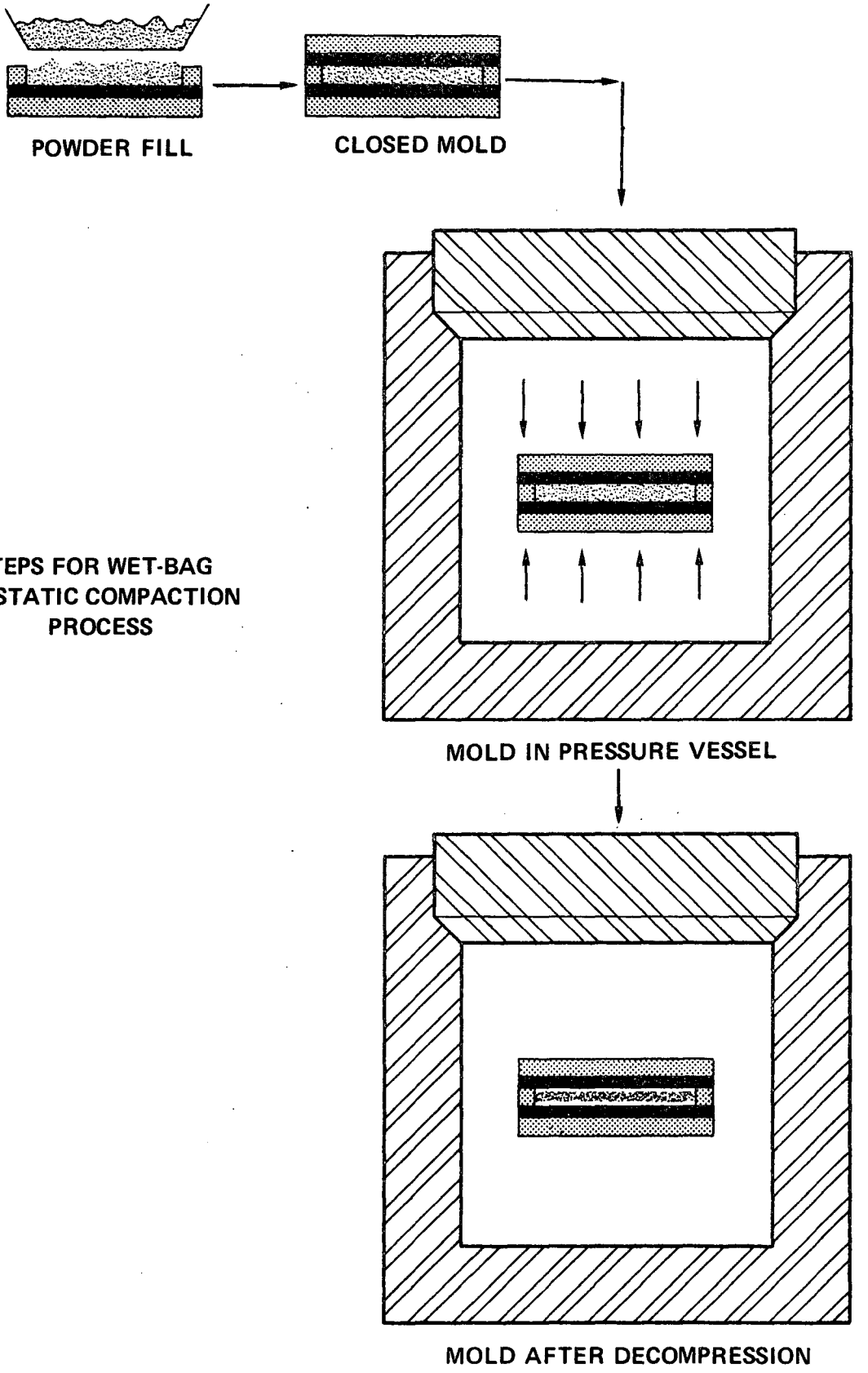


FIGURE 2. STEPS FOR WET-BAG ISOSTATIC COMPACTION PROCESS

## II. EXPERIMENTAL

The experimental work involved pore-former preparation, nickel powder preparation, blending of the two powders, compaction of the powder blend, removal of the pore-former, sintering of the "green" plaque, and electrode fabrication and testing. The following is a brief outline of these procedures.

### A. PLAQUE PREPARATION

Figure 3 illustrates the process flow of the various operations required in the fabrication of the plaques. Each operation is described in some detail in the paragraphs that follow.

1. **Pore-Former:** Of the various materials considered in this program as candidates for use as pore-formers (sodium chloride, urea, thiosemicarbazide, camphor), $(NH_4)_2CO_3$ was found to be the most convenient material to use for this purpose. It was prepared as follows:

   - Fisher purified grade powder was placed in a pan in a dry room (R.H. 3-5%) overnight to allow loss of any excess moisture.
   - The powder was then placed in a porcelaim ball mill and ground for 15 to 20 minutes utilizing 13/16 in. diameter Burundum grinding media.
   - After grinding, the powder was placed in a stack of standard seives and placed on a sieve shaker for 15 minutes. The -37$\mu$ fraction was separated and placed aside, and the remaining fractions were labeled and saved for future use and/or grinding. At this point in the processing, samples of each lot of $(NH_4)_2CO_3$ used were taken for density determination. Results for the four lots of powder used, as determined on an air pychometer were: 1.659 g/cc, 1.614 g/cc, 1.653 g/cc, and 1.575 g/cc. This gives an average value for all lots of 1.625 ± 0.062 g/cc. The narrow range of densities shows the materials were adequate for their intended purpose.

     When a sufficient fraction of -37$\mu$ powder was obtained, it was placed in a three-inch micro-mesh seive stack (44 $\mu$, 30$\mu$, 20$\mu$, 10$\mu$) and placed on a shaker for 15 minutes. The various fractions were then stored in separate labeled jars until needed. All operations on the pore-formers (grinding, seiving, and storage) were performed in a dry room (R.H. 3-5%).

2. **Nickel Powder:** Inco 287 powder was used in this work except where otherwise stated. It was prepared by placing a sample in a vacuum oven for one hour at 210°C. After removal from the oven, the powder was placed in the dry room to cool. When cool, the powder was placed in the standard seives and processed on the shaker for 15 minutes. The -37$\mu$ (400 mesh) fraction was stored in the dry room and the remaining fractions discarded.

3. **Powder Blending:** To prepare a blend for an 80 % porous structure, for example, the nickel and $(NH_4)_2CO_3$ were weighed out on a Mettler P162 balance to obtain Ni:$(NH_4)_2CO_3$ ratio of 1.5:1 by weight, the ratio required to yield a 80 % plaque. The normal working weight was 200 grams. This was used to aid in handling and to avoid changes in composition due to storage. The powders were then mixed and placed in a standard seive (the seive used was one size larger than the pore-former fraction used, except for the sizes smaller than 37$\mu$ for which the 400-mesh seive was

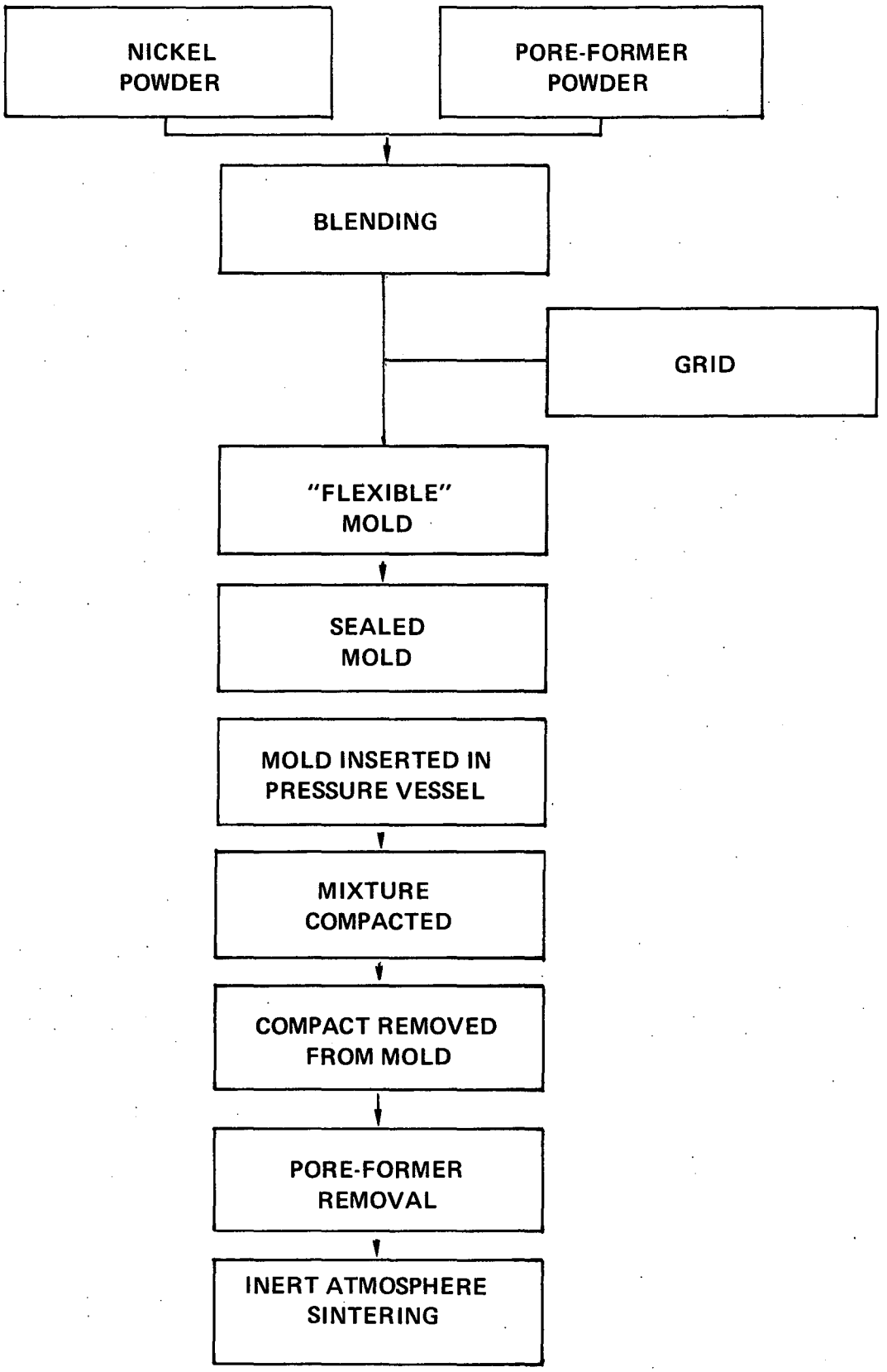


FIGURE 3. PROCESS FLOW CHART, PLAQUE FABRICATION

employed) and brushed through with a bristle paintbrush. This procedure was followed to minimize lumping of the pore-former. Following the brushing process, the blend was placed in a Patterson-Kelley twin-shell dry blender and allowed to mix for 30 minutes. After mixing, the material was again brushed through a seive and then stored in the dry room. All the above operations were carried out in the dry room. The blend for a 60 % porous structure was prepared in a similar manner except that the Ni to $(NH_4)_2CO_3$ ratio was 9:1, the value required to prepare a plaque of 60 % porosity.

4. **Powder Compaction:** The blend was then loaded into the cavity of a flexible mold (Figure 4) which already contained an annealed 20-mesh, 7-mil wire, woven screen, by brushing through an appropriate size seive (for the -37$\mu$ size pore-former, a 45$\mu$ seive was used). The essential feature of this mold was the two flexible ends which permitted compaction, via the rubber parts, from both sides of the specimen. This mold allowed the preparation of a part three inches in diameter. All excess material was struck off, and the mold closed and inserted into an Autoclave Engineers four-inch isostatic press and compacted at a pressure of 7000 psi for one minute.

5. **Pore-Former Removal:** After compaction, the "green" sintered specimen was removed from the mold and the $(NH_4)_2CO_3$ pore-former was removed by placing the sample in a vacuum oven and decomposing under vacuum at 210° C for 20 minutes.

6. **Green Plaque Sintering:** The "green" plaques were then removed from the decomposition oven and immediately placed into a vacuum furnace where they were sintered in a TM Vacuum Products oven at a pressure of less than 50$\mu$ at 1600° F for 10 minutes. Helium was used as a back fill and cooling media.

7. **Plaque Inspection:** After sintering, all plaques were examined visually for irregularities, trimmed, and weighed and measured to determine their apparent densities.

   Selected specimens were analyzed in terms of geometry (thickness, porosity, etc.), pore-size, (from photomicrographs), mechanical strength, and uniformity as judged from X-ray radiographs.

## B. PLAQUE CHARACTERIZATION

1. **Plaque Geometry:** Plaque dimensions in this study were 2.35 x 1.62 in. and approximately 30 mils thick. The thickness variation within one sample was determined by multiple readings with a micrometer with 0.8 inch diameter anvil and the average value used to determine the variation from sample to sample. Also recorded were screen weights and powder weights for each sample prepared.

2. **Mechanical Testing:** Mechanical strengths were measured for selected specimens on an Instron Tensile Tester by a three-point bend method.

3. **Photomicrographs:** Scanning electron photomicrographs of selected specimens were taken and measurements made on them to determine induced pore size and ratio of induced to interstitial porosity. Examination of photomicrographs was also used as a criteria for microscopic uniformity, along with such items as $Cd(OH)_2$ crystal size and distribution, in virgin and cycled electrodes.

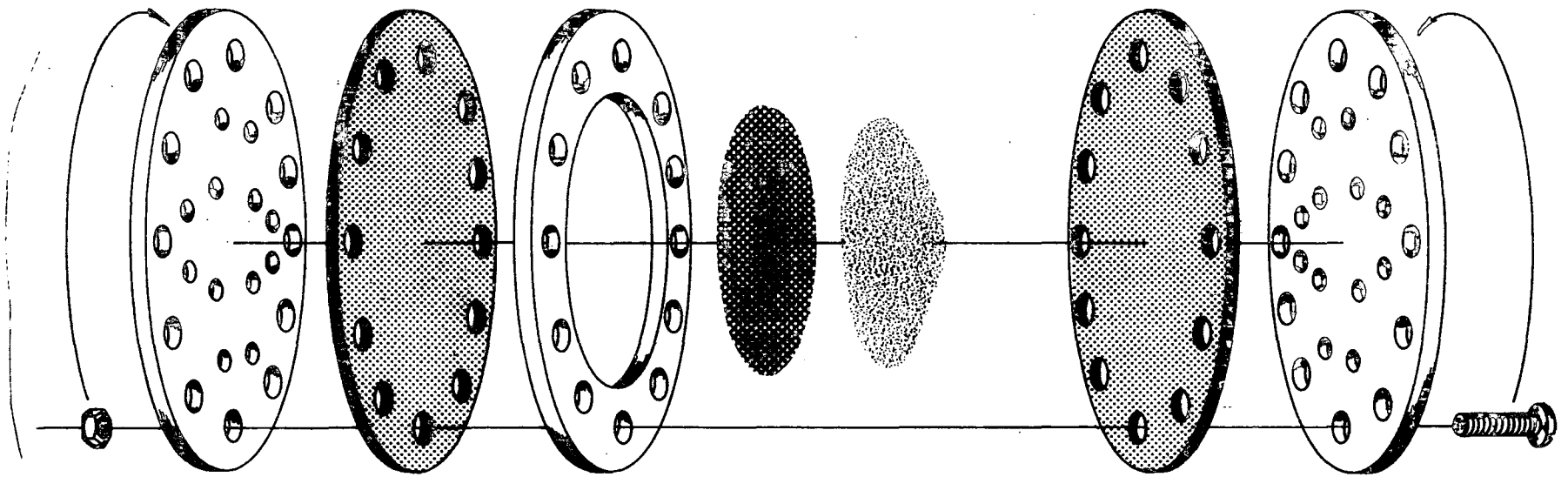


FIGURE 4. EXPLODED VIEW OF FLEXIBLE MOLD USED TO ISOSTATICALLY COMPACT POWDERS

4. **X-Ray Radiographs:** Qualitative examination of x-ray radiographs was employed as an important technique for judging the macroscopic uniformity of all specimens at various stages of preparation and testing.

5. **B.E.T. Surface Area:** Surface areas of selected sintered plaques were determined with a Numinco-Orr Surface Area Pore-Volume Analyzer, Model 2100, using Krypton as the adsorbate. Surface areas were utilized for comparison with other properties.

## C. CADMIUM ELECTRODE PROCESSING

The structures prepared as described above were impregnated by a proprietary process[1] in a manner that minimizes plaque damage. All electrodes in this study were loaded to 40.183 ± 0.883 g CdO per cubic inch of plaque (0.507 ± 0.031 Ah/in.$^2$ $Cd(OH)_2$ loading). It was felt that a constant loading per cubic inch of free space would yield electrodes far too low in energy density.

The electrodes were then placed in 30 % KOH (prepared from mercury cell grade 45 % KOH) and charged against nickel dummies to a minimum of 50 % overcharge (based on the calculated theoretical capacity) during a 16-hour charge cycle. They were then discharged to 0.0 volts versus a nickel oxide reference electrode at a current of 200 mA, washed free of KOH in hot deionized water and air dried at 70° C for one hour.

## D. ELECTROCHEMICAL TESTING

Cadmium electrodes thusly prepared were cycled in 2.35 x 1.62 in. sizes in specially constructed prismatic hardware in a nickel-cadmium-nickel sandwich configuration, using nickel electrodes of sufficient capacity to assure negative limited performance under all test conditions. These cells were cycled on fully automatic equipment to 100 % depth (0.00 volts) using the regime shown below:

| CYCLE NO. | CHARGE RATE | DISCHARGE RATE |
|---|---|---|
| 1-3 | 150 mA For 16 Hr | 240 mA |
| 4 | 150 mA For 16 Hr | 1.20 A |
| 5 | 150 mA For 16 Hr | 2.40 A |
| 6 | 150 mA For 16 Hr | 4.80 A |
| 7-End | 1.20 A For 1 Hr | 1.20 A |

All the charge and discharge data were recorded on a Leeds & Northrup Speedomax Type G multipoint recorder and a statistically significant sample size was tested for each type of electrode prepared.

The use of negative limited cells assured that these electrodes will receive more tortuous treatment than they would receive in a practical cell. In this way, performance differences and aging characteristics between different type electrodes would show themselves with the expenditure of a minimum amount of test effort. Tests of longer duration, up to 250 cycles, performed on state-of-the-art electrodes showed no additional degradation beyond that attained in the first 56 cycles.

## E. DATA REDUCTION

The large bulk of data collected during the characterizing and testing of the specimens of this study was reduced and correlated by use of a Honeywell Time-Sharing terminal and an array of standard and special computer routines that permitted rapid and accurate data processing.

## III. RESULTS

### A. BULK PROPERTIES OF ISOSTATICALLY COMPACTED PLAQUES

As briefly mentioned earlier, measurements of bulk plaque properties such as length, width, thickness, screen and sample weights were routinely made. In addition, powder weights, sample and sintered powder porosities, were calculated. These are summarized in tabular form below:

| PROPERTY | $\bar{X}$ ± 95 % CONFIDENCE LIMIT |
|---|---|
| Screen Weights* | 0.204 ± 0.007 g/in.$^2$ |
| Width | 1.629 ± 0.005 in. |
| Length | 2.354 ± 0.029 in. |
| Avg Thickness Variation In A Group** | 3.571 ± 0.215 % |
| Powder Content 60 % Specimens | 3.066 ± 0.045 g/cc |
| Powder Content 80 % Specimens | 1.417 ± 0.031 g/cc |
| Powder Porosity 80 % Specimens | 84.08 ± 0.35 % |
| Powder Porosity 60 % Specimens | 65.55 ± 0.51 % |

* Did not follow normal distribution – perhaps 2 different batches

** $\Sigma$ % variation within a group/n

n = number of groups

$$\% \text{ variation} = \frac{\text{Max. value} - \text{Min. value}}{\text{Max. value}} \times 100.0$$

In spite of the fact that no rigorous effort was made to optimize uniformity on the bulk scale, a very high degree of uniformity is inherent in the process. Within the rather tight limits defined above, one would not expect the experimental results to be confounded with the above mentioned parameters.

A comparison of the uniformity of isostatically compacted plaques with those produced by other means has been made elsewhere[2].

### B. MECHANICAL STRENGTHS OF ISOSTATICALLY COMPACTED PLAQUES

The mechanical strengths of cadmium electrode substrates are important properties to consider when one is preparing electrodes that are expected to be long lived. Furthermore, mechanical strengths are useful tools for general characterization of electrodes and plaques.

The samples whose mechanical strengths were to be evaluated were tested on a Instron three-point bend test jig shown schematically below:

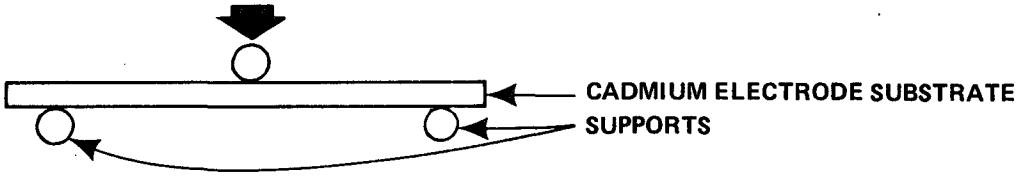


THREE-POINT BEND TEST JIG

The sample is supported by two rigidly mounted outer supports with a center-to-center distance of two inches. A third member is brought down to bear on the sample on its midpoint at a constant velocity. The sample is thusly slowly bent and eventually cracked. The load required to do this is obviously a measure of the mechanical strength of the electrode and should be a measure of the interparticle bonding of the plaque.

The load measurements are actually performed on an Instron Tensile Tester with the mobile pin attached to the crosshead of the instrument. The load required to crack the sample was determined with a one-pound load cell. Samples were cut to approximately one-inch widths, with the exact width being measured with a vernier at the fracture. Loads required to fracture the sample are usually in the 0.5 lb range.

An analysis of the bending moments gives for the yield stress, S, in units of psi:

$$S = \frac{3}{2} \frac{PL}{Wh^2}$$

Where:

P = load measured in pounds

L = sample length (two inches in this work)

W = sample width

h = sample thickness

Stresses expressed in this way were determined for randomly selected substrates.

The mechanical strengths are shown as a function of porosity in Figure 5. A least squares fit is given. The detailed data are in Appendix A.

The values of the mechanical strengths are seen to vary linearly between 900 and about 8000 psi between porosities of 80 and 60 %. A variation in mechanical strengths with induced pore size was noted with the larger pore-size materials having in general higher strengths. The differences in mechanical properties with varying induced pore-size was extremely small and will not be elaborated on at this particular time. The mechanical strength is shown to be a rapidly varying function of porosity; much greater than one might anticipate if only the metal content of the plaque were considered.

Especially noteworthy are the exceptionally high values of mechanical strength of the 60 % plaques, in the 8000 psi range. Conventional gravity sintered plaques sintered under the same conditions had mechanical strengths of 643 for a 79.2 % porous plaque. If the performance of electrodes prepared from the compacted 60 % plaques is on a par with the gravity sintered materials, important benefits, like life for example, may be realized.

### C. B.E.T. SURFACE AREAS OF SUBSTRATES

Surface areas of special specimens were determined using a modified B.E.T. method and Krypton as the adsorbate. The surface areas were in the range of 0.11 to 0.17 $m^2$/gm of powder content in the plaque. The contribution of the screen weight to the total plaque weight was arithmetically eliminated for the sake of this discussion.

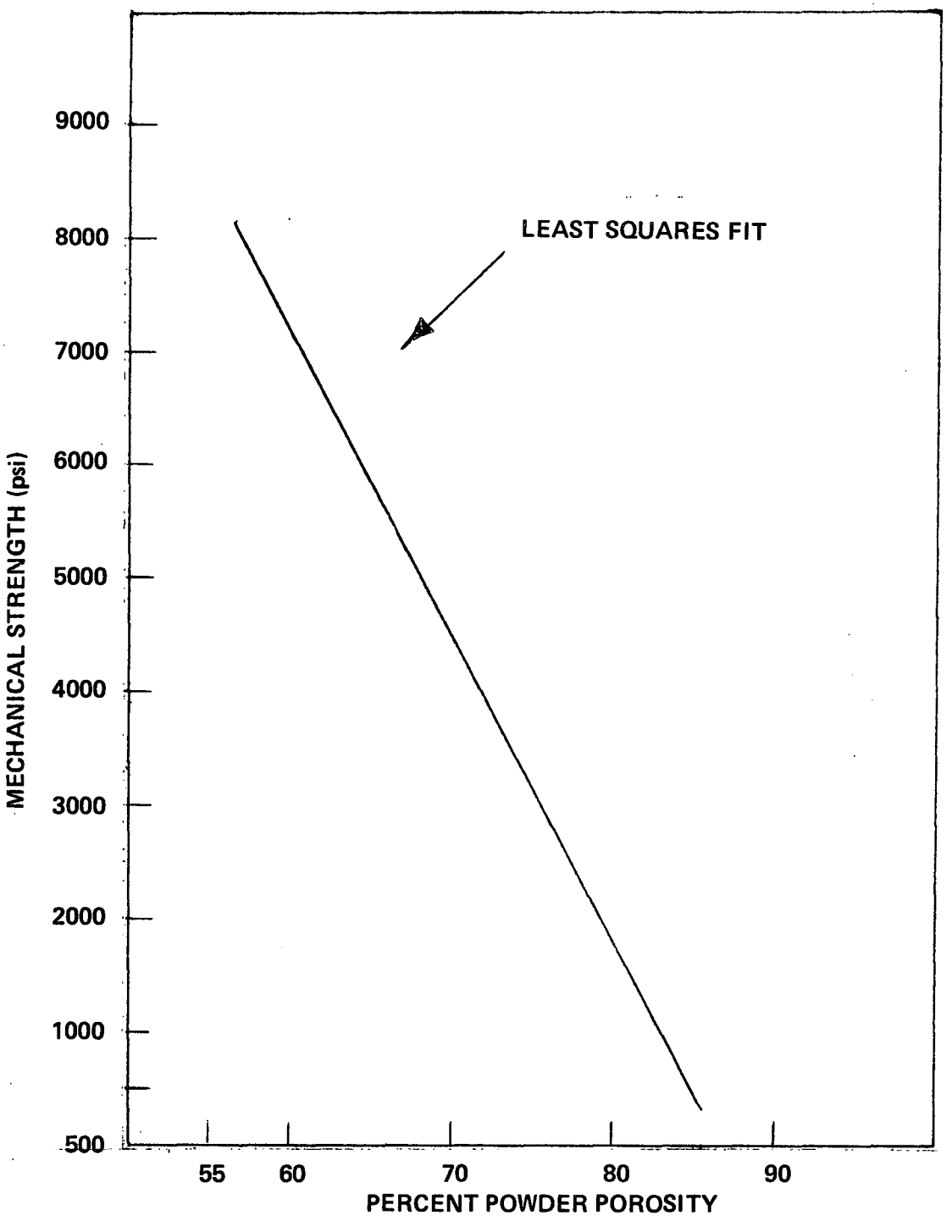


FIGURE 5. RELATION BETWEEN MECHANICAL STRENGTH AND POROSITY

The specimens whose surface area was measured did have support screens however. The specific surface areas in terms of powder weights are shown as a function of total porosity including screen in Figure 6. The 87 % porosity materials were studied previously in a privately funded project. The specific surface area is seen to be a linear function of porosity in this range for the two different pore sizes. The reduction in surface area with decreasing porosity is a reflection of the packing of the nickel powder. With the low porosity materials a particle has more neighbors to bond with during pressing and form necks with during sintering. There is, therefore, a marked decrease in powder surface area with decreasing porosity.

The surface areas of the compacted plaques also show some dependence on induced pore-size. This effect is rather small however. One may easily visualize changes in the number of interparticle bonds and therefore, surface area when the size and quantity of pore-former particles are varied. The use of larger pore-former particles with the same quantity of metal powder results in a material with a thicker pore wall. The additional powder around the pore-former seemingly packs differently for different sized pore-formers. As a result each particle will have a different number of neighbors to form necks with during sintering depending upon the size of the pore-former. The surface area will, therefore, exhibit small differences.

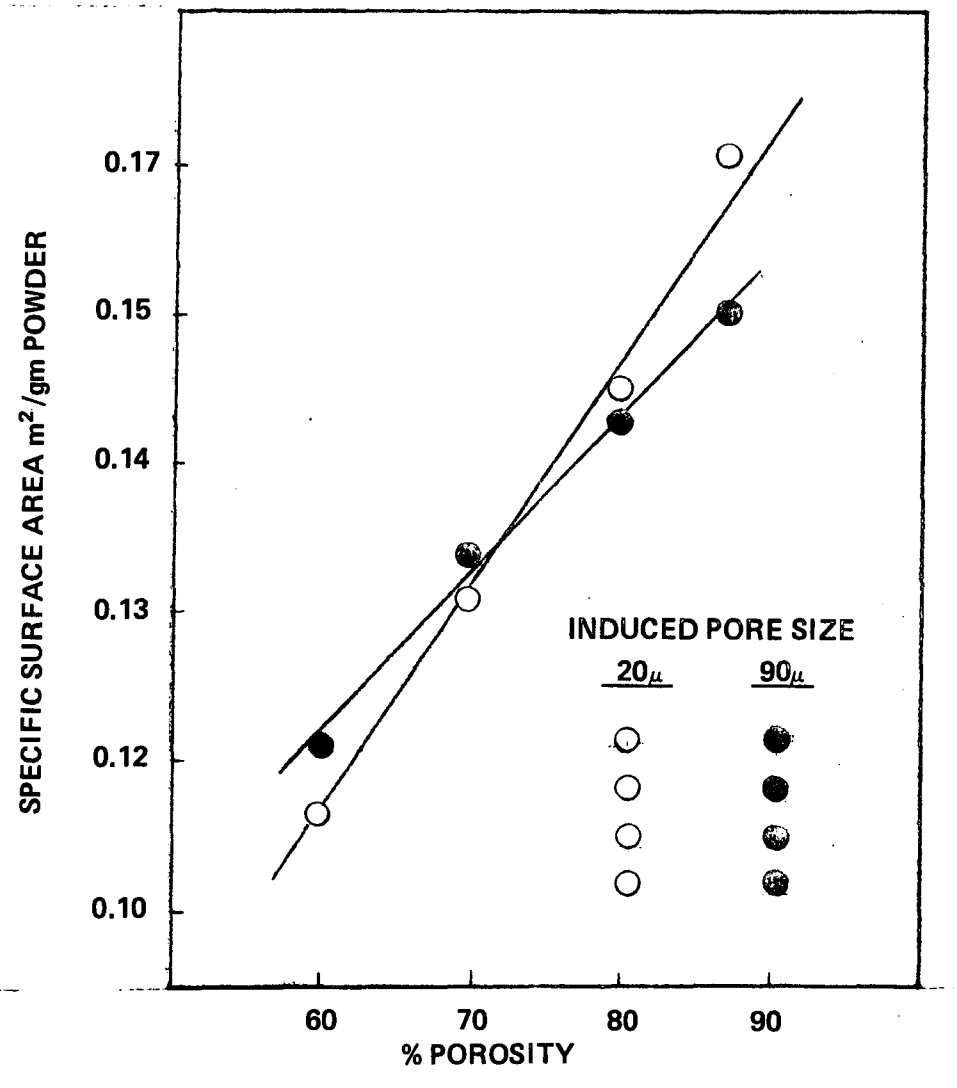


**FIGURE 6. SPECIFIC SURFACE AREA AS A FUNCTION OF PLAQUE POROSITY**

Figure 6 shows the two lines intersecting. On the basis of the above discussion, one would not expect this to happen. In reality, different ratios of pore-former to nickel powder are required to prepare plaques of differing porosity irrespective of the pore-size. One would expect that where the results are anomalous, the same ratio of pore-former to nickel powder ratio was not employed.

## D. RESULTS OF CYCLE TESTING

As described earlier, accelerated life testing of the cadmium electrodes prepared was performed in specially constructed negative limited cells at high charge and discharge rates. This is an extremely punishing regime for cadmium electrodes. It was employed in an effort to minimize the amount of experimental effort in evaluating the differences between various electrodes. The results are therefore not necessarily typical of cadmium electrodes in conventional positive limited systems in which they are never discharged to 100 % depth. The results are therefore best used only for comparative study of this type. Testing of 80 % porosity plaques of 90, 50, 25, and 15 $\mu$ induced pore size and 60 % porosity plaques at the 90, 50, 25, and 15$\mu$ induced pore-size levels has been completed. Also, performance of state-of-the-art electrodes (gravity sintered plaques) were evaluated for the purpose of comparison. In addition, a blended powder, Inco 287 with Sheritt-Gordon 1$\mu$ powder, was evaluated.

Test results for the state-of-the-art electrodes are given in Figure 7. Cycle by cycle data is given in Appendix B. The points are averages of eight cells and the error bars represent the 95 % confidence interval from the average. We are now in a position to evaluate test results of our new plaques on a comparative basis.

### 1. Test Results For 80 % Porous Plaques

Accelerated cycle test results for cadmium electrodes prepared from isostatically compacted plaques of 80 % porosity and 15, 25, 50, and 90$\mu$ induced pore size are shown in Figures 8 through 11, respectively. Cycle by cycle data is given in Appendix B. Periodic oscillations in the test data were observed at times as for example in Figure 7. We have no explanation for this observation. No outstanding differences between these groups of cells was evident. There were some differences however. The group of electrodes prepared from the 80 % 25$\mu$ pore-size plaques had higher efficiencies than the other groups of cells, especially during later stages of the test program. Electrodes prepared from the plaques with 50$\mu$ and 90$\mu$ induced pore-sizes, although they were slightly lower in efficiency, were more uniform in performance. This difference was due to the ease of handling and blending pore-former particles with nickel particles, which manifested itself in better general plaque uniformity (see following sections). Special difficulties were encountered with the preparation and blending of the 15$\mu$ pore-former.

It thus appears that there is little or no contribution of induced pore-size to electrode efficiency at these porosity levels. And more significantly, all these groups of cells are comparable to the state-of-the-art electrodes. The electrodes prepared from the 80 % 25$\mu$ plaques were better throughout the test.

Cycle test data were generated for an 80 % porous plaque containing 60 % Inco 287 and 40 % Sheritt-Gordon 1$\mu$ nickel powder. The test results are given in Figure 12 and are comparable to the 80 % 25$\mu$ electrodes, that is, there is no statistically significant difference between them.

### 2. Test Results For 60 % Porous Plaques

Accelerated cycle testing was also completed for cadmium electrodes prepared from 60 % plaques at the 15, 25, 50, and 90$\mu$ pore-size levels. Test results are given in Figure 13 through 16, respectively. The electrodes prepared from the 25$\mu$ induced pore plaques had the best efficiencies of the group. The 60 % 25$\mu$ electrodes

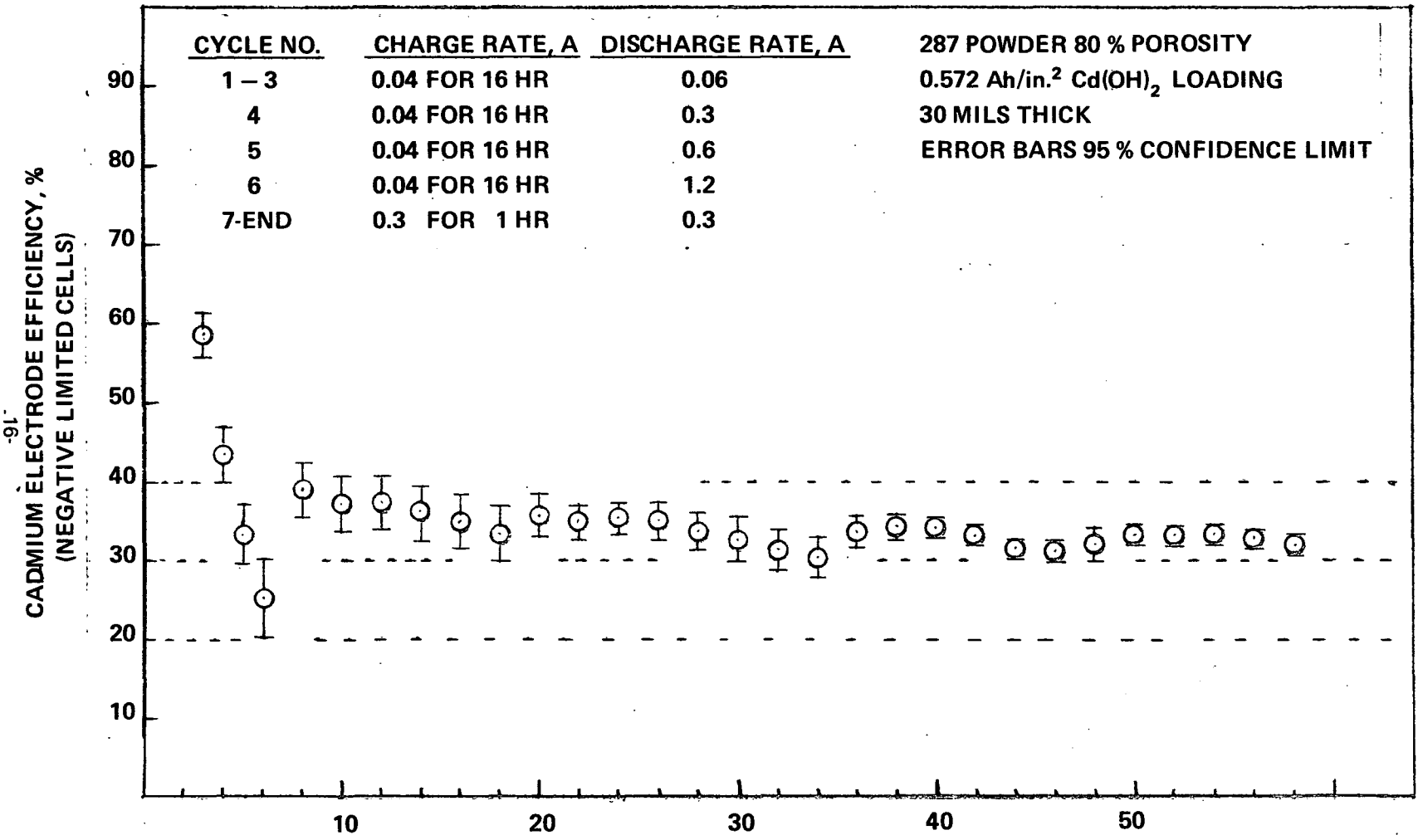


FIGURE 7. CYCLE LIFE OF STATE-OF-THE-ART CADMIUM ELECTRODE

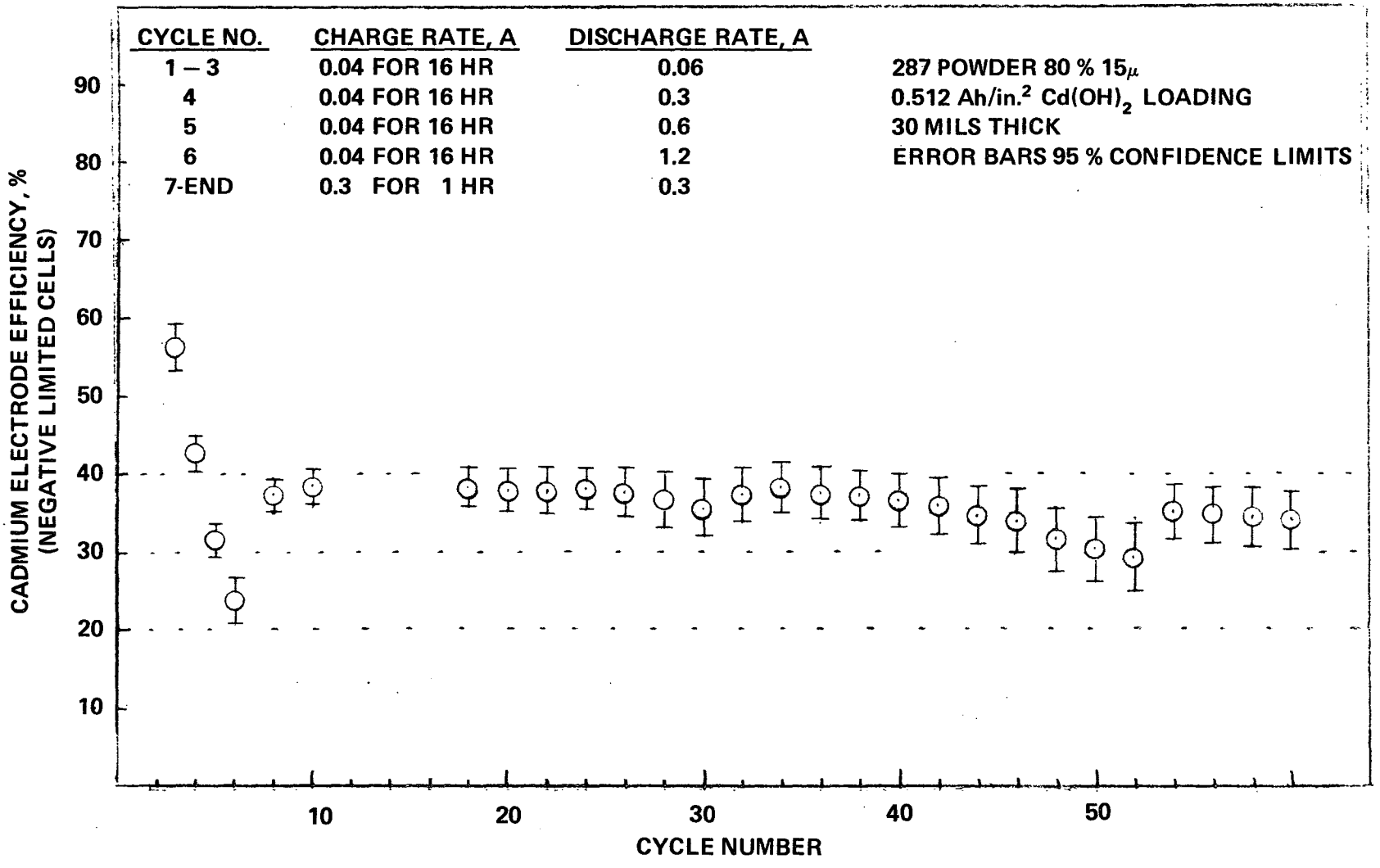


FIGURE 8. CYCLE LIFE OF CADMIUM ELECTRODES PREPARED FROM ISOSTATICALLY COMPACTED PLAQUES 80 % POROSITY 15μ INDUCED PORES

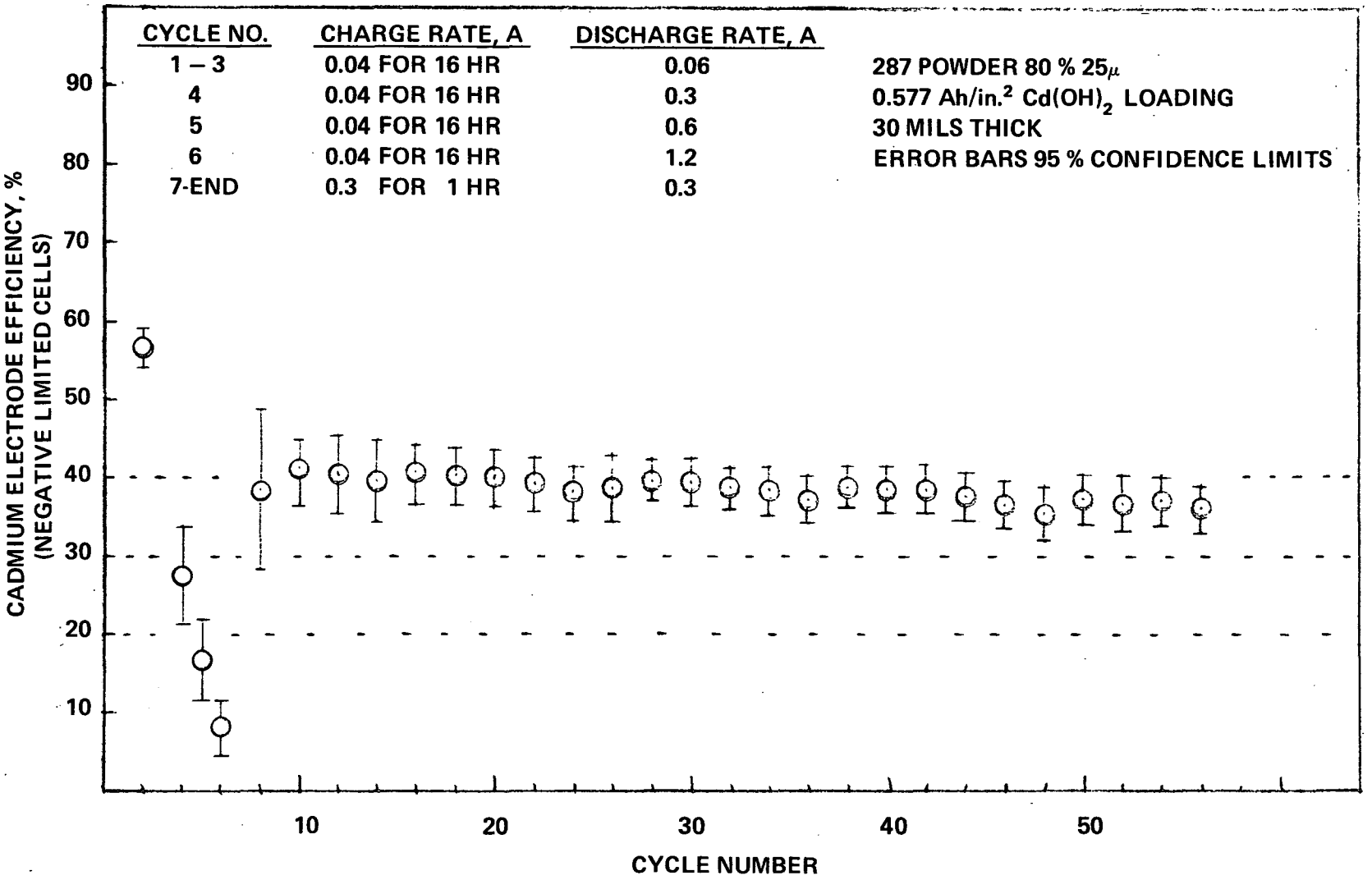


FIGURE 9. CYCLE LIFE OF CADMIUM ELECTRODES PREPARED FROM ISOSTATICALLY COMPACTED PLAQUES 80 % POROSITY 25μ INDUCED PORES

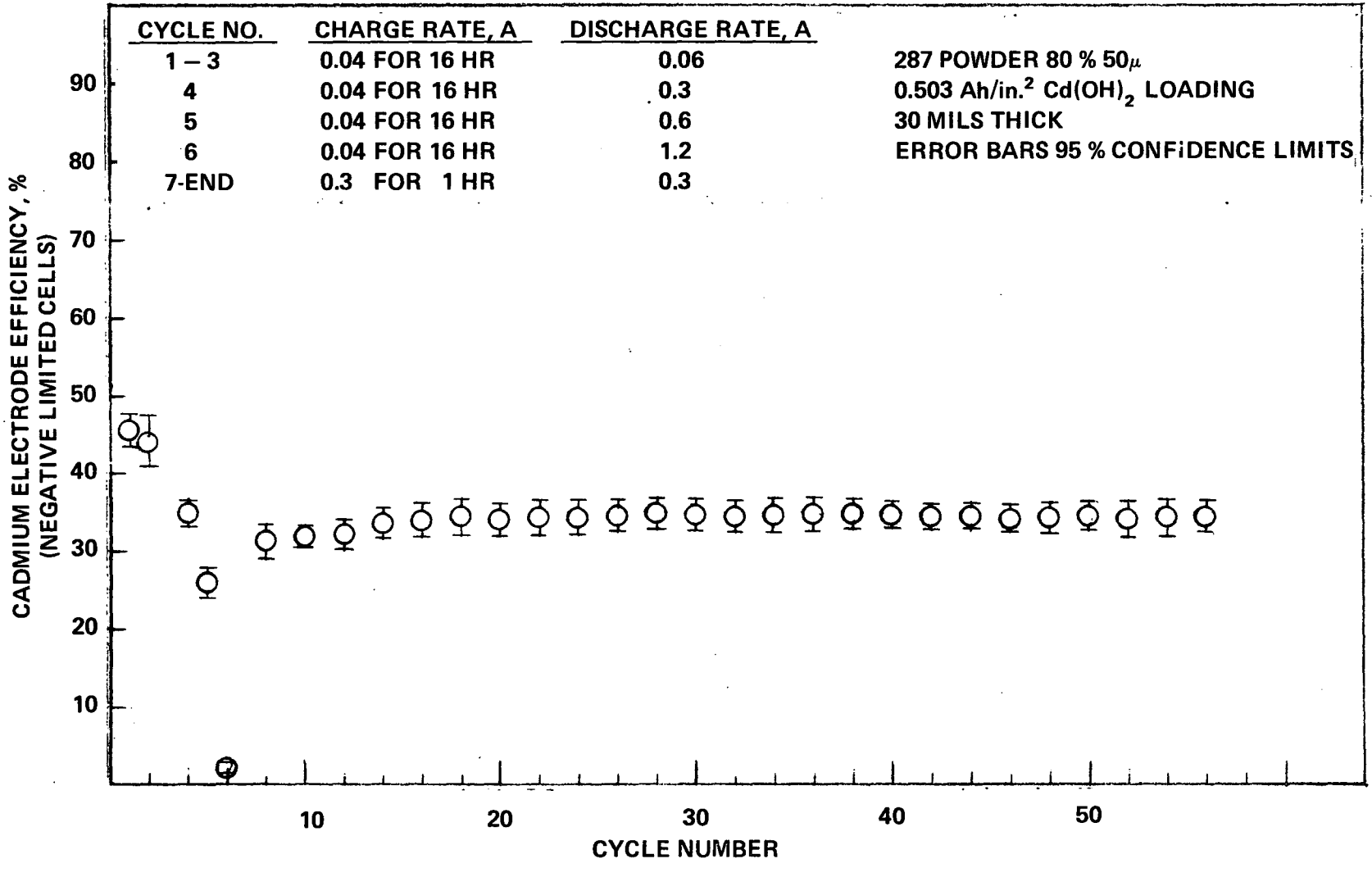


FIGURE 10. CYCLE LIFE OF CADMIUM ELECTRODES PREPARED FROM ISOSTATICALLY COMPACTED PLAQUES 80 % POROSITY 50μ INDUCED PORES

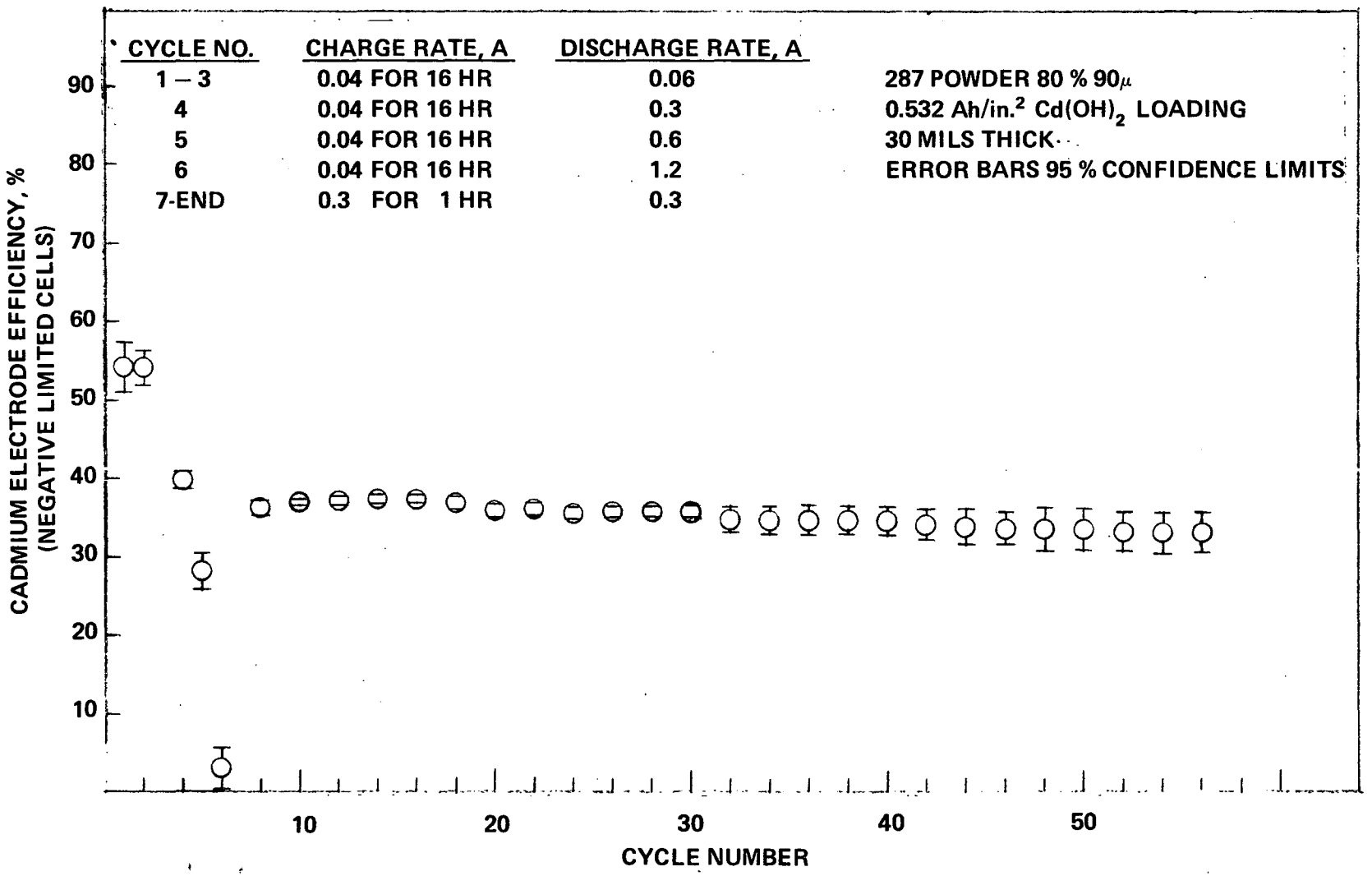


FIGURE 11. CYCLE LIFE OF CADMIUM ELECTRODES PREPARED FROM ISOSTATICALLY COMPACTED PLAQUES 80 % POROSITY 90μ INDUCED PORES

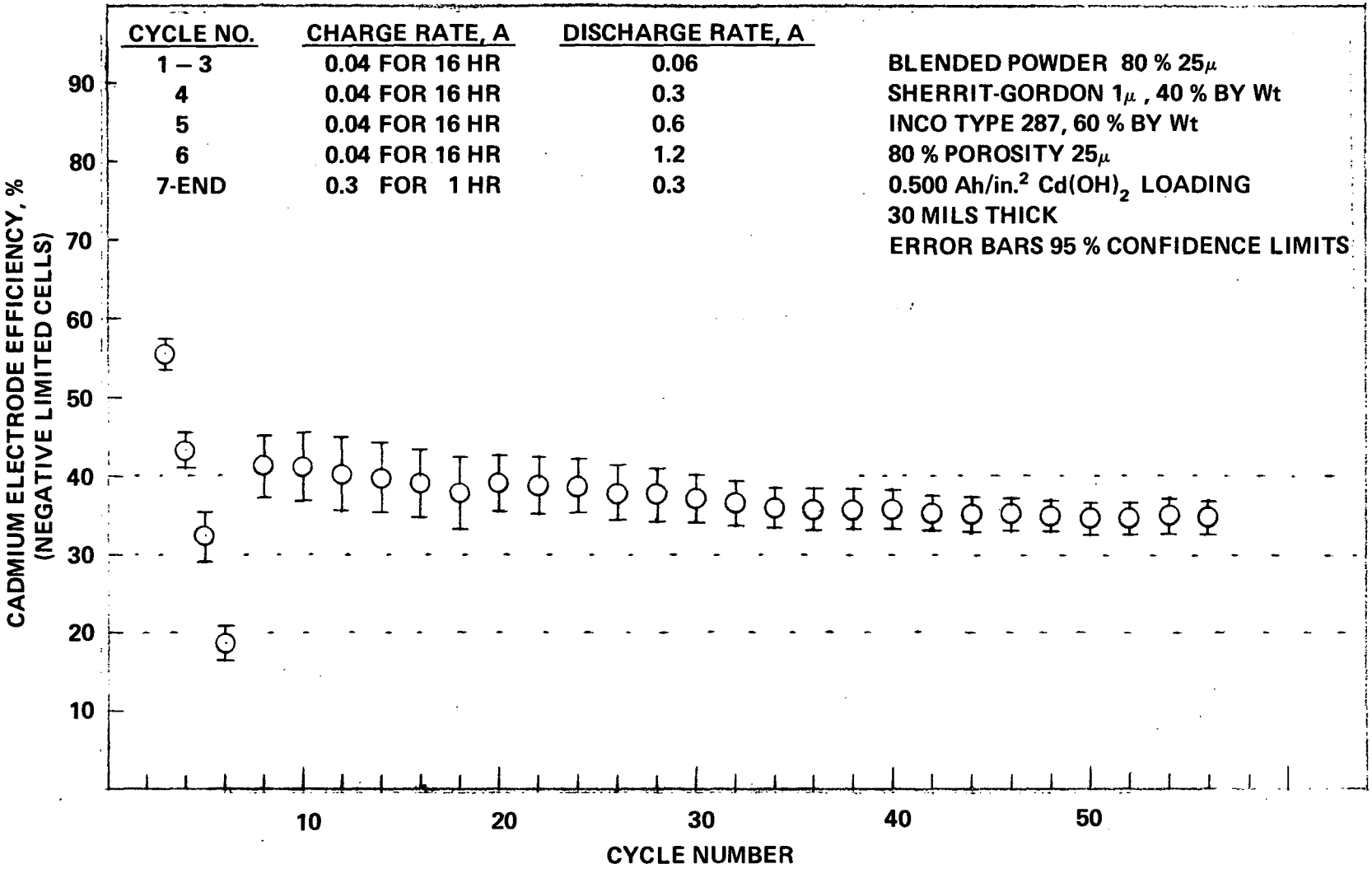


FIGURE 12. CYCLE LIFE OF CADMIUM ELECTRODES PREPARED FROM ISOSTATICALLY COMPACTED PLAQUES 80 % POROSITY 25μ INDUCED PORES BLENDED POWDER

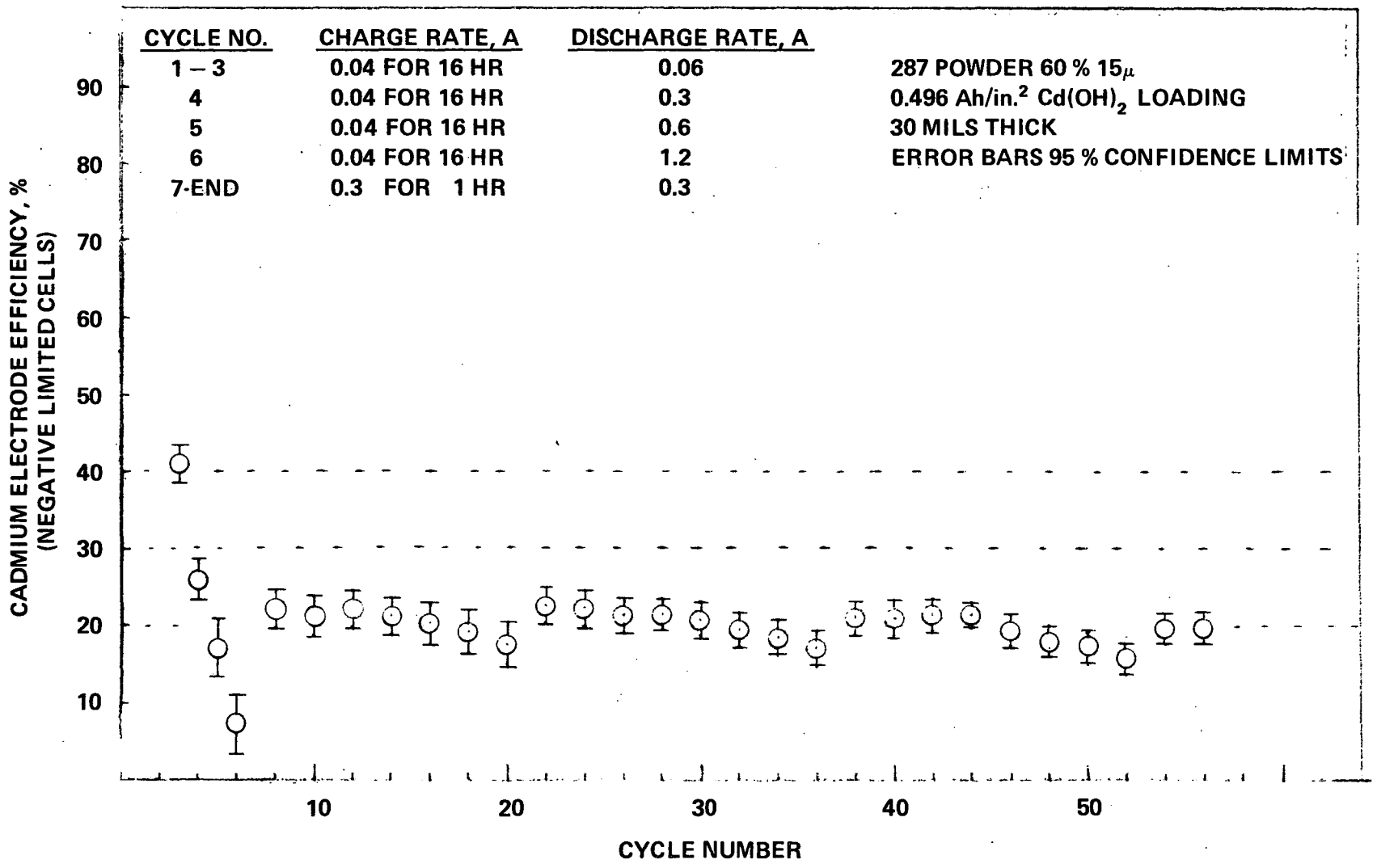


FIGURE 13. CYCLE LIFE OF CADMIUM ELECTRODES PREPARED FROM ISOSTATICALLY COMPACTED PLAQUES 60 % POROSITY 15μ INDUCED PORES

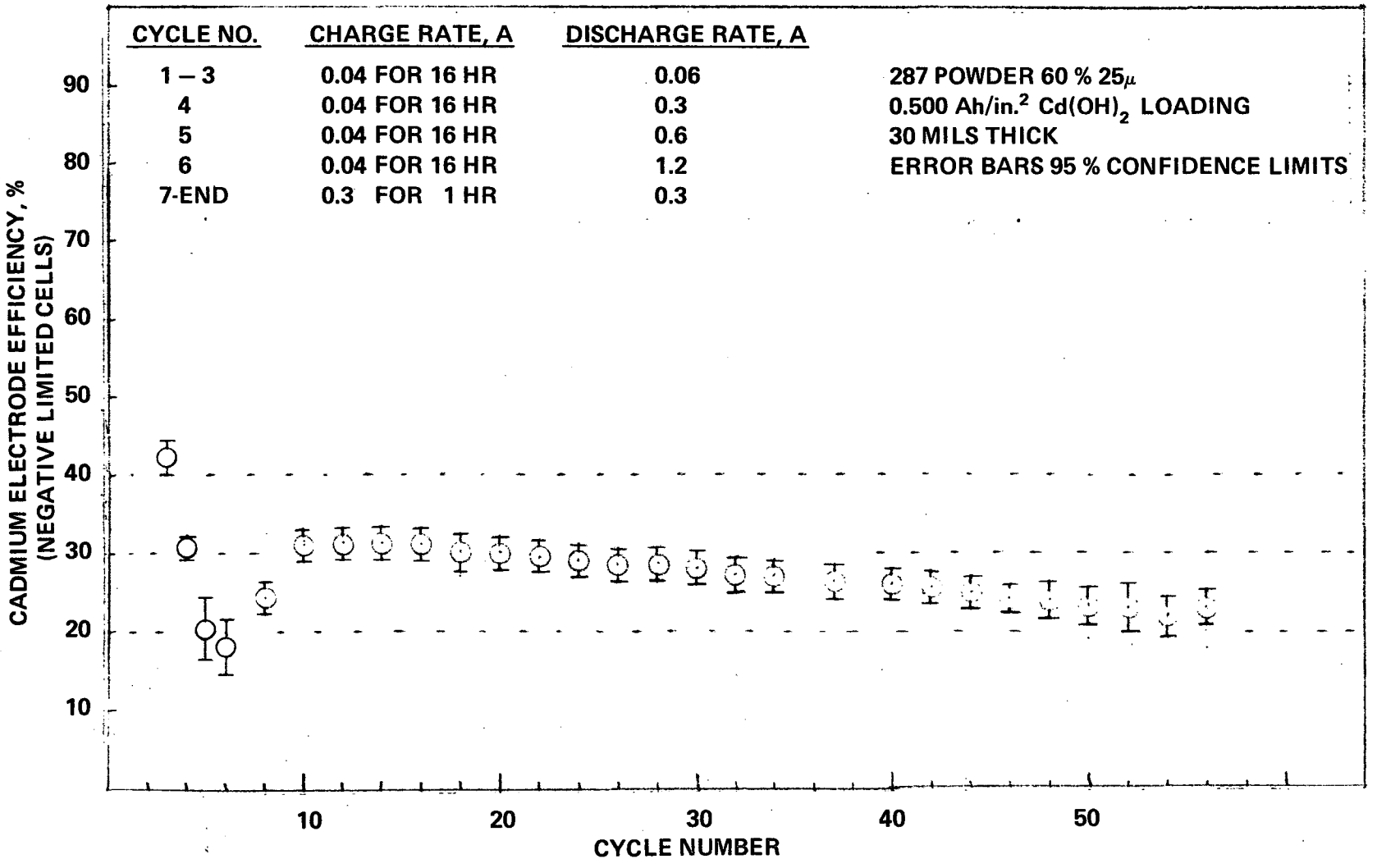


FIGURE 14. CYCLE LIFE OF CADMIUM ELECTRODES PREPARED FROM ISOSTATICALLY COMPACTED PLAQUES 60 % POROSITY 25μ INDUCED PORES

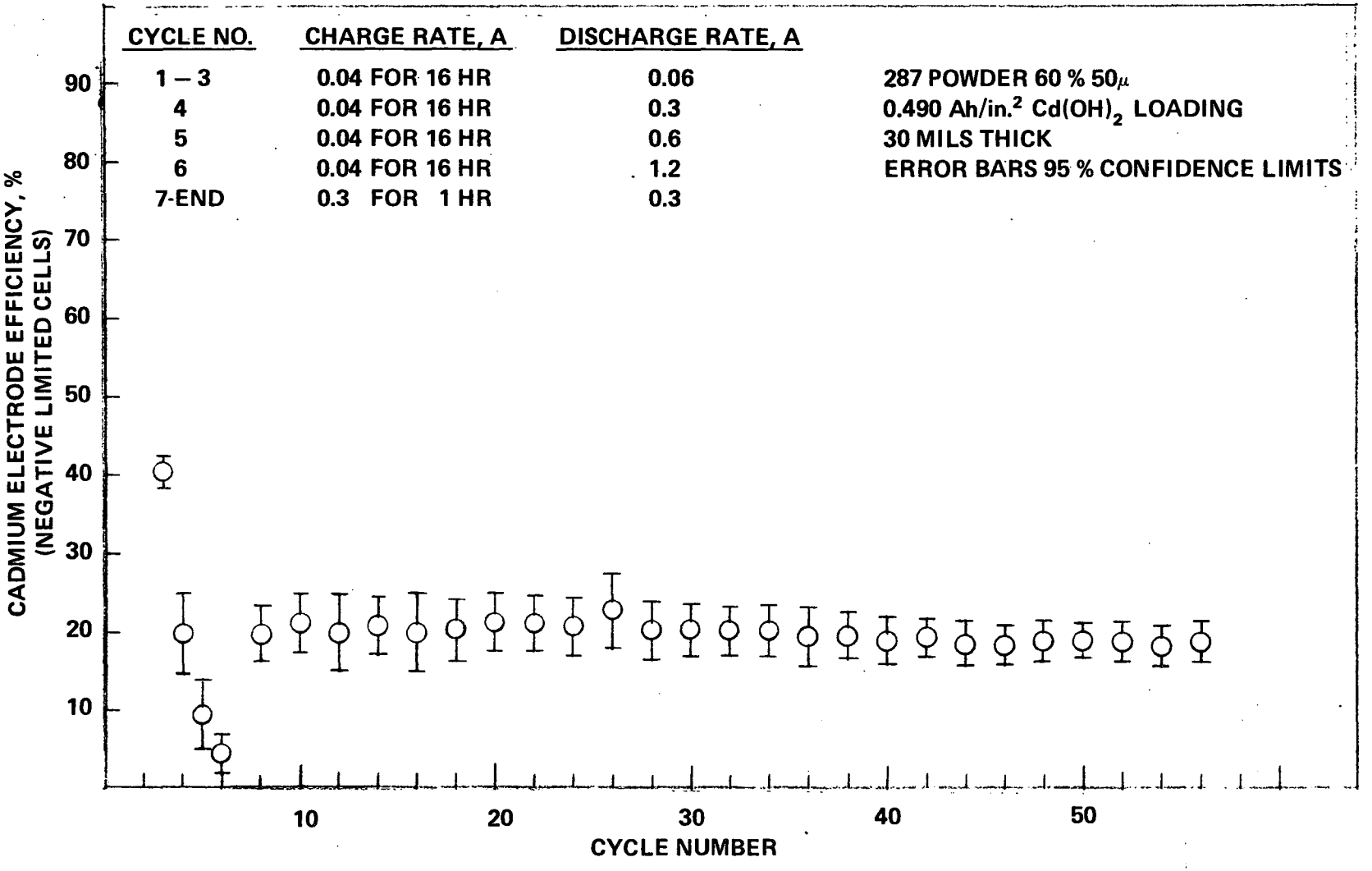


FIGURE 15. CYCLE LIFE OF CADMIUM ELECTRODES PREPARED FROM ISOSTATICALLY COMPACTED PLAQUES 60 % POROSITY 50μ INDUCED PORES

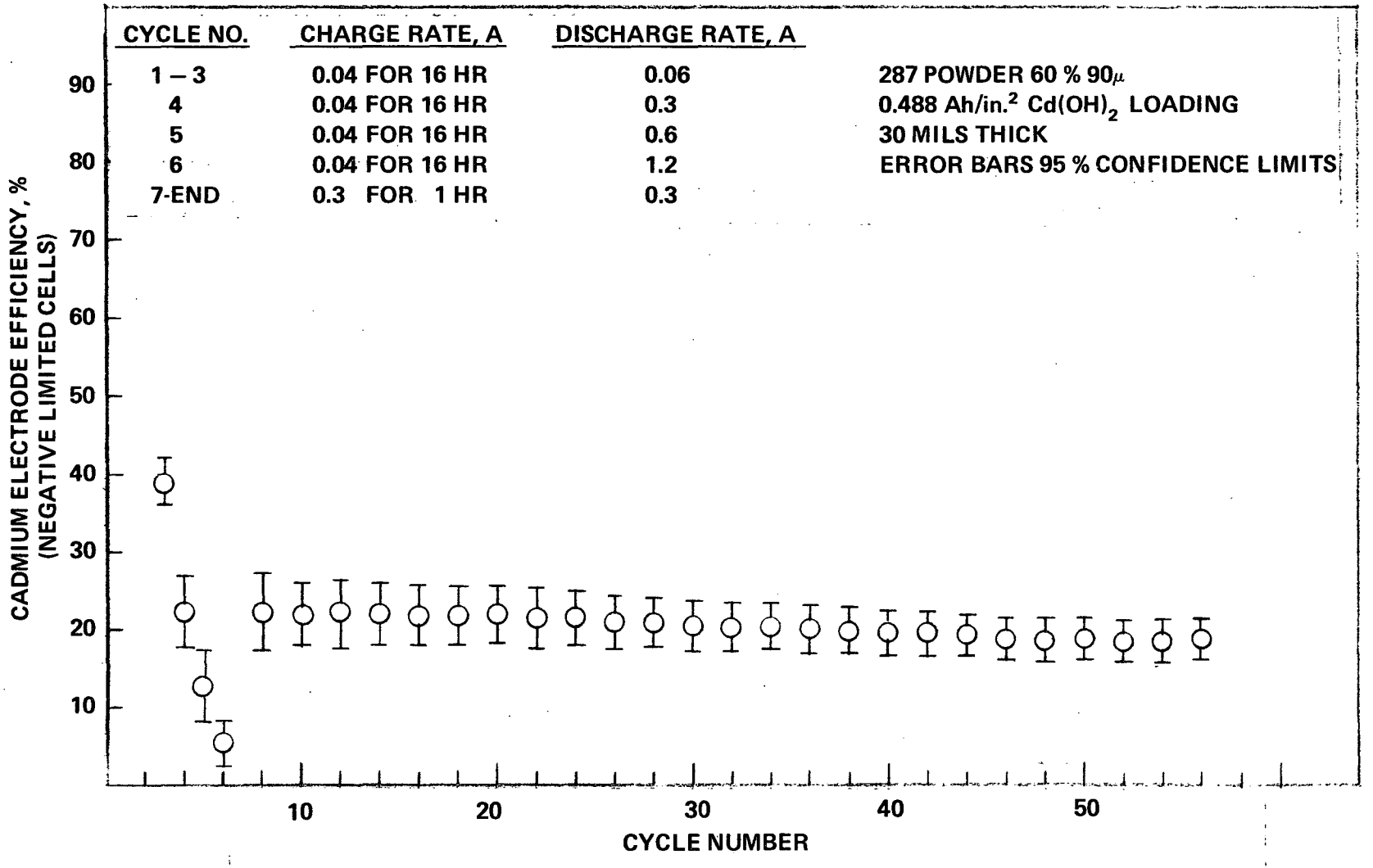


FIGURE 16. CYCLE LIFE OF CADMIUM ELECTRODES PREPARED FROM ISOSTATICALLY COMPACTED PLAQUES 60 % POROSITY 90μ INDUCED PORES

are however, lower in efficiency than the 80 % electrodes but not by a great deal, about 10 % across the board. In view of their exceptional mechanical properties, as compared to the 80 % structures (see Figure 5) and good efficiency and with the prospect of improving the efficiency, these are extremely interesting and promising structures, in the opinion of the authors.

### 3. Test Summaries

A summary of the test results of the accelerated cycle data obtained to date is given in Table 1. The degradation of capacity rates was determined via a linear regression analysis of the test data, using the seventh to the last cycle. A straight line was found to fit the data well. The differences in the test data were small, a numerical summary makes it easier to compare the isostatically compacted electrodes and conventional electrodes prepared from gravity sintered plaques from the point of view of efficiency and degradation rates. As far as degradation rates are concerned there are no statistically significant differences, with one exception, between all the electrodes tested. The electrodes prepared from the 60 % 25$\mu$ plaques inexplicably have higher degradation rates than all the other electrodes. It therefore seems that the degradation rate under the test conditions employed is independent of the plaque properties and therefore can not be used as a criterion for cell life. If there is any distinguishing feature in the data it would have to be the electrode efficiencies where some real differences are observed. From this point of view the 80 % structures with pore sizes 25 or less have efficiencies higher than conventional electrodes.

It is seen that electrodes prepared from the higher induced porosities, 91 % versus 49 %, have considerably higher efficiencies at the end of 50 tortuous cycles. We cannot account for this difference on the basis of increased loading per unit volume of the free space of the 60 % electrodes. (Recall that all electrodes had the same loading per unit total volume.) On the basis of their loadings alone, we expected 60 and 80 % porous electrodes to have essentially the same efficiencies. The low efficiencies of the 60 % electrodes are perhaps related to their low induced porosity. Further work will be required if this phenomenon is to be clarified.

**TABLE 1. SUMMARY OF CYCLE TEST DATA**
**Least Squares Fit To Y = A + BX**
**Y = Efficiency, X = Cycle Number**

| ELECTRODES | % $P_{ind}$(1) | A(2) | B(3) | SMOOTHED EFFICIENCY AT CYCLE 50 |
|---|---|---|---|---|
| State-of-the-Art (Thermal) | 0 | 37.33 | -0.100 ± 0.058 | 32.3 ± 2.4 |
| From 60 % 15 Plaques | 40 | 22.22 | -0.0694 ± 0.054 | 18.7 ± 2.3 |
| From 60 % 25 Plaques | 40 | 33.20 | -0.182 ± 0.052 | 24.1 ± 2.2 |
| From 60 % 50 Plaques | 40 | 21.98 | -0.064 ± 0.086 | 18.8 ± 3.6 |
| From 60 % 90 Plaques | 40 | 23.22 | -0.085 ± 0.082 | 19.0 ± 3.5 |
| From 80 % 15 Plaques | 91 | 40.28 | -0.120 ± 0.076 | 34.3 ± 3.2 |
| From 80 % 25 Plaques | 91 | 41.51 | -0.0873 ± 0.092 | 37.1 ± 3.9 |
| From 80 % 25 Plaques (Blended Powders) | 91 | 41.64 | -0.140 ± 0.079 | 34.6 ± 3.3 |
| From 80 % 50 Plaques | 91 | 32.54 | +0.048 ± 0.048 | 34.9 ± 2.0 |
| From 80 % 90 Plaques | 91 | 38.00 | -0.086 ± 0.031 | 33.7 ± 1.3 |

(1) Percent Porosity Induced, calculated

(2) Electrode Efficiency at the Zero Cycle, if it is possible to extrapolate through the first 7 cycles ± average 95 % confidence limit

(3) Rate of degradation of the electrode efficiency per cycle ± 95% confidence limit

## E. SCANNING ELECTRON MICROSCOPY OF ISOSTATICALLY COMPACTED PLAQUES AND CADMIUM ELECTRODES

The scanning electron microscope (SEM) is a uniquely suited tool for examining the extent of uniformity of the microstructures of the plaque materials prepared in this work. This is mainly due to the striking superiority of the SEM micrographs as compared to optical micrographs. This important benefit is in addition to other very considerable advantages such as:

- Not requiring special and lengthy polishing of a flat surface which is difficult for soft battery plate materials we are dealing with.
- No need to etch the specimen to differentiate the different materials and phases present.
- Surfaces do not have to be replicated as is required in conventional electron microscopy. The utility of the SEM will be evident as the micrographs are presented.

Aside from qualitatively judging the extent of uniformity, attempts were made to measure the total porosity and interstitial porosity from the photomicrographs.

It was not possible to determine these properties with any degree of accuracy from the SEM photomicrographs due to its extreme depth of field. It was not possible to identify all the pores since one could not readily distinguish nickel particles at different planes (levels) in the plaque. However, it was a relatively simple matter to determine the average induced pore size by measuring a representative sampling of the induced pores at the 100X magnification, of the micrographs given in the following text and in Appendix D. Results are given below in Table 2. These measurements are very sensitive to the judgement of the observer.

**TABLE 2. INDUCED PORE SIZE OF ISOSTATICALLY COMPACTED PLAQUES**

| PLAQUE | INDUCED PORE SIZE, $\mu$ |
|---|---|
| 60% 15$\mu$ | 10-15 |
| 80% 15$\mu$ | 10-15 |
| 60% 25$\mu$ | 16 |
| 80% 25$\mu$ | 16 |
| 60% 50$\mu$ | 33 |
| 80% 50$\mu$ | 35 |
| 60% 90$\mu$ | 72 |
| 80% 90$\mu$ | 70 |

Figures 17 and 18 are representative SEM photomicrographs, 60 and 80 % 25$\mu$ , of isostatically compacted structures and are qualitatively quite revealing as far as microscopic uniformity is concerned. Part (a) of each figure at approximately 100X magnification shows the nature of the induced porosity, rather large pores (measured values given in Table 2 for all groups of plaques prepared), uniformly distributed throughout the plaque. The 80 % porosity material apparently being a little bit more uniform in this respect. The actual size of the induced pores are considerably less than sizes of the pore-former particles. The reduction in size is probably due for the most part to shrinkage during sintering. The photomicrographs at the 1000X magnification show the induced and interstitial porosity in more detail, especially the interstitial porosity and its relation to the induced

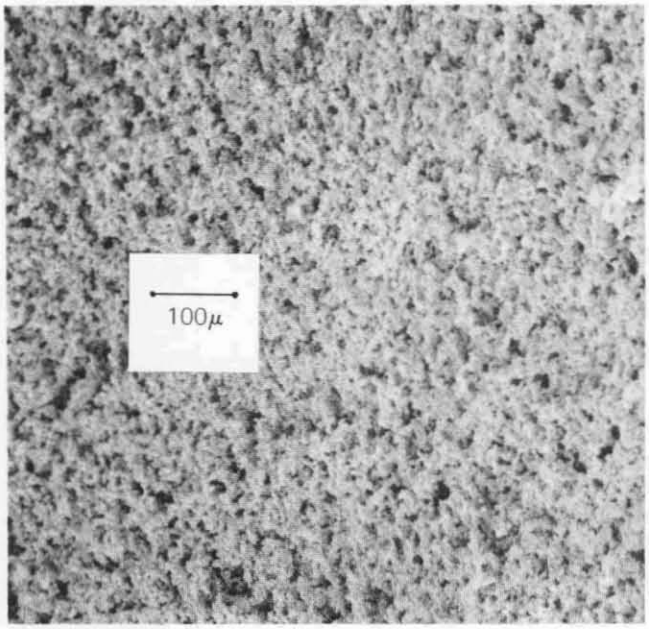


110X

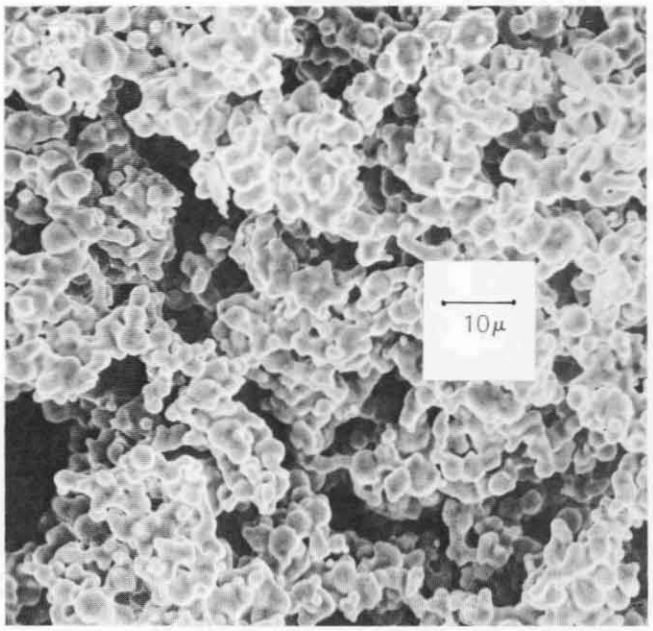


1000X



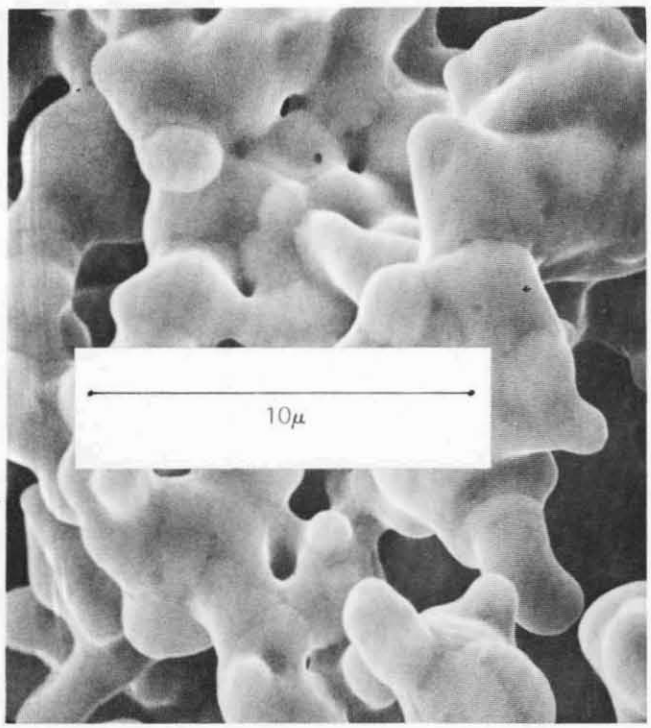


5000X

**FIGURE 17. SEM PHOTOMICROGRAPHS OF ISOSTATICALLY COMPACTED PLAQUES, 80 % 25μ**

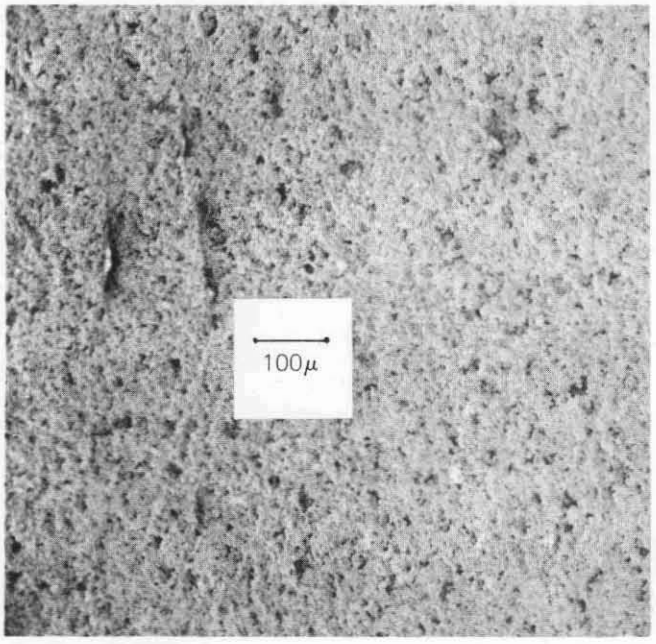


95X

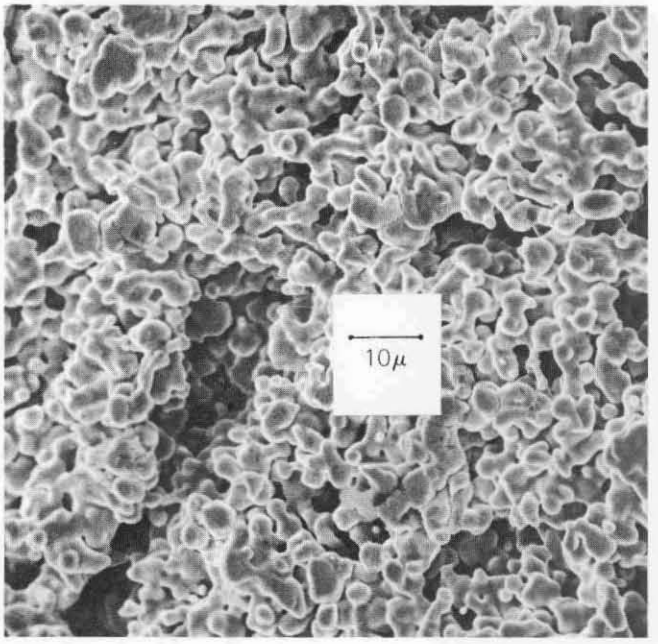


1000X



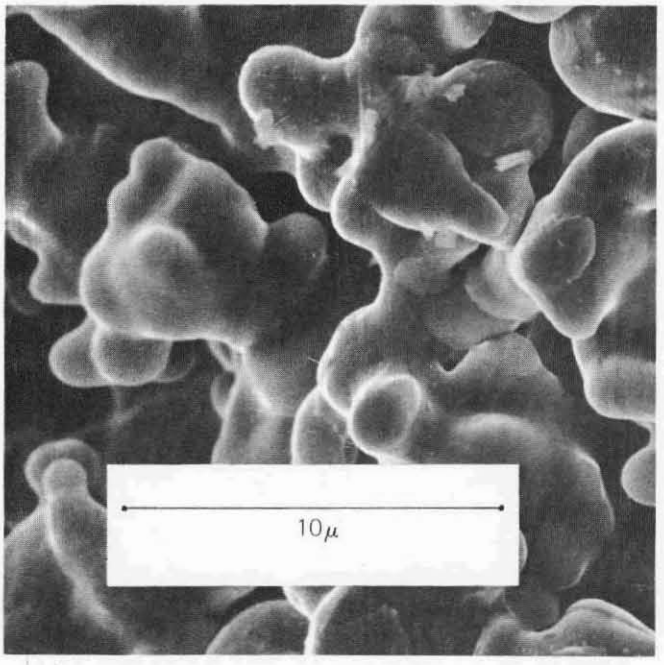


5000X

**FIGURE 18. SEM PHOTOMICROGRAPHS OF ISOSTATICALLY COMPACTED PLAQUES, 60 % 25μ**

porosity. Small interstitial pores well under 10$\mu$ are evident which no doubt contribute substantially to the total porosity and performance of the electrode. No very extensive agglomerates of material are visible, that is, all the porosity is seemingly interconnected. Part (c) at 5000X magnification reveals some interesting fine points about the sintered nickel structures. These show the interstitial porosity exclusively. The small interstitial pores are again evident. Also, linear boundaries are apparent. These represent grooves from the sintering of two nickel powder particles. Also evident are dots on the nickel structures. These are micro pits where three or more particles were sintered together. There is a far greater population of these dots for the compacted 80 % porous structures. This is indicative of more interparticle bonding and no doubt contributes to the increased strengths of the compacted materials over the conventional gravity sintered materials.

These observations are contrasted with the details shown in Figure 19 for a state-of-the-art gravity sintered plaque prepared under identical conditions of sintering time and temperature. Very large irregular pores not uniformly distributed are evident. Also present in the gravity sintered structure are islands of large agglomerates of nickel metal. The gravity sintered specimens do not have the well-developed necks and the high population of dimples as the compacted specimens.

The compacted plaques characteristically have well-developed necks. The increased and improved interparticle contact between powder particles and the compressed plaques is the primary factor governing their improved strength.

Routinely at the end of the accelerated test program, SEM photomicrographs of selected specimens of the cycled cadmium electrodes were taken in an effort to measure morphological changes that occurred during the cycle testing. Typical examples are shown in Figure 20 and 21 for electrodes made from 60 % 25$\mu$ and 80 % 15$\mu$ plaques. The $Cd(OH)_2$ crystal size through the plaque structure is important because the crystal size is perhaps a key property governing the performance degradation of cadmium electrodes during cycling.

Also of importance in the micrographs is the presence of base nickel. A typical example of a formed but not cycled electrode is given in Figure 22. Note that the plaque substructure is completely covered with $Cd(OH)_2$ crystals. Apparently with prolonged cycling, morphological changes occurred in which cadmium active mass migrated from the nickel surfaces onto other cadmium hydroxide particles. Also prominent in the micrographs is the evidence of corrosion of the nickel substrate. The previously discussed pits are considerably enlarged after cycling. At present we do not know whether this is due to electrode processing or to the cycling.

Additional SEM photomicrographs of isostatically compacted plaques (60 and 80 %, 15-90$\mu$) and electrodes made from same are included in Appendix D and E.

The $Cd(OH)_2$ crystal sizes, $\bar{d}$, were measured from the micrographs and are summarized below in Table 3 with other pertinent data, the smoothed 50th cycle efficiency.

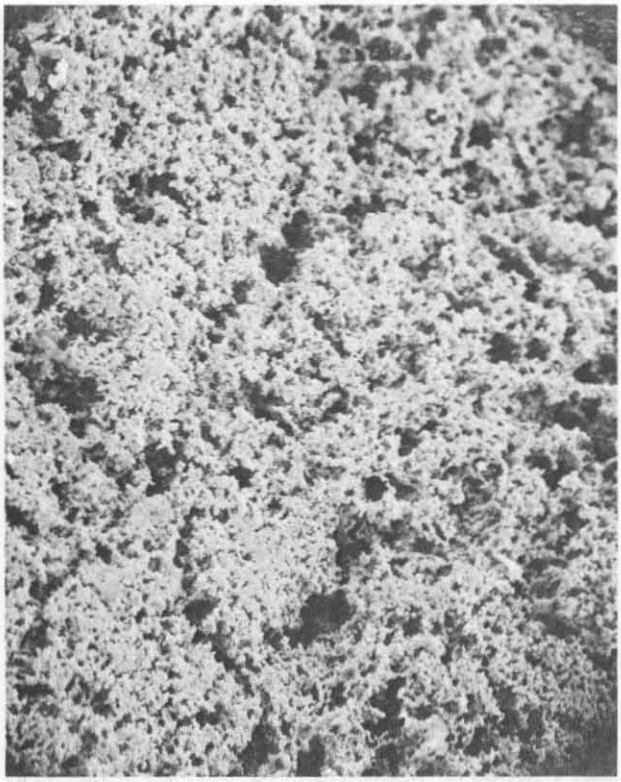

135X

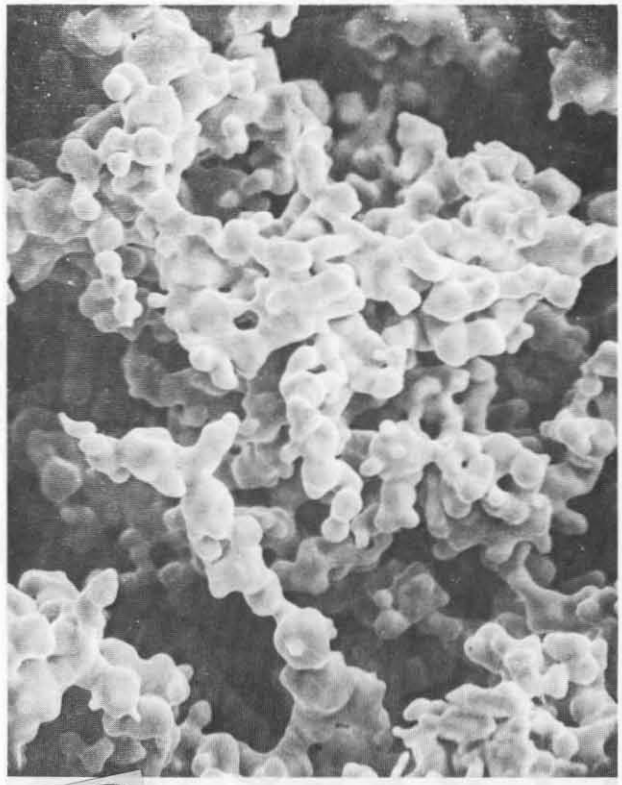

1350X



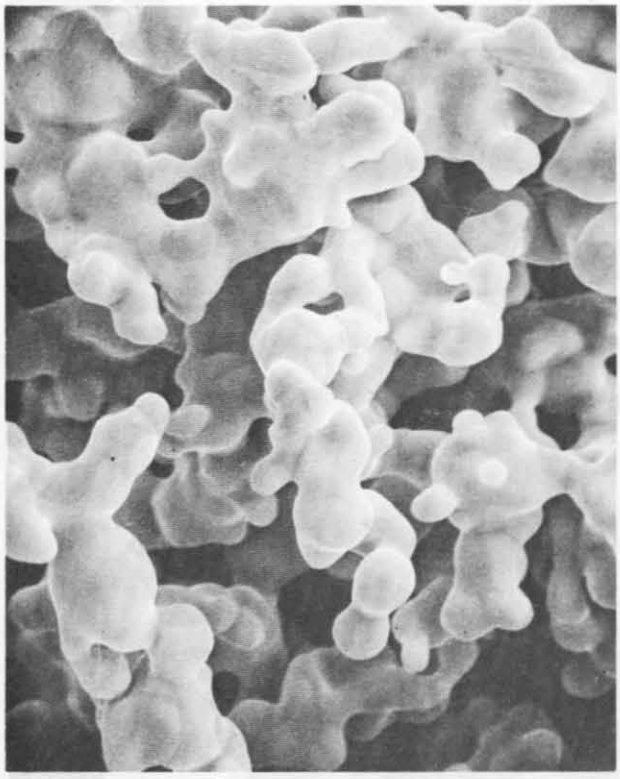

2305X

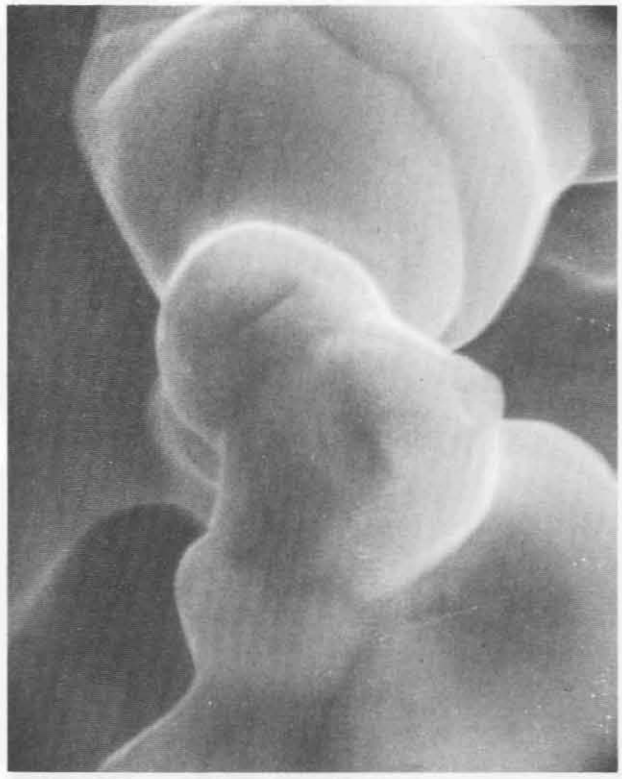

13,520X

FIGURE 19. SEM PHOTOMICROGRAPHS OF STATE-OF-THE-ART GRAVITY SINTERED PLAQUES

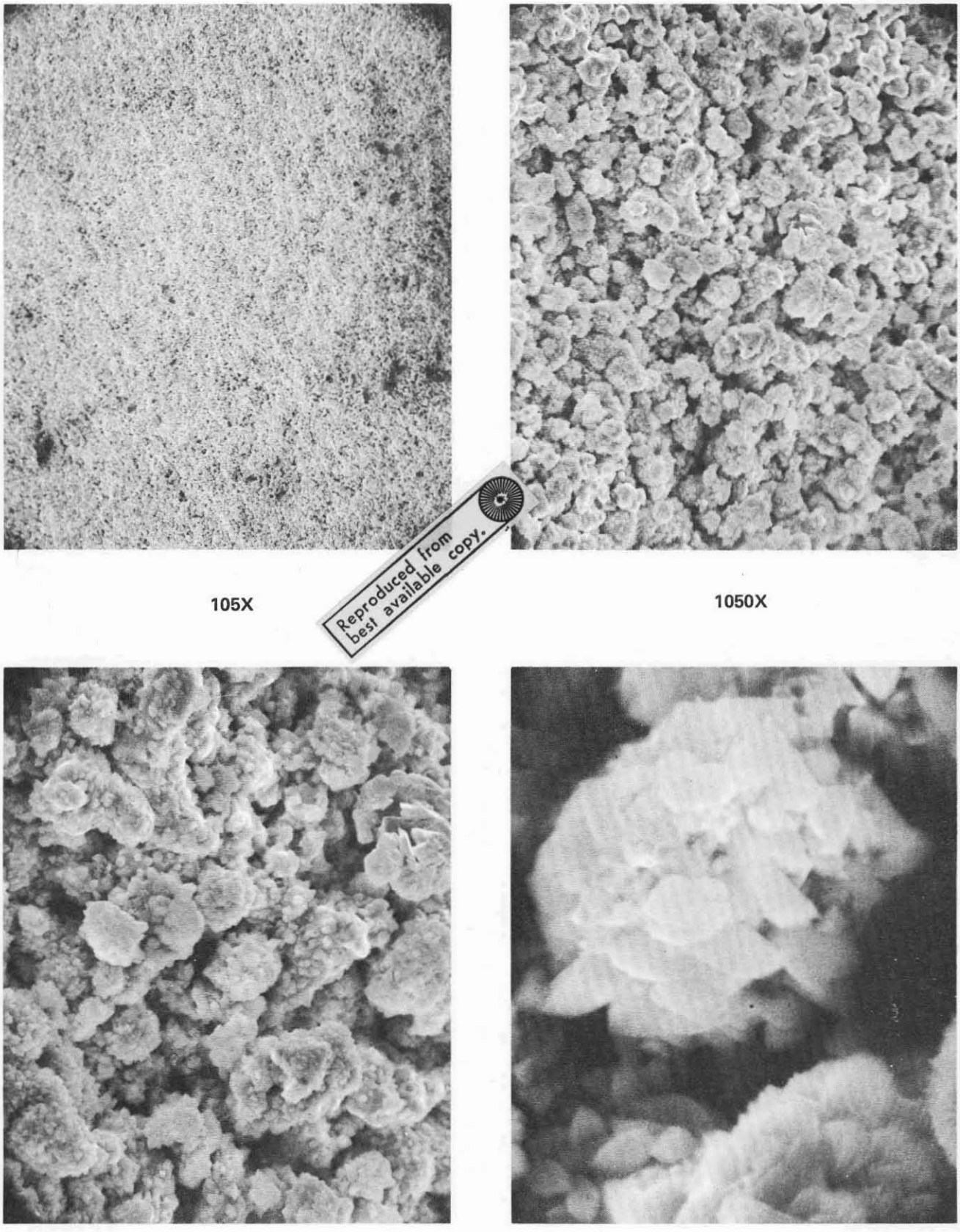

105X

1050X

2100X

10,500X



FIGURE 20. SEM PHOTOMICROGRAPHS OF CYCLED ELECTRODES MADE FROM ISOSTATICALLY COMPACTED PLAQUES, 60 % 25$\mu$

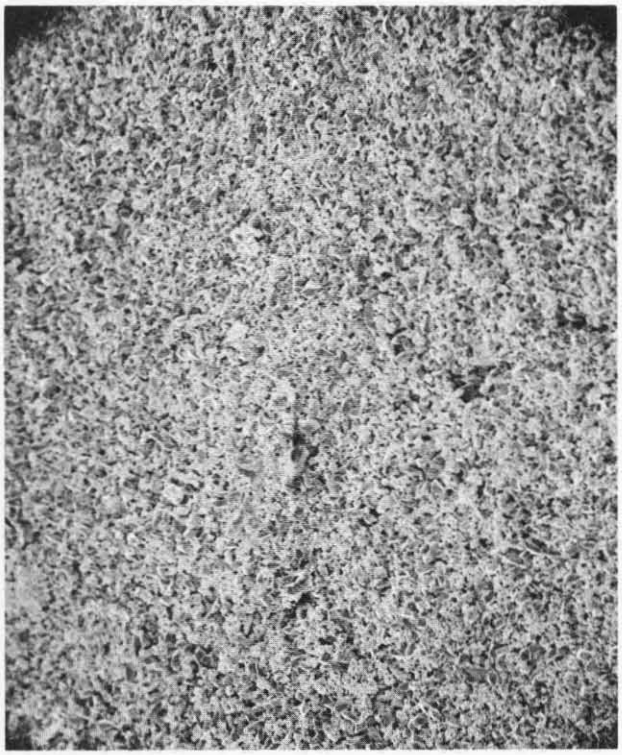

105X

1050X

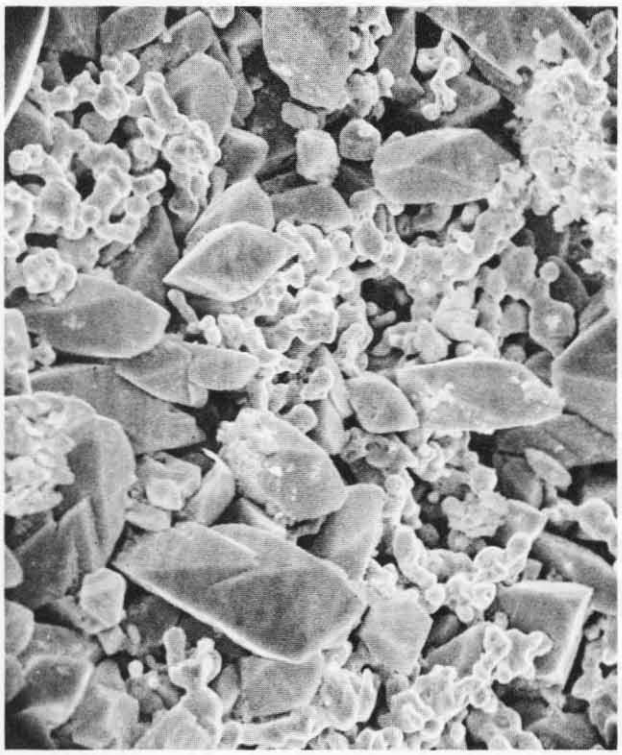

2100X

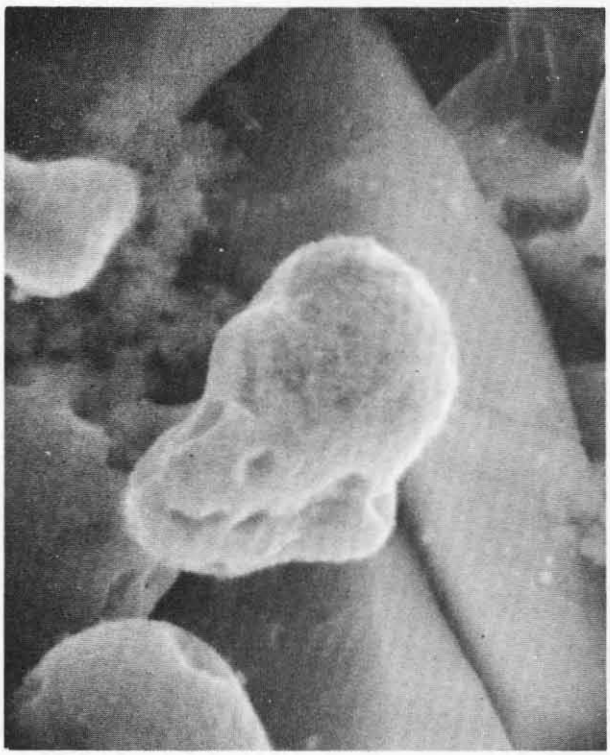

10,500X

FIGURE 21. SEM PHOTOMICROGRAPHS OF CYCLED ELECTRODES MADE FROM ISOSTATICALLY COMPACTED PLAQUES 80 % 15$\mu$

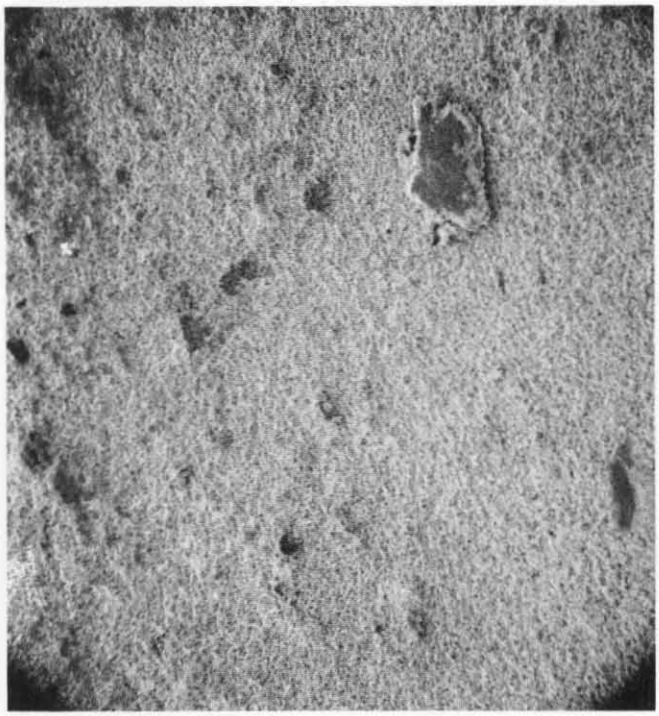

105X

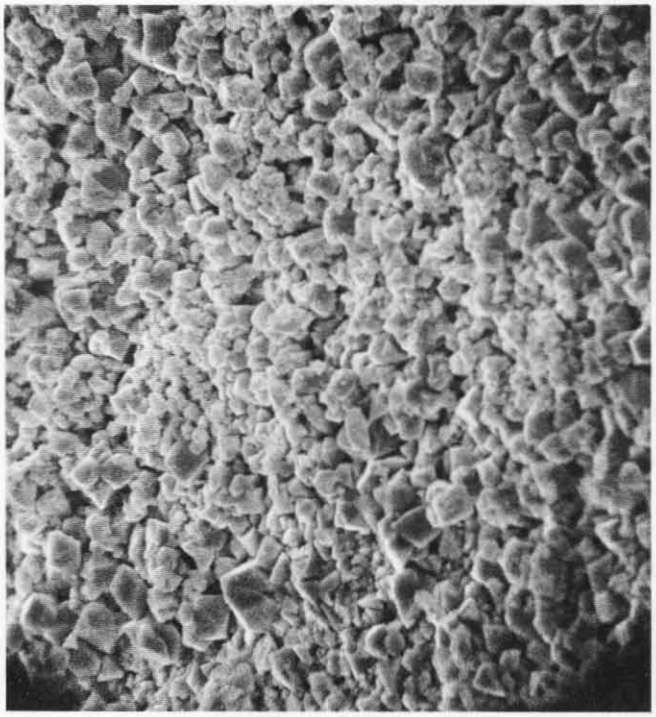

1050X

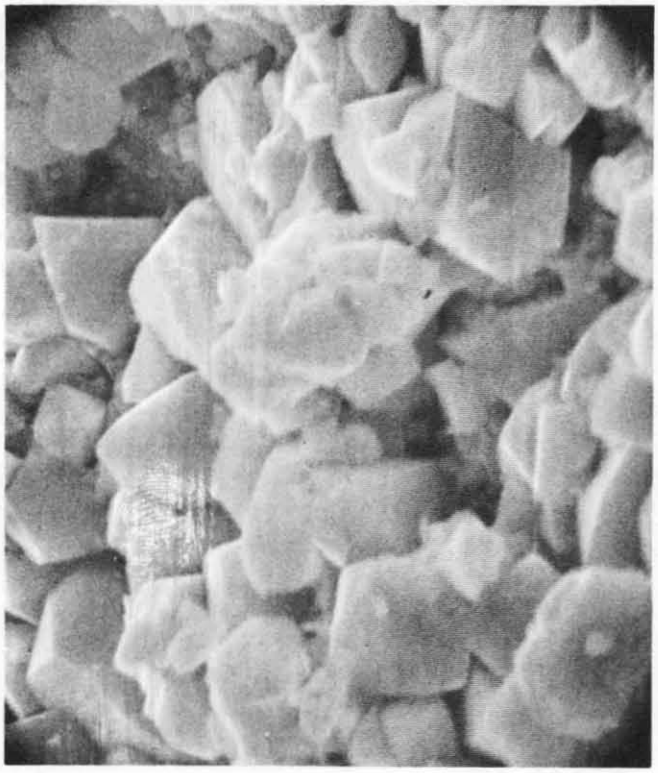

5250X



FIGURE 22. SEM PHOTOMICROGRAPHS OF FORMED ELECTRODE MADE FROM ISOSTATICALLY COMPACTED PLAQUE, INCO 287 POWDER, 60 % 50$\mu$

TABLE 3. $Cd(OH)_2$ CRYSTAL SIZE AFTER CYCLING

| ELECTRODE TYPE | SMOOTHED 50th CYCLE EFFICIENCY | $\bar{d}$ ($\mu$) |
|---|---|---|
| 60 % 15$\mu$ | 18.7 | 2.3 |
| 60 % 25$\mu$ | 24.1 | 1.4 |
| 60 % 50$\mu$ | 18.8 | 1.0 |
| 60 % 90$\mu$ | 19.0 | 0-1.0 |
| 80 % 15$\mu$ | 34.3 | 9.8 |
| 80 % 25$\mu$ | 37.1 | 6.8 |
| 80 % 50$\mu$ | 34.9 | 7.3 |
| 80 % 90$\mu$ | 33.7 | 4.7 |

It is very clear that the $Cd(OH)_2$ crystal size is dependent upon the substrate porosity, the 60 % porous substrates have crystal sizes in the 0-2$\mu$ range and the 80 % porous substrates have crystal sizes of about 7-10$\mu$. This difference in crystal sizes is conspicuous when one compares Figures 20 and 21. It must be pointed out, however, that the crystal size is perhaps confounded with the depth of discharge and perhaps porosity of the two different groups of electrodes. One would generally expect better efficiencies for electrodes with the smaller crystal sizes, yet the opposite was observed.

No definite relationship between crystal size and electrode efficiency was apparent. A trend of decreasing crystal size with increasing induced pore size was evident.

As an additional point of interest, the formed but uncycled electrodes had average crystal sizes of 3.0$\mu$, so that upon cycling, crystal sizes of the electrodes with the 60 % porous substrates decreased while those with the 80 % porous substrates increased.

At this point, it is worthwhile to repeat that the above treatment of crystal size is approximate because of the difficulty in interpreting the size of the crystals.

It thus appears, if we may say from such a limited quantity of data, that the $Cd(OH)_2$ crystal size in these electrodes at the loading levels studied is dependent upon both the plaque pore size and porosity.

## F. X-RAY RADIOGRAPHY OF PLAQUES AND ELECTRODES

The intensity of an X-ray beam is attenuated locally as it passes through a homogeneous or heterogeneous body. This is due to the adsorption or scattering of the X-ray beam by the material concerned. As a result, the X-ray beam emerging from the object can form, at the surface of a photographic film, areas of differing intensity which as a whole comprise the X-ray image. This is the so-called technique of X-ray radiography. It was used here as a qualitative tool for the measurement of microscopic uniformity of plaques prepared, and followed through after loading with active material, formation, and cycling. This was done in an effort to monitor the bulk uniformity of components in a qualitative way at various stages in the electrode testing and processing regime. Measurements were made on virgin plaque, formed or unformed virgin electrodes, and the electrode at the conclusion of the testing.

The intensity of the radiographs in the format in which they are given is dependent on numerous factors. Some of the more important factors are the intensity of the X-ray beam, exposure time (on negative and print), film type, etc. These are aside from the optical density of the specimen material. Since we were only interested in density gradations within a particular specimen, no rigorous effort was made to carefully control the photographic steps so that a given intensity on the radiograph would correspond to an actual density value. As a result, comparing densities from specimen to specimen has no meaning since these are biased by the photographic processing.

Radiographs representing samples of each porosity and pore-size are shown in Figures 24 through 32. Figure 23 shows radiographs of state-of-the-art electrodes induced for comparison. A careful visual comparison shows several intersting features. First, the bulk uniformity of the isostatically compacted plaques was good, compared to state-of-the-art. An increasing degree of uniformity was evident as the size of the pore-former was increased. This was probably due to increased ease of processing and preparing a uniform powder blend. Uniformity of the isostatically compacted plaques could still be improved by tightening of the process variables; no exceptional effort could be made to this end since so many other parameters had to be defined in this exploratory study.

A trend toward increased uniformity with increased induced pore size was also noted with the impregnated plaques. The apparent lack of uniformity of some of the impregnated plaques is due to the impregnation procedure employed. Particularly noticeable is the mottling of the plaques, and high density areas on one edge. This high density area on one edge is due to attitude effects during impregnation. The electrodes were prepared in racks standing on edge[2], allowing gravitational effects to force the higher loading on the lowest edge. The mottling effect can be attributed to the process itself and apparently not to the plaques. Modified impregnation procedures designed to the need of the particular type of plaques may be required to improve uniformity of electrodes. The cycle test results were not affected by these particular nonuniformities.

Further, examination of the radiographs of these same electrodes after cycling, showed that they were identical to the radiographs of the unformed or formed electrodes. This indicated that there were no bulk material location changes in the electrode during cycle testing.

Another interesting aspect of these electrodes, which was made very apparent by the radiographs of the electrodes after cycling, was the amount of cracking observed. A large part of these cracks were apparent upon visual examination, but others were invisible subsurface cracks. Cracking during cycle test can be detrimental to the performance of the electrode due to increasing internal resistance and general reduction in current collection efficiency. The exact cause of this phenomena is not known; however, it may be due to electrode dimensional changes generating stresses during charge and discharge. Also, it is very important to note that the 80 % porous substrate material was far more susceptible to cracking (see Mechanical Strengths in Figure 5) than was the stronger 60 % porous substrate materials. The gravity sintered (state-of-the-art) exhibited the most severe cracking.

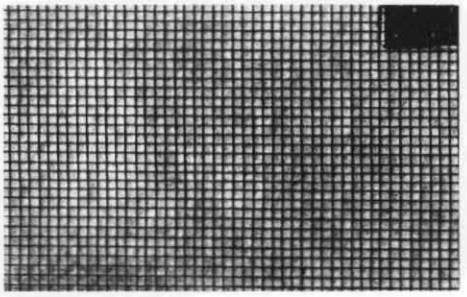

Raw Plaque Prepared By
Gravity Sintering Technique

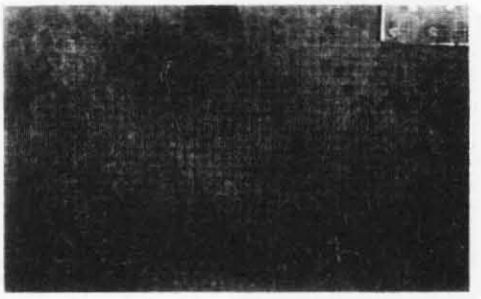

Unformed Electrode Prepared
From A Gravity Sintered Plaque

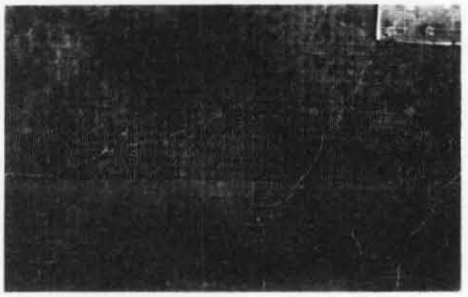

Formed, Uncycled Electrode

Cycled Electrode

FIGURE 23. TYPICAL "STATE-OF-THE-ART" ELECTRODE
PREPARED FROM GRAVITY SINTERED PLAQUE

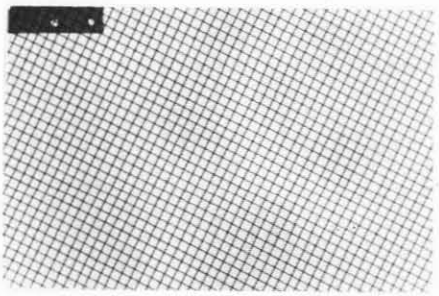

Raw Plaque Prepared
By Isostatic Compaction

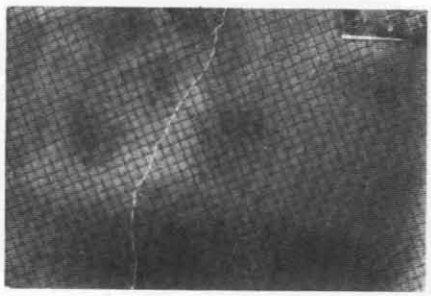

Formed Electrode Prepared From An
Isostatically Compacted Plaque

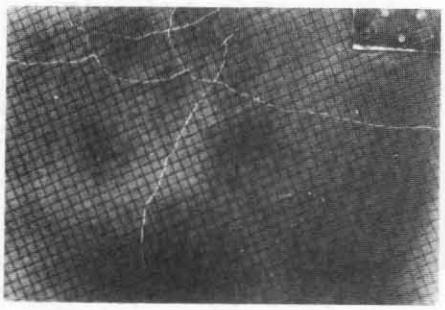

Cycled Electrode After 56 Cycles

**FIGURE 24. ELECTRODE PREPARED FROM ISOSTATICALLY COMPACTED PLAQUE, 80 % 15$\mu$ PORE SIZE**

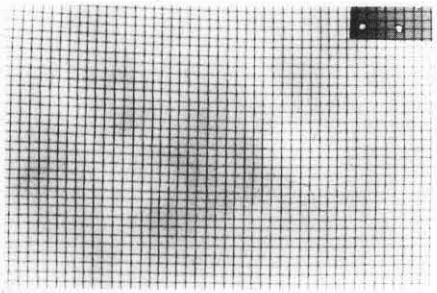

Raw Plaque Prepared
By Isostatic Compaction

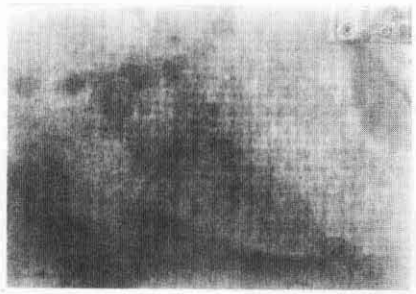

Formed Electrode Prepared From An
Isostatically Compacted Plaque



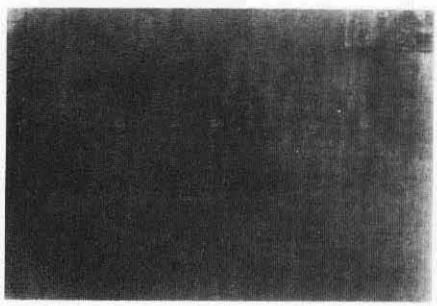

Cycled Electrode After 56 Cycles

FIGURE 25. ELECTRODE PREPARED FROM ISOSTATICALLY COMPACTED PLAQUE, 60 % 15$\mu$ INDUCED PORE SIZE

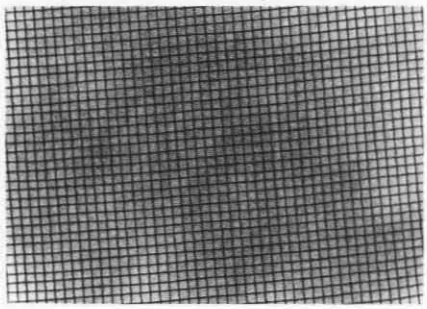

Raw Plaque Prepared
By Isostatic Compaction

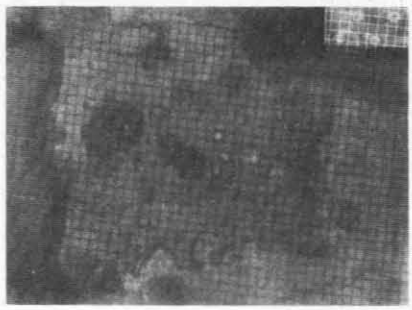

Unformed Electrode Prepared From An
Isostatically Compacted Plaque

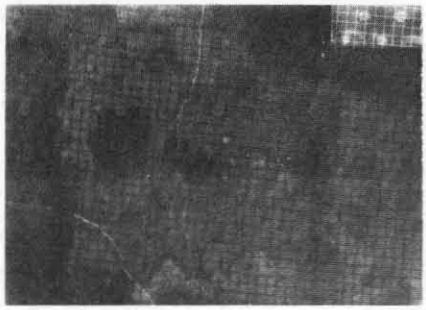

Cycled Electrode After 56 Cycles

FIGURE 26. ELECTRODE PREPARED FROM ISOSTATICALLY COMPACTED PLAQUE, 80 % 25$\mu$ INDUCED PORE SIZE

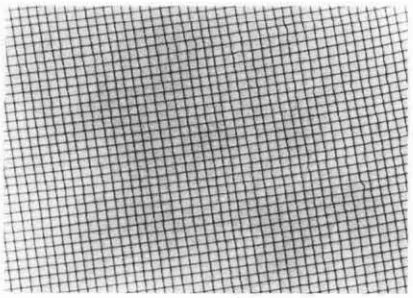

Raw Plaque Prepared
By Isostatic Compaction

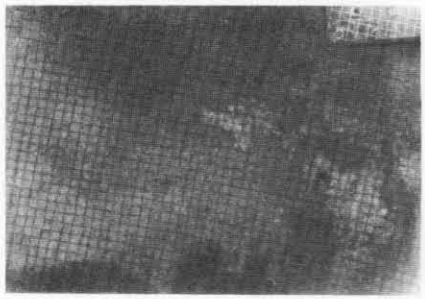

Unformed Electrode

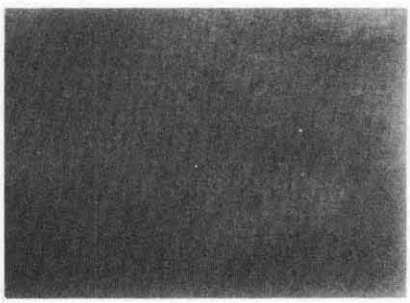

Formed Electrode

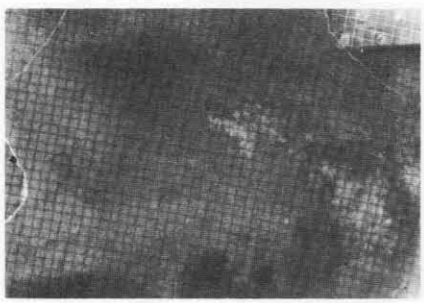

Cycled Electrode After 60 Cycles

FIGURE 27. ELECTRODE PREPARED FROM ISOSTATICALLY COMPACTED PLAQUE 60 % 25$\mu$ INDUCED PORE SIZE

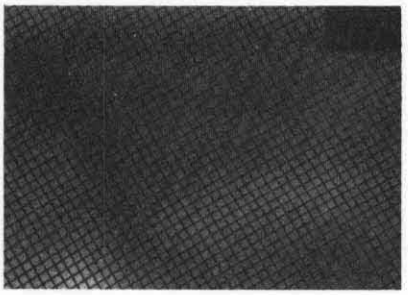

Raw Plaque Prepared
By Isostatic Compaction

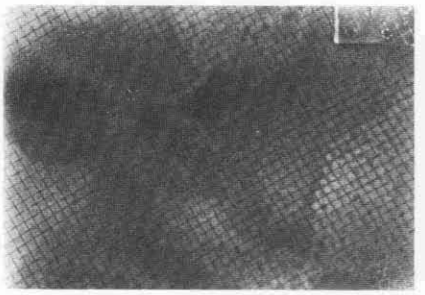

Unformed Electrode

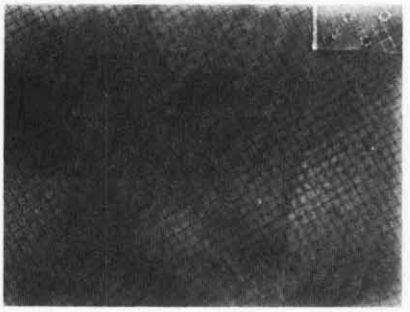

Formed Electrode

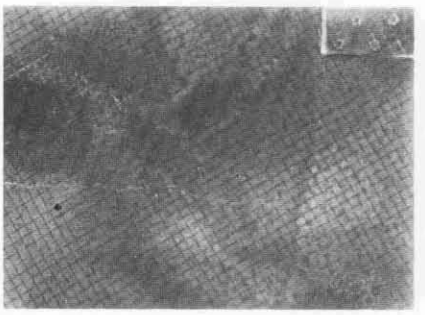

Cycled Electrode After 56 Cycles

FIGURE 28. ELECTRODE PREPARED FROM ISOSTATICALLY COMPACTED PLAQUE 80 % 25$\mu$ INDUCED PORE SIZE, BLENDED POWDER

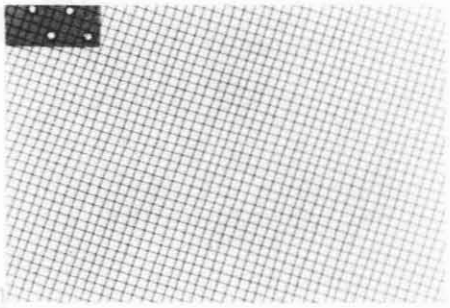

Raw Plaque Prepared
By Isostatic Compaction

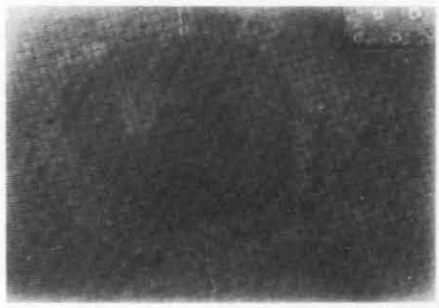

Unformed Electrode



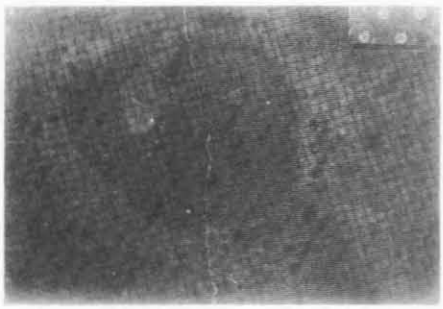

Cycled Electrode After 56 Cycles

FIGURE 29. ELECTRODE PREPARED FROM ISOSTATICALLY COMPACTED PLAQUE, 80 % 50$\mu$ INDUCED PORE SIZE

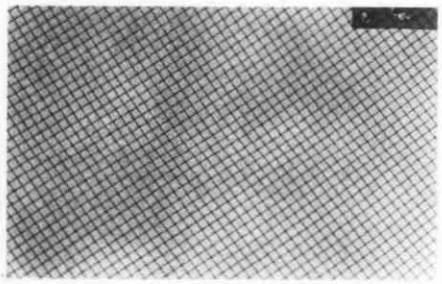

Raw Plaque Prepared
By Isostatic Compaction

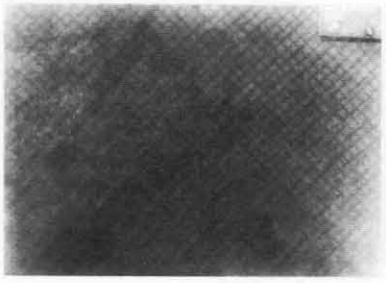

Unformed Electrode

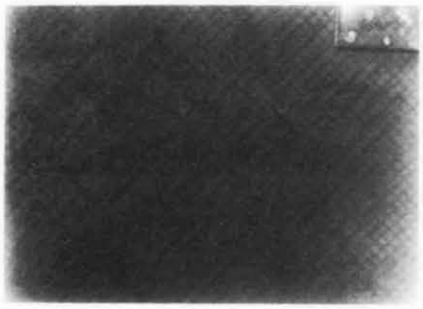

Cycled Electrode After 56 Cycles

FIGURE 30. ELECTRODE PREPARED FROM ISOSTATICALLY COMPACTED PLAQUE 60 % 50$\mu$ INDUCED PORE SIZE

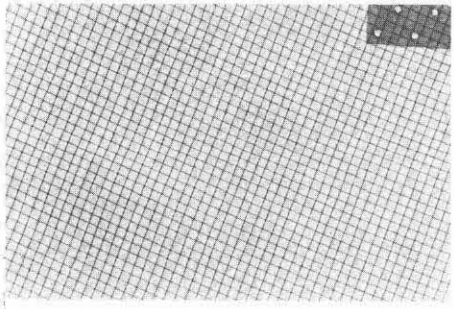

Raw Plaque Prepared
By Isostatic Compaction

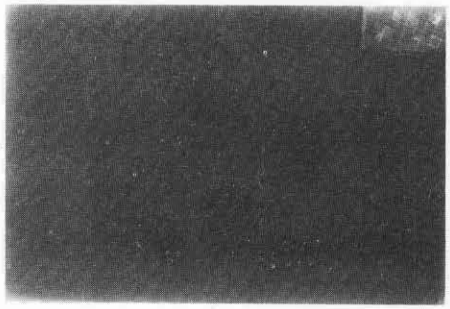

Unformed Electrode

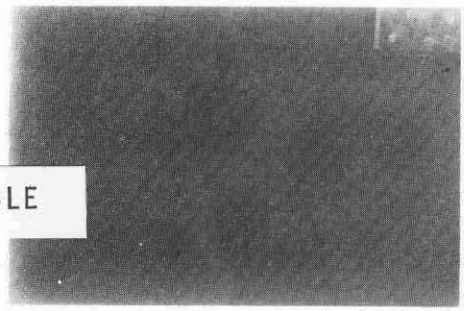

NOT REPRODUCIBLE

Cycled Electrode After 56 Cycles

**FIGURE 31. ELECTRODE PREPARED FROM ISOSTATICALLY COMPACTED PLAQUE, 80 % 90$\mu$ INDUCED PORE SIZE**

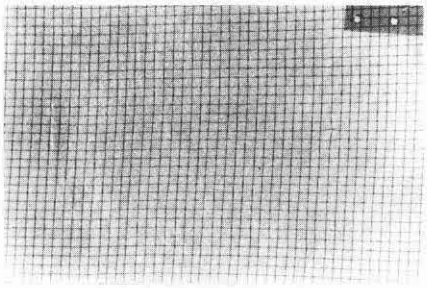

Raw Plaque Prepared
By Isostatic Compaction

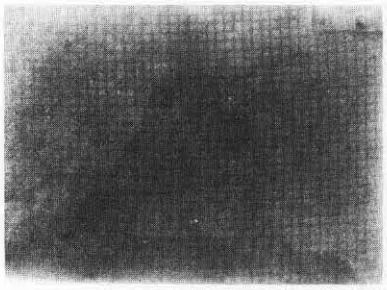

Unformed Electrode



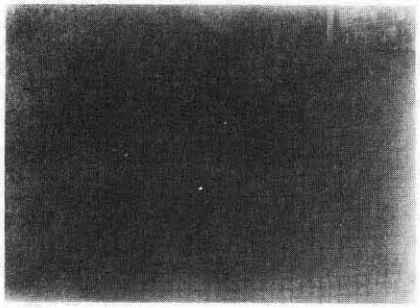

Cycled Electrode After 56 Cycles

FIGURE 32. ELECTRODE PREPARED FROM ISOSTATICALLY COMPACTED PLAQUE 60 % 90$\mu$ INDUCED PORE SIZE

## IV. CONCLUSIONS

An exploratory study of a technique for preparing improved cadmium electrode substrates with precisely controlled microstructures for possible use in aerospace nickel-cadmium cells has been completed. Cadmium electrodes were prepared having 60 % and 80 % porosities, each at 15, 25, and 90 $\mu$ induced pore size levels, and cycle tested using an accelerated regime. The results reveal several very good prospects for improved aerospace cadmium electrodes. These are:

1. Cadmium electrodes prepared from 60 % porosity 25 $\mu$ induced pore size plaques had efficiencies only 5-10 percentage points lower than state-of-the-art electrodes judging from the results of an accelerated test regime. These plaques had vastly superior mechanical properties, about 8000 psi as compared to 645 psi for the conventional gravity sintered material in use today. This added strength was observed to eliminate cracking and physical degradation of the electrodes during processing and cycling. The electrical performance of these electrodes was poorer than state-of-the-art electrodes.

   It is reasonable to assume that efficiencies of such electrodes may be raised without greatly sacrificing mechanical properties.

2. Cadmium electrodes prepared from 80 % porous 25 $\mu$ induced pore size plaques, under the tortuous test regime employed, proved to be the best electrodes made during the course of this program from the point of view of highest efficiency. They were superior to state-of-the-art electrodes in this respect, in addition to having somewhat superior mechanical strengths and better uniformity.

3. Of a more developmental type of interest that may be refined to yield practical results, it was observed that:

   - The plaque pore size and porosity were found to be contributing factors to $Cd(OH)_2$ crystal size, reportedly an important property governing the performance and life of cadmium electrodes. No relation between crystal size and efficiency was found.
   - The induced porosity was observed to be a factor in electrode performance. Higher induced porosity apparently yielded better electrodes. This property was confounded with loading, however.
   - The best performance at both the 60 % and 80 % porosities were observed with the 25 $\mu$ induced sizes. The higher induced pore sizes, the 50 and 90 $\mu$, were more uniform as shown in X-ray radiographs.
   - Morphological changes of $Cd(OH)_2$, determined from SEM photomicrographs, were identified after the cycling procedure. With the 60 % structures the crystals apparently decreased in size with cycling, while with the 80 % porosity structures the crystals increased in size.

- Active material loading uniformity on the bulk scale was measured in the X-ray radiographs. There were no observable bulk changes in uniformity with cycling.
- Some small degree of corrosion of the plaques was evident from photomicrographs. The corrosion was due either to processing or cycling.
- Plaques were thoroughly characterized with the use of the SEM. Induced pore-sizes were evaluated, interstitial pores described and various fine structures, pits and scars, identified.
- BET surface areas were measured and varied between 0.11 and 0.17 $m^2/gm$ depending upon plaque pore size and porosity.
- Three-point bend tests were performed on selected specimens and varied between about 900 and 8000 psi between porosities of 80 % and 60 %. As a point of comparison, a 79 % gravity sintered material had a bend strength of 643 psi.

## V. RECOMMENDATIONS FOR FUTURE WORK

An initial study of improved plaque materials prepared via a powder metallurgical technique allowing control over porosity and pore size has yielded cadmium electrodes that are better than state-of-the-art electrodes, in terms of efficiency and mechanical strength. There are a number of areas that are worthy of exploration that are likely to yield still further improved cadmium electrodes with respect to reproducibility, uniformity, and long life.

1. Optimize performance of high strength substrates; e.g., 60 % porous, to the level of the 80 % structures. This should involve improved processing steps. Increased induced porosities should help also.
2. Better active material loading technique to attain more uniform, more efficient active material loading.
3. Evaluate selected optimized substrate more thoroughly; i.e., much longer cycle life testing in practical cells over a wider range of test conditions.
4. Determine effect of pore size on oxygen recombinations in practical cells.
5. Further develop techniques for mold filling and powder handling and classification techniques to improve reproducibility and uniformity of the plaque.

## REFERENCES


1. A.M. Heuninckx, "Process for Making Sintered Type Cadmium Electrodes", U.S. Patent 2,952,570 (1960).

2. C.J. Menard and E. Luksha, "Nickel Plaque Substrate for Cadmium Electrodes for Aerospace Nickel-Cadmium Cells", Southern California-Nevada Section of ECS, Los Angeles, California, 4 December 1970.


## BIBLIOGRAPHY


Bates, L.M., "Some Physical Factors Affecting Radiographic Image Quality: Their Theoretical Basis and Measurement", Public Health Service Publication No. 999-RH-38, August 1969.

Brunauer, S., Emmett, P.H., and Teller, E., *J. Am. Chem. Soc.,* **60**, 309 (1938).

Hughel, T.J., et al., "The Scanning Electron Microscope As A Tool for Battery Plate Research", Power Sources 1970, Preprint Paper 3.

"Industrial Radiography", Published by Agfa-Gevaert Inc., Teterboro, New Jersey.

McClellan, A.L., and Harnsberger, H.F., *J. Colloid and Interface Science,* **23**, 577 (1967).

Parry, J.M., "Development of Uniform and Predictable Battery Materials for Nickel-Cadmium Aerospace Cells", NASA Report, NAS5-11561 (1969).

Schwarzhopf, P., and Pearson, D.A., "Fabrication of Polyporosity Microstructures", U.S. Patent 3,362,818 (1968).

Sherfey, J., "Metal Structures With Parallel Pores of Uniform Size", NASA TN D-6259, April 1971.

Ibid, NASA Preprint X-735-70-307, July 1970.

U.S. Patent 2,672,415, 16 March 1954.

# APPENDIX A

## SUMMARY OF MECHANICAL STRENGTH DATA

Table 4 Results of a Least Squares Fit on Mechanical Strength Data

| Actual Powder Porosity | Measured Mechanical Strength | Calculated Mechanical Strength | Percent Difference | Induced Pore-Size |
|---|---|---|---|---|
| 56.77 % | 9014 psi | 8197 psi | - 9.0 | 25μ |
| 58.21 | 8803 | 7802 | -11.3 | 15μ |
| 58.46 | 8225 | 7734 | - 5.9 | 15μ |
| 59.68 | 7747 | 7401 | - 4.4 | 15μ |
| 63.68 | 5368 | 6310 | +17.5 | 90μ |
| 64.00 | 6267 | 6222 | - 0.7 | 50μ |
| 64.94 | 5488 | 5965 | + 8.7 | 90μ |
| 65.01 | 5995 | 5946 | - 0.8 | 25μ |
| 65.55 | 5080 | 5799 | +14.1 | 25μ |
| 66.26 | 5578 | 5606 | + 0.4 | 25μ |
| 66.34 | 5636 | 5584 | - 0.9 | 90μ |
| 66.53 | 6080 | 5531 | - 9.0 | 50μ |
| 67.23 | 4257 | 5340 | +25.4 | 15μ |
| 67.42 | 4763 | 5289 | +11.0 | 15μ |
| 68.46 | 4375 | 5002 | +14.3 | 15μ |
| 81.88 | 1265 | 1340 | + 5.9 | 90μ |
| 82.50 | 917 | 1172 | +27.7 | 25μ |
| 82.64 | 1100 | 1134 | + 3.0 | 25μ |
| 82.82 | 946 | 1085 | +14.7 | 25μ |
| 82.86 | 1048 | 1075 | + 2.5 | 25μ |
| 82.89 | 841 | 1066 | +26.7 | 25μ |
| 83.96 | 1044 | 773 | -25.9 | 90μ |
| 84.00 | 828 | 763 | - 7.8 | 90μ |
| 84.77 | 788 | 551 | -30.1 | 50μ |
| 84.93 | 750 | 508 | -32.2 | 25μ |
| 84.97 | 800 | 498 | -37.7 | 50μ |
| 84.98 | 550 | 495 | - 9.9 | 50μ |
| 85.11 | 776 | 459 | -40.7 | 25μ |
| 85.11 | 411 | 459 | +11.6 | 25μ |
| 85.41 | 747 | 377 | -49.5 | 15μ |

# APPENDIX B

## SUMMARY OF CYCLE TEST DATA FOR "STATE-OF-THE-ART" ELECTRODES

TABLE 5

SUMMARY OF CYCLE TEST DATA FOR "STATE-OF-THE-ART" ELECTRODES

| "STATE OF THE ART" Gould Standard Process | | | | "STATE OF THE ART" Precipitation Process | | | |
|---|---|---|---|---|---|---|---|
| Cycle Number | Average Capacity | Average Efficiency | 95% Confidence Limit for Efficiency | Cycle Number | Average Capacity | Average Efficiency | 95% Confidence Limit for Efficiency |
| 1 | 1.1218 | 56.688 | ±2.082 | 1 | 1.1124 | 60.638 | ±5.462 |
| 2 | 1.1406 | 57.638 | ±2.208 | 2 | 1.1006 | 59.975 | ±5.425 |
| 3 | 1.1613 | 58.675 | ±2.771 | 3 | 1.0301 | 56.138 | ±5.545 |
| 4 | 0.8616 | 43.525 | ±3.519 | 4 | 0.7269 | 39.513 | ±9.339 |
| 5 | 0.6610 | 33.375 | ±4.405 | 5 | 0.5184 | 28.150 | ±10.432 |
| 6 | 0.3035 | 15.263 | ±5.030 | 6 | 0.2634 | 14.357 | ±5.196 |
| 7 | 0.7494 | 37.851 | ±3.187 | 7 | 0.6222 | 38.300 | ±3.141 |
| 8 | 0.7733 | 39.046 | ±3.442 | 8 | 0.6388 | 38.579 | ±2.952 |
| 9 | 0.7629 | 38.514 | ±3.608 | 9 | 0.6386 | 38.804 | ±2.908 |
| 10 | 0.7397 | 37.344 | ±3.617 | 10 | 0.6276 | 38.257 | ±3.307 |
| 11 | 0.7547 | 38.109 | ±3.023 | 11 | 0.6201 | 38.170 | ±3.439 |
| 12 | 0.7434 | 37.538 | ±3.315 | 12 | 0.6147 | 37.678 | ±3.765 |
| 13 | 0.7235 | 36.529 | ±3.293 | 13 | 0.6060 | 37.278 | ±3.869 |
| 14 | 0.7153 | 36.109 | ±3.467 | 14 | 0.5951 | 36.883 | ±4.034 |
| 15 | 0.7046 | 35.567 | ±3.445 | 15 | 0.5972 | 36.816 | ±4.202 |
| 16 | 0.6932 | 35.000 | ±3.288 | 16 | 0.5832 | 36.032 | ±4.236 |
| 17 | 0.6780 | 34.219 | ±3.504 | 17 | 0.5675 | 35.691 | ±4.373 |
| 18 | 0.6646 | 33.546 | ±3.452 | 18 | 0.5519 | 35.142 | ±4.114 |
| 19 | 0.6466 | 32.635 | ±3.183 | 19 | 0.6044 | 37.228 | ±4.149 |
| 20 | 0.7093 | 35.841 | ±2.555 | 20 | 0.5985 | 36.787 | ±4.255 |
| 21 | 0.6967 | 35.203 | ±2.365 | 21 | 0.6422 | 39.757 | ±4.196 |
| 22 | 0.6974 | 35.239 | ±1.952 | 22 | 0.5951 | 36.692 | ±4.157 |
| 23 | 0.6896 | 34.829 | ±1.957 | 23 | 0.6479 | 39.057 | ±4.097 |
| 24 | 0.7039 | 35.558 | ±1.902 | 24 | 0.5963 | 36.609 | ±4.534 |
| 25 | 0.6966 | 35.189 | ±2.291 | 25 | 0.5799 | 35.760 | ±4.352 |
| 26 | 0.6941 | 35.063 | ±2.357 | 26 | 0.5560 | 34.715 | ±4.343 |
| 27 | 0.6818 | 34.437 | ±2.234 | 27 | 0.5456 | 34.016 | ±4.458 |
| 28 | 0.6714 | 33.915 | ±2.245 | 28 | 0.5262 | 32.997 | ±4.420 |
| 29 | 0.6650 | 33.585 | ±2.255 | 29 | 0.5310 | 33.627 | ±4.633 |
| 30 | 0.6535 | 32.999 | ±2.411 | 30 | 0.5209 | 33.019 | ±4.670 |
| 31 | 0.6381 | 32.222 | ±2.380 | 31 | 0.5162 | 32.727 | ±3.735 |
| 32 | 0.6255 | 31.589 | ±2.403 | 32 | 0.5026 | 31.755 | ±4.653 |
| 33 | 0.6161 | 31.111 | ±2.545 | 33 | 0.5476 | 34.607 | ±3.984 |
| 34 | 0.6058 | 30.589 | ±2.505 | 34 | 0.5583 | 34.929 | ±4.129 |
| 35 | 0.6784 | 34.278 | ±2.015 | 35 | 0.5640 | 35.092 | ±4.028 |
| 36 | 0.6714 | 33.924 | ±1.926 | 36 | 0.5586 | 34.683 | ±4.041 |
| 37 | 0.6781 | 34.271 | ±1.814 | 37 | 0.5783 | 36.346 | ±5.560 |
| 38 | 0.6839 | 34.567 | ±1.497 | 38 | 0.5605 | 34.808 | ±4.080 |
| 39 | 0.6910 | 34.928 | ±1.106 | 39 | 0.5511 | 34.363 | ±4.087 |
| 40 | 0.6801 | 34.365 | ±1.416 | 40 | 0.5441 | 33.910 | ±4.134 |
| 41 | 0.6678 | 33.742 | ±1.731 | 41 | 0.5334 | 33.401 | ±4.076 |
| 42 | 0.6567 | 33.180 | ±1.434 | 42 | 0.5256 | 32.937 | ±4.298 |
| 43 | 0.6439 | 32.534 | ±1.729 | 43 | 0.5165 | 32.436 | ±4.401 |
| 44 | 0.6333 | 31.994 | ±1.834 | 44 | 0.5004 | 31.870 | ±4.387 |
| 45 | 0.6321 | 31.930 | ±1.915 | 45 | 0.4936 | 31.304 | ±4.383 |
| 46 | 0.6170 | 31.170 | ±1.730 | 46 | 0.4854 | 31.045 | ±4.438 |
| 47 | 0.6089 | 30.759 | ±1.839 | 47 | | Recorder Failure | |
| 48 | 0.6404 | 32.368 | ±2.044 | 48 | 0.4567 | 29.430 | ±4.642 |
| 49 | 0.6348 | 32.086 | ±2.128 | 49 | 0.4424 | 28.724 | ±4.574 |
| 50 | 0.6609 | 33.428 | ±1.505 | 50 | 0.4265 | 28.141 | ±4.786 |
| 51 | 0.6594 | 33.351 | ±1.590 | 51 | 0.4221 | 27.786 | ±5.018 |
| 52 | 0.6641 | 33.591 | ±1.541 | 52 | 0.4090 | 27.131 | ±5.072 |
| 53 | 0.6669 | 33.731 | ±1.448 | 53 | 0.3911 | 26.135 | ±5.138 |
| 54 | 0.6658 | 33.679 | ±1.477 | 54 | 0.3856 | 25.817 | ±5.338 |
| 55 | 0.6597 | 33.375 | ±1.396 | 55 | 0.3731 | 25.085 | ±5.802 |
| 56 | 0.6522 | 32.994 | ±1.494 | 56 | 0.3636 | 24.650 | ±5.889 |

# APPENDIX C

## SUMMARY OF CYCLE TEST DATA FOR ELECTRODES PREPARED FROM ISOSTATICALLY COMPACTED PLAQUES

TABLE 6

SUMMARY OF CYCLE TEST DATA FOR ELECTRODES PREPARED FROM ISOSTATICALLY COMPACTED PLAQUES

| 60% Porosity 15μ Induced Pore-Size | | | | 80% Porosity 15μ Induced Pore-Size | | | |
|---|---|---|---|---|---|---|---|
| Cycle Number | Average Capacity | Average Efficiency | 95% Confidence Limit for Efficiency | Cycle Number | Average Capacity | Average Efficiency | 95% Confidence Limit for Efficiency |
| 1 | 0.7404 | 39.625 | ±2.523 | 1 | 0.8466 | 57.825 | ±2.814 |
| 2 | 0.7501 | 40.113 | ±2.088 | 2 | 0.7648 | 52.150 | ±2.654 |
| 3 | 0.7696 | 41.100 | ±2.414 | 3 | 0.8265 | 56.350 | ±2.795 |
| 4 | 0.4844 | 25.850 | ±2.677 | 4 | 0.6268 | 42.713 | ±2.260 |
| 5 | 0.3211 | 17.125 | ±3.528 | 5 | 0.4635 | 31.575 | ±2.113 |
| 6 | 0.1373 | 7.313 | ±3.734 | 6 | 0.3478 | 23.663 | ±3.101 |
| 7 | 0.4053 | 21.592 | ±2.168 | 7 | 0.5416 | 36.922 | ±1.617 |
| 8 | 0.4102 | 21.849 | ±2.188 | 8 | 0.5523 | 37.640 | ±1.906 |
| 9 | 0.3762 | 21.901 | ±2.282 | 9 | 0.5634 | 38.411 | ±1.743 |
| 10 | 0.4009 | 21.338 | ±2.482 | 10 | 0.5704 | 38.875 | ±2.040 |
| 11 | 0.4270 | 22.754 | ±2.235 | 11 | 0.5666 | 38.611 | ±2.201 |
| 12 | 0.4182 | 22.284 | ±2.367 | 12 | | Recorder Failure | |
| 13 | 0.4064 | 21.648 | ±2.435 | 13 | | " | |
| 14 | 0.3996 | 21.278 | ±2.398 | 14 | | " | |
| 15 | 0.3915 | 20.834 | ±2.544 | 15 | | " | |
| 16 | 0.3801 | 20.216 | ±2.715 | 16 | | " | |
| 17 | 0.3730 | 19.836 | ±2.677 | 17 | | " | |
| 18 | 0.3621 | 19.253 | ±2.812 | 18 | 0.5659 | 38.557 | ±2.571 |
| 19 | 0.3062 | 18.226 | ±2.662 | 19 | 0.5602 | 38.171 | ±2.602 |
| 20 | 0.3343 | 17.773 | ±2.715 | 20 | 0.5583 | 38.036 | ±2.692 |
| 21 | 0.3324 | 17.728 | ±3.117 | 21 | 0.5573 | 37.920 | ±2.779 |
| 22 | 0.4709 | 22.702 | ±2.330 | 22 | 0.5584 | 38.047 | ±2.896 |
| 23 | 0.4209 | 22.432 | ±2.248 | 23 | 0.5634 | 38.382 | ±2.896 |
| 24 | 0.4192 | 22.347 | ±2.285 | 24 | 0.5587 | 38.068 | ±2.805 |
| 25 | 0.4105 | 21.860 | ±2.192 | 25 | 0.5581 | 38.019 | ±2.915 |
| 26 | 0.4017 | 21.389 | ±2.347 | 26 | 0.5545 | 37.776 | ±3.036 |
| 27 | 0.4151 | 22.130 | ±2.202 | 27 | 0.5444 | 37.082 | ±3.166 |
| 28 | 0.4054 | 21.605 | ±2.028 | 28 | 0.5418 | 36.904 | ±3.295 |
| 29 | 0.4065 | 21.656 | ±2.206 | 29 | 0.5391 | 36.709 | ±3.509 |
| 30 | 0.3936 | 20.964 | ±2.078 | 30 | 0.5249 | 35.736 | ±3.619 |
| 31 | 0.3897 | 20.743 | ±2.136 | 31 | 0.5263 | 35.836 | ±3.735 |
| 32 | 0.3665 | 19.505 | ±2.317 | 32 | 0.5505 | 37.481 | ±3.381 |
| 33 | 0.3573 | 19.010 | ±2.243 | 33 | 0.5516 | 37.561 | ±3.105 |
| 34 | 0.3495 | 18.583 | ±2.337 | 34 | 0.5654 | 38.512 | ±3.231 |
| 35 | 0.3320 | 17.649 | ±2.370 | 35 | 0.5598 | 38.140 | ±2.914 |
| 36 | 0.3251 | 17.294 | ±2.149 | 36 | 0.5568 | 37.931 | ±3.024 |
| 37 | 0.3045 | 16.191 | ±2.155 | 37 | 0.5551 | 37.819 | ±2.840 |
| 38 | 0.3964 | 21.123 | ±2.009 | 38 | 0.5532 | 37.687 | ±3.002 |
| 39 | 0.3947 | 21.032 | ±1.873 | 39 | 0.5446 | 37.101 | ±3.166 |
| 40 | 0.3955 | 21.058 | ±2.181 | 40 | 0.5418 | 36.907 | ±3.204 |
| 41 | 0.4037 | 21.509 | ±1.954 | 41 | 0.5361 | 36.510 | ±3.325 |
| 42 | 0.4051 | 21.590 | ±1.975 | 42 | 0.5304 | 36.117 | ±3.498 |
| 43 | 0.3959 | 21.098 | ±1.989 | 43 | 0.5246 | 35.725 | ±3.767 |
| 44 | 0.3887 | 20.708 | ±1.945 | 44 | 0.5113 | 34.819 | ±3.728 |
| 45 | 0.3839 | 20.453 | ±2.035 | 45 | 0.5064 | 34.470 | ±3.901 |
| 46 | 0.3650 | 19.430 | ±1.859 | 46 | 0.5024 | 34.198 | ±3.901 |
| 47 | 0.3583 | 19.074 | ±1.928 | 47 | 0.4833 | 32.908 | ±4.024 |
| 48 | 0.3389 | 18.031 | ±1.983 | 48 | 0.4693 | 31.949 | ±4.065 |
| 49 | 0.3374 | 17.950 | ±2.040 | 49 | 0.4610 | 31.386 | ±3.992 |
| 50 | 0.3219 | 17.119 | ±2.056 | 50 | 0.4491 | 30.580 | ±4.010 |
| 51 | 0.3038 | 16.181 | ±2.136 | 51 | 0.4110 | 27.955 | ±4.674 |
| 52 | 0.2964 | 15.758 | ±1.956 | 52 | 0.4332 | 29.476 | ±4.376 |
| 53 | 0.2892 | 15.359 | ±2.074 | 53 | 0.4242 | 28.871 | ±4.476 |
| 54 | 0.3720 | 19.808 | ±1.964 | 54 | 0.5183 | 35.284 | ±3.513 |
| 55 | 0.3786 | 20.174 | ±1.952 | 55 | 0.5205 | 35.439 | ±3.498 |
| 56 | 0.3704 | 19.718 | ±1.991 | 56 | 0.5121 | 34.872 | ±3.599 |

TABLE 7

SUMMARY OF CYCLE TEST DATA FOR ELECTRODES PREPARED FROM ISOSTATICALLY COMPACTED PLAQUES

| | 60% POROSITY 25μ INDUCED PORE SIZE | | | | 80% POROSITY 25μ INDUCED PORE SIZE | | |
|---|---|---|---|---|---|---|---|
| Cycle No. | Average Capacity | Average Efficiency | 95% Confidence Limit for Efficiency | Cycle No. | Average Capacity | Average Efficiency | 95% Confidence Limit for Efficiency |
| 1 | 0.7574 | 38.813 | ±2.552 | 1 | 0.9501 | 54.238 | ±2.529 |
| 2 | 0.7924 | 40.988 | ±2.253 | 2 | 1.1013 | 56.463 | ±2.532 |
| 3 | 0.8191 | 42.313 | ±1.983 | 3 | 1.0615 | 38.988 | ±5.175 |
| 4 | 0.5833 | 30.757 | ±1.631 | 4 | 0.7640 | 27.488 | ±6.445 |
| 5 | 0.3904 | 20.425 | ±3.984 | 5 | 0.5445 | 16.600 | ±5.203 |
| 6 | 0.1528 | 8.138 | ±3.336 | 6 | 0.3271 | 8.138 | ±3.336 |
| 7 | 0.5528 | 28.472 | ±2.038 | 7 | 0.7388 | 41.073 | ±4.874 |
| 8 | 0.4866 | 24.662 | ±1.781 | 8 | 0.6943 | 38.546 | ±10.264 |
| 9 | 0.6232 | 32.278 | ±2.185 | 9 | 0.7414 | 41.495 | ±4.954 |
| 10 | 0.6252 | 32.239 | ±2.033 | 10 | 0.7380 | 41.369 | ±4.605 |
| 11 | 0.6352 | 32.469 | ±1.965 | 11 | 0.7301 | 40.996 | ±4.867 |
| 12 | 0.6118 | 31.549 | ±2.066 | 12 | 0.7257 | 40.729 | ±4.996 |
| 13 | 0.6110 | 31.501 | ±2.132 | 13 | 0.7145 | 40.126 | ±4.990 |
| 14 | 0.6046 | 31.450 | ±2.139 | 14 | 0.7062 | 39.800 | ±5.216 |
| 15 | 0.6033 | 31.093 | ±2.209 | 15 | 0.7290 | 40.484 | ±5.242 |
| 16 | 0.6004 | 30.942 | ±2.293 | 16 | 0.7302 | 40.830 | ±4.030 |
| 17 | 0.5980 | 30.819 | ±2.267 | 17 | 0.7219 | 40.254 | ±4.002 |
| 18 | 0.5913 | 30.464 | ±2.392 | 18 | 0.7257 | 40.269 | ±3.599 |
| 19 | 0.5681 | 30.198 | ±2.617 | 19 | 0.7260 | 40.517 | ±3.402 |
| 20 | 0.5877 | 30.330 | ±2.109 | 20 | 0.7141 | 40.007 | ±3.486 |
| 21 | 0.5775 | 29.801 | ±2.063 | 21 | 0.7075 | 39.684 | ±3.275 |
| 22 | 0.5726 | 29.812 | ±2.141 | 22 | 0.7025 | 39.297 | ±3.332 |
| 23 | 0.5639 | 29.156 | ±2.190 | 23 | 0.6902 | 38.830 | ±3.480 |
| 24 | 0.5662 | 29.250 | ±2.121 | 24 | 0.6811 | 38.376 | ±3.597 |
| 25 | 0.5545 | 28.640 | ±2.139 | 25 | 0.6746 | 38.119 | ±3.675 |
| 26 | 0.5625 | 28.982 | ±1.931 | 26 | 0.7018 | 38.829 | ±4.109 |
| 27 | 0.5421 | 28.370 | ±2.049 | 27 | 0.7113 | 39.549 | ±3.060 |
| 28 | 0.5591 | 28.816 | ±1.990 | 28 | 0.7185 | 39.735 | ±2.714 |
| 29 | 0.5493 | 28.329 | ±2.131 | 29 | 0.7127 | 39.579 | ±2.729 |
| 30 | 0.5432 | 28.195 | ±2.094 | 30 | 0.7146 | 39.468 | ±2.894 |
| 31 | 0.5464 | 28.177 | ±2.193 | 31 | 0.7096 | 39.382 | ±2.734 |
| 32 | 0.5320 | 27.426 | ±2.206 | 32 | 0.7002 | 39.038 | ±2.739 |
| 33 | 0.5266 | 27.160 | ±2.229 | 33 | 0.6964 | 38.821 | ±2.815 |
| 34 | 0.5294 | 27.381 | ±2.183 | 34 | 0.6915 | 38.583 | ±3.055 |
| 35 | 0.5121 | 26.758 | ±2.511 | 35 | 0.6788 | 37.953 | ±3.054 |
| 36 | | Recorder Failure | | 36 | 0.6641 | 37.163 | ±3.091 |
| 37 | 0.4232 | 26.706 | ±2.287 | 37 | 0.6503 | 36.481 | ±3.166 |
| 38 | | Recorder Failure | | 38 | 0.7017 | 38.761 | ±2.613 |
| 39 | | Recorder Failure | | 39 | 0.6907 | 38.520 | ±2.872 |
| 40 | 0.5060 | 26.126 | ±2.080 | 40 | 0.7025 | 38.789 | ±3.044 |
| 41 | 0.4056 | 25.610 | ±2.019 | 41 | 0.6982 | 28.687 | ±3.115 |
| 42 | 0.4997 | 25.815 | ±1.910 | 42 | 0.7031 | 38.754 | ±3.063 |
| 43 | 0.4766 | 25.375 | ±2.089 | 43 | 0.6903 | 38.256 | ±2.899 |
| 44 | 0.4793 | 25.070 | ±2.014 | 44 | 0.6823 | 37.933 | ±3.031 |
| 45 | 0.4900 | 25.286 | ±1.806 | 45 | 0.6759 | 37.492 | ±3.100 |
| 46 | 0.4851 | 24.646 | ±1.694 | 46 | 0.6617 | 36.798 | ±3.327 |
| 47 | 0.4763 | 24.887 | ±2.331 | 47 | 0.6565 | 36.592 | ±3.384 |
| 48 | 0.4718 | 24.311 | ±2.326 | 48 | 0.6408 | 35.747 | ±3.561 |
| 49 | 0.4660 | 24.028 | ±2.156 | 49 | 0.6402 | 35.745 | ±3.676 |
| 50 | 0.4586 | 23.638 | ±2.469 | 50 | 0.6827 | 37.661 | ±3.194 |
| 51 | 0.4504 | 23.307 | ±2.634 | 51 | 0.6780 | 37.544 | ±3.044 |
| 52 | 0.4498 | 23.177 | ±2.725 | 52 | 0.6896 | 37.940 | ±3.400 |
| 53 | 0.4308 | 22.190 | ±2.800 | 53 | 0.6745 | 37.274 | ±3.242 |
| 54 | 0.4322 | 22.196 | ±2.826 | 54 | 0.6776 | 37.229 | ±3.183 |
| 55 | 0.4530 | 23.424 | ±2.291 | 55 | 0.6684 | 36.961 | ±3.133 |
| 56 | 0.4507 | 23.280 | ±2.136 | 56 | 0.6518 | 36.264 | ±2.901 |

TABLE 8

SUMMARY OF CYCLE TEST DATA FOR ELECTRODES PREPARED FROM ISOSTATICALLY COMPACTED PLAQUES

80% Porosity

25μ Induced Pore-Size
(Blended Powders)

| Cycle Number | Average Capacity | Average Efficiency | 95% Confidence Limit for Efficiency |
|---|---|---|---|
| 1 | | Recorder Failure | |
| 2 | 0.9163 | 55.721 | ±1.903 |
| 3 | 0.9174 | 55.750 | ±1.846 |
| 4 | 0.7130 | 43.338 | ±2.201 |
| 5 | 0.5336 | 32.375 | ±3.249 |
| 6 | 0.2764 | 16.825 | ±4.838 |
| 7 | 0.6522 | 40.078 | ±3.731 |
| 8 | 0.6716 | 41.275 | ±3.864 |
| 9 | 0.6627 | 41.308 | ±4.527 |
| 10 | 0.6607 | 41.324 | ±4.288 |
| 11 | 0.6472 | 40.719 | ±4.540 |
| 12 | 0.6466 | 40.304 | ±4.458 |
| 13 | 0.6422 | 40.030 | ±4.387 |
| 14 | 0.6207 | 39.761 | ±4.325 |
| 15 | 0.6352 | 39.601 | ±4.225 |
| 16 | 0.6270 | 39.092 | ±4.088 |
| 17 | 0.6255 | 39.000 | ±3.982 |
| 18 | 0.6031 | 37.932 | ±4.551 |
| 19 | 0.6295 | 38.868 | ±4.067 |
| 20 | 0.6373 | 39.146 | ±3.652 |
| 21 | 0.6630 | 39.203 | ±3.614 |
| 22 | 0.6312 | 38.773 | ±3.576 |
| 23 | 0.6329 | 38.883 | ±3.454 |
| 24 | 0.6293 | 38.667 | ±3.418 |
| 25 | 0.6230 | 38.287 | ±3.249 |
| 26 | 0.6152 | 37.801 | ±3.371 |
| 27 | 0.6196 | 38.078 | ±3.218 |
| 28 | 0.6125 | 37.643 | ±3.192 |
| 29 | 0.6052 | 37.197 | ±3.037 |
| 30 | 0.6048 | 37.184 | ±2.918 |
| 31 | 0.5987 | 36.802 | ±2.946 |
| 32 | 0.5957 | 36.627 | ±2.835 |
| 33 | 0.5919 | 36.396 | ±2.767 |
| 34 | 0.5857 | 36.022 | ±2.719 |
| 35 | 0.5896 | 36.262 | ±2.633 |
| 36 | 0.5816 | 35.769 | ±2.620 |
| 37 | 0.5836 | 35.895 | ±2.525 |
| 38 | 0.5827 | 35.845 | ±2.473 |
| 39 | 0.5844 | 35.957 | ±2.385 |
| 40 | 0.5802 | 35.698 | ±2.419 |
| 41 | 0.5775 | 35.536 | ±2.336 |
| 42 | 0.5763 | 35.467 | ±2.198 |
| 43 | 0.5706 | 35.123 | ±2.105 |
| 44 | 0.5719 | 35.201 | ±2.145 |
| 45 | 0.5701 | 35.084 | ±2.181 |
| 46 | 0.5727 | 35.253 | ±2.115 |
| 47 | 0.5723 | 35.229 | ±2.159 |
| 48 | 0.5693 | 35.046 | ±2.074 |
| 49 | 0.5661 | 34.850 | ±2.045 |
| 50 | 0.5643 | 34.739 | ±2.043 |
| 51 | 0.5614 | 34.557 | ±2.100 |
| 52 | 0.5638 | 34.713 | ±1.997 |
| 53 | 0.5688 | 35.015 | ±2.065 |
| 54 | 0.5715 | 35.183 | ±2.074 |
| 55 | 0.5670 | 34.905 | ±2.079 |
| 56 | 0.5658 | 34.836 | ±2.053 |

TABLE 9

SUMMARY OF CYCLE TEST DATA FOR ELECTRODES PREPARED FROM ISOSTATICALLY COMPACTED PLAQUES

| 60% Porosity 50μ Induced Pore-Size | | | | 80% Porosity 50μ Induced Pore-Size | | | |
|---|---|---|---|---|---|---|---|
| Cycle Number | Average Capacity | Average Efficiency | 95% Confidence Limit for Efficiency | Cycle Number | Average Capacity | Average Efficiency | 95% Confidence Limit for Efficiency |
| 1 | 0.7916 | 40.636 | ±2.037 | 1 | 0.9870 | 45.572 | ±2.269 |
| 2 | 0.7970 | 40.928 | ±1.325 | 2 | 0.9556 | 44.146 | ±3.194 |
| 3 | 0.7922 | 40.688 | ±1.143 | 3 | 0.9012 | 41.600 | ±2.493 |
| 4 | 0.3908 | 19.924 | ±5.091 | 4 | 0.7556 | 34.886 | ±1.386 |
| 5 | 0.1878 | 9.538 | ±4.455 | 5 | 0.5606 | 25.876 | ±1.992 |
| 6 | 0.0886 | 4.500 | ±2.427 | 6 | 0.0466 | 2.156 | ±0.533 |
| 7 | 0.3886 | 19.869 | ±3.883 | 7 | 0.6486 | 29.944 | ±2.094 |
| 8 | 0.3891 | 19.894 | ±3.563 | 8 | 0.6788 | 31.341 | ±2.016 |
| 9 | 0.4130 | 21.138 | ±3.570 | 9 | 0.6794 | 31.374 | ±1.569 |
| 10 | 0.4161 | 21.281 | ±3.724 | 10 | 0.6897 | 31.849 | ±1.483 |
| 11 | 0.4022 | 20.562 | ±4.374 | 11 | 0.6968 | 32.181 | ±1.461 |
| 12 | 0.3904 | 19.954 | ±4.845 | 12 | 0.7006 | 32.355 | ±1.497 |
| 13 | 0.4276 | 21.861 | ±3.956 | 13 | 0.7115 | 32.858 | ±1.547 |
| 14 | 0.4075 | 20.843 | ±3.719 | 14 | 0.7249 | 33.472 | ±2.057 |
| 15 | 0.4216 | 21.569 | ±3.624 | 15 | 0.7295 | 33.682 | ±2.197 |
| 16 | 0.3930 | 20.089 | ±4.988 | 16 | 0.7334 | 33.862 | ±2.246 |
| 17 | 0.4335 | 22.188 | ±4.232 | 17 | 0.7365 | 34.002 | ±2.573 |
| 18 | 0.4012 | 20.519 | ±3.928 | 18 | 0.7465 | 34.472 | ±2.123 |
| 19 | 0.3949 | 20.179 | ±5.210 | 19 | 0.7357 | 33.968 | ±2.212 |
| 20 | 0.4207 | 21.526 | ±3.603 | 20 | 0.7353 | 33.950 | ±2.148 |
| 21 | 0.3989 | 20.393 | ±4.803 | 21 | 0.7399 | 34.163 | ±2.239 |
| 22 | 0.4170 | 21.338 | ±3.473 | 22 | 0.7407 | 34.201 | ±2.163 |
| 23 | 0.4165 | 21.295 | ±3.556 | 23 | 0.7439 | 34.350 | ±2.164 |
| 24 | 0.4075 | 20.836 | ±3.723 | 24 | 0.7400 | 34.168 | ±2.278 |
| 25 | 0.3861 | 19.733 | ±5.258 | 25 | 0.7503 | 34.645 | ±2.128 |
| 26 | 0.4100 | 22.974 | ±4.788 | 26 | 0.7478 | 34.532 | ±2.066 |
| 27 | 0.4062 | 20.772 | ±3.417 | 27 | 0.7523 | 34.738 | ±2.106 |
| 28 | 0.4007 | 20.487 | ±3.629 | 28 | 0.7531 | 34.778 | ±2.058 |
| 29 | 0.4186 | 21.421 | ±3.213 | 29 | 0.7510 | 34.683 | ±1.932 |
| 30 | 0.4015 | 20.531 | ±3.344 | 30 | 0.7521 | 34.732 | ±1.971 |
| 31 | 0.4018 | 20.554 | ±3.219 | 31 | 0.7538 | 34.815 | ±1.910 |
| 32 | 0.3986 | 20.385 | ±3.295 | 32 | 0.7462 | 34.461 | ±1.978 |
| 33 | 0.3994 | 20.438 | ±3.195 | 33 | 0.7480 | 34.550 | ±1.675 |
| 34 | 0.3981 | 20.358 | ±3.339 | 34 | 0.7507 | 34.670 | ±2.091 |
| 35 | 0.3820 | 19.529 | ±3.719 | 35 | 0.7461 | 34.474 | ±1.917 |
| 36 | 0.3820 | 19.528 | ±3.714 | 36 | 0.7556 | 34.897 | ±1.966 |
| 37 | 0.3778 | 19.328 | ±3.398 | 37 | 0.7542 | 34.836 | ±1.878 |
| 38 | 0.3876 | 19.836 | ±2.741 | 38 | 0.7526 | 34.759 | ±2.022 |
| 39 | 0.3823 | 19.566 | ±2.769 | 39 | 0.7488 | 34.592 | ±1.830 |
| 40 | 0.3718 | 19.016 | ±2.972 | 40 | 0.7491 | 34.603 | ±1.749 |
| 41 | 0.3826 | 19.578 | ±2.586 | 41 | 0.7469 | 34.508 | ±1.633 |
| 42 | 0.3771 | 19.308 | ±2.399 | 42 | 0.7494 | 34.623 | ±1.573 |
| 43 | 0.3693 | 18.895 | ±2.647 | 43 | 0.7439 | 34.369 | ±1.774 |
| 44 | 0.3647 | 18.663 | ±2.759 | 44 | 0.7472 | 34.526 | ±1.688 |
| 45 | 0.3684 | 18.855 | ±2.357 | 45 | 0.7461 | 34.472 | ±1.810 |
| 46 | 0.3571 | 18.273 | ±2.640 | 46 | 0.7430 | 34.331 | ±1.784 |
| 47 | 0.3502 | 17.907 | ±3.546 | 47 | 0.7458 | 34.455 | ±1.884 |
| 48 | 0.3693 | 18.895 | ±2.706 | 48 | 0.7449 | 34.415 | ±1.898 |
| 49 | 0.3627 | 18.563 | ±2.454 | 49 | 0.7458 | 34.456 | ±1.940 |
| 50 | 0.3668 | 18.785 | ±2.305 | 50 | 0.7475 | 34.537 | ±1.869 |
| 51 | 0.3599 | 18.416 | ±2.592 | 51 | 0.7452 | 34.428 | ±1.994 |
| 52 | 0.3668 | 18.777 | ±2.617 | 52 | 0.7432 | 34.337 | ±2.093 |
| 53 | 0.3607 | 18.459 | ±2.472 | 53 | 0.7446 | 34.405 | ±2.024 |
| 54 | 0.3599 | 18.419 | ±2.479 | 54 | 0.7470 | 34.415 | ±2.098 |
| 55 | 0.3385 | 17.312 | ±3.581 | 55 | 0.7500 | 34.652 | ±2.016 |
| 56 | 0.3660 | 18.731 | ±2.648 | 56 | 0.7465 | 34.489 | ±2.046 |

TABLE 10

SUMMARY OF CYCLE TEST DATA FOR ELECTRODES PREPARED FROM ISOSTATICALLY COMPACTED PLAQUES

| | 60% POROSITY 90μ INDUCED PORE SIZE | | | | 80% POROSITY 90μ INDUCED PORE SIZE | | |
|---|---|---|---|---|---|---|---|
| Cycle No. | Average Capacity | Average Efficiency | 95% Confidence Limit for Efficiency | Cycle No. | Average Capacity | Average Efficiency | 95% Confidence Limit for Efficiency |
| 1 | 0.7600 | 38.026 | ±2.697 | 1 | 1.4996 | 54.284 | ±3.331 |
| 2 | 0.7784 | 38.928 | ±2.293 | 2 | 1.4960 | 54.184 | ±2.066 |
| 3 | 0.7744 | 38.772 | ±2.282 | 3 | 1.4438 | 52.318 | ±1.556 |
| 4 | 0.4448 | 22.318 | ±4.599 | 4 | 1.1030 | 40.006 | ±1.166 |
| 5 | 0.2526 | 12.698 | ±4.569 | 5 | 0.7840 | 28.410 | ±2.074 |
| 6 | 0.1072 | 5.410 | ±2.751 | 6 | 0.0912 | 3.324 | ±2.338 |
| 7 | 0.4210 | 21.133 | ±3.974 | 7 | 0.9544 | 34.602 | ±1.292 |
| 8 | 0.4418 | 22.233 | ±5.034 | 8 | 1.0088 | 36.574 | ±0.939 |
| 9 | 0.4398 | 22.077 | ±3.946 | 9 | 1.0136 | 36.738 | ±0.897 |
| 10 | 0.4383 | 22.006 | ±4.001 | 10 | 1.0242 | 37.134 | ±0.434 |
| 11 | 0.4454 | 22.364 | ±4.139 | 11 | 1.0266 | 37.383 | ±0.495 |
| 12 | 0.4442 | 22.293 | ±3.865 | 12 | 1.0278 | 37.271 | ±0.632 |
| 13 | 0.4410 | 22.132 | ±3.942 | 13 | 1.0329 | 37.464 | ±0.886 |
| 14 | 0.4400 | 22.089 | ±3.889 | 14 | 1.0343 | 37.525 | ±0.636 |
| 15 | 0.4412 | 22.138 | ±3.747 | 15 | 1.0308 | 37.386 | ±0.473 |
| 16 | 0.4363 | 21.905 | ±3.854 | 16 | 1.0328 | 37.462 | ±0.563 |
| 17 | 0.4399 | 22.076 | ±3.619 | 17 | 1.0233 | 37.129 | ±0.823 |
| 18 | 0.4356 | 21.856 | ±3.690 | 18 | 1.0201 | 37.016 | ±0.807 |
| 19 | 0.4380 | 21.977 | ±3.605 | 19 | 1.0028 | 36.388 | ±0.822 |
| 20 | 0.4364 | 21.894 | ±3.622 | 20 | 0.9947 | 36.087 | ±0.663 |
| 21 | 0.4361 | 21.872 | ±3.341 | 21 | 0.9995 | 36.263 | ±0.676 |
| 22 | 0.4283 | 21.495 | ±3.658 | 22 | 0.9921 | 35.997 | ±0.766 |
| 23 | 0.4334 | 21.738 | ±3.478 | 23 | 0.9957 | 36.119 | ±0.594 |
| 24 | 0.4285 | 21.490 | ±3.368 | 24 | 0.9844 | 35.716 | ±0.786 |
| 25 | 0.4250 | 21.316 | ±3.379 | 25 | 0.9931 | 36.022 | ±0.678 |
| 26 | 0.4213 | 21.127 | ±3.291 | 26 | 0.9926 | 35.997 | ±0.582 |
| 27 | 0.4212 | 21.119 | ±3.290 | 27 | 0.9933 | 36.029 | ±0.634 |
| 28 | 0.4199 | 21.048 | ±3.120 | 28 | 0.9873 | 35.810 | ±0.838 |
| 29 | 0.4226 | 21.188 | ±3.168 | 29 | 0.9848 | 35.723 | ±0.693 |
| 30 | 0.4115 | 20.629 | ±3.155 | 30 | 0.9887 | 35.858 | ±0.788 |
| 31 | 0.4079 | 20.448 | ±3.129 | 31 | 0.9852 | 35.727 | ±0.767 |
| 32 | 0.4069 | 20.399 | ±3.082 | 32 | 0.9625 | 34.927 | ±1.584 |
| 33 | 0.4102 | 20.557 | ±2.933 | 33 | 0.9656 | 35.023 | ±1.436 |
| 34 | 0.4080 | 20.451 | ±3.020 | 34 | 0.9604 | 34.835 | ±1.684 |
| 35 | 0.4019 | 20.143 | ±3.045 | 35 | 0.9529 | 34.562 | ±1.844 |
| 36 | 0.4022 | 20.157 | ±3.055 | 36 | 0.9592 | 34.785 | ±1.918 |
| 37 | 0.3999 | 20.032 | ±2.748 | 37 | 0.9579 | 34.735 | ±1.949 |
| 38 | 0.3994 | 20.006 | ±2.947 | 38 | 0.9569 | 34.702 | ±2.049 |
| 39 | 0.3966 | 19.867 | ±2.888 | 39 | 0.9545 | 34.610 | ±1.924 |
| 40 | 0.3956 | 19.819 | ±2.903 | 40 | 0.9574 | 34.716 | ±1.946 |
| 41 | 0.3949 | 19.780 | ±2.759 | 41 | 0.9438 | 34.227 | ±2.065 |
| 42 | 0.3940 | 19.734 | ±2.802 | 42 | 0.9439 | 34.228 | ±1.994 |
| 43 | 0.3881 | 19.430 | ±2.598 | 43 | 0.9380 | 34.009 | ±1.980 |
| 44 | 0.3872 | 19.393 | ±2.647 | 44 | 0.9404 | 34.095 | ±2.091 |
| 45 | 0.3855 | 19.305 | ±2.711 | 45 | 0.9391 | 34.047 | ±2.051 |
| 46 | 0.3774 | 18.896 | ±2.726 | 46 | 0.9306 | 33.738 | ±2.051 |
| 47 | 0.3840 | 19.229 | ±2.687 | 47 | 0.9347 | 33.885 | ±2.407 |
| 48 | 0.3750 | 18.781 | ±2.834 | 48 | 0.9315 | 33.768 | ±2.481 |
| 49 | 0.3761 | 18.829 | ±2.672 | 49 | 0.9318 | 33.778 | ±2.433 |
| 50 | 0.3802 | 19.025 | ±2.737 | 50 | 0.9284 | 33.663 | ±2.530 |
| 51 | 0.3705 | 18.551 | ±2.753 | 51 | 0.9252 | 33.544 | ±2.546 |
| 52 | 0.3722 | 18.634 | ±2.661 | 52 | 0.9229 | 33.461 | ±2.464 |
| 53 | 0.3732 | 18.684 | ±2.834 | 53 | 0.9212 | 33.392 | ±2.501 |
| 54 | 0.3721 | 18.627 | ±2.775 | 54 | 0.9184 | 33.301 | ±2.635 |
| 55 | 0.3710 | 18.565 | ±2.620 | 55 | 0.9216 | 33.410 | ±2.624 |
| 56 | 0.3775 | 18.891 | ±2.633 | 56 | 0.9192 | 33.323 | ±2.600 |

# APPENDIX D

## ADDITIONAL SEM PHOTOMICROGRAPHS OF ISOSTATICALLY COMPACTED PLAQUES (80 % POROSITY 15 – 90$\mu$) AND ELECTRODES MADE FROM SAME

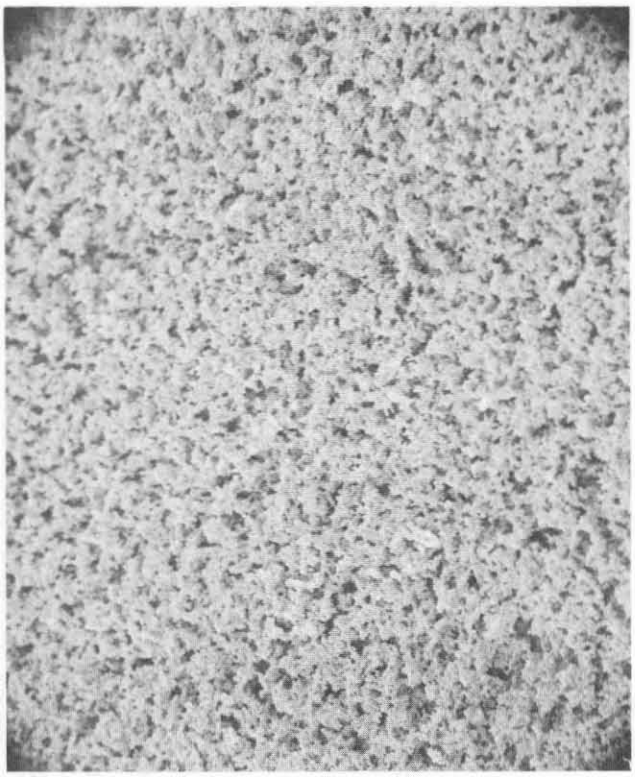

110X

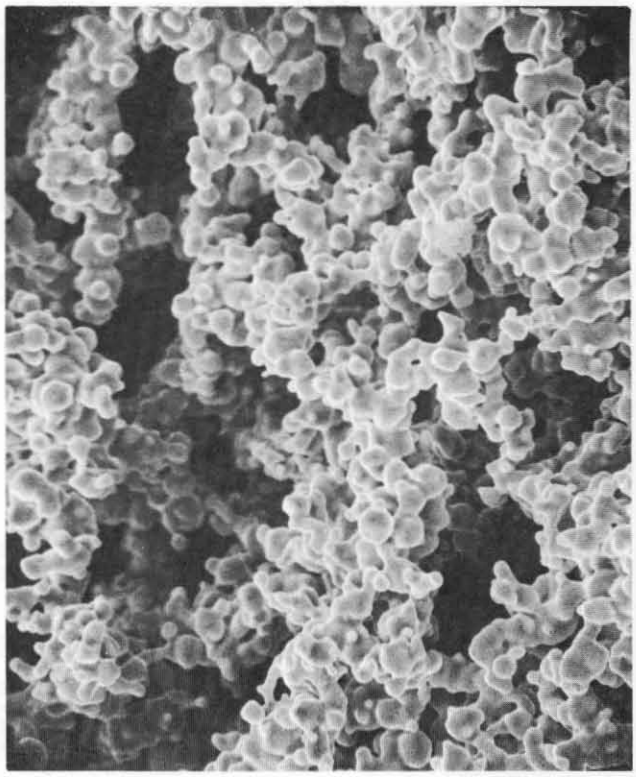

1100X

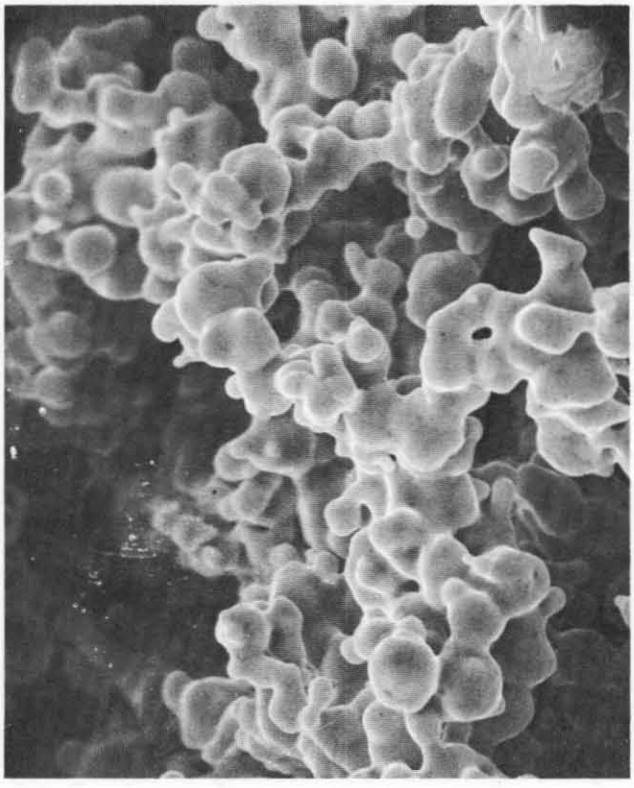

2200X

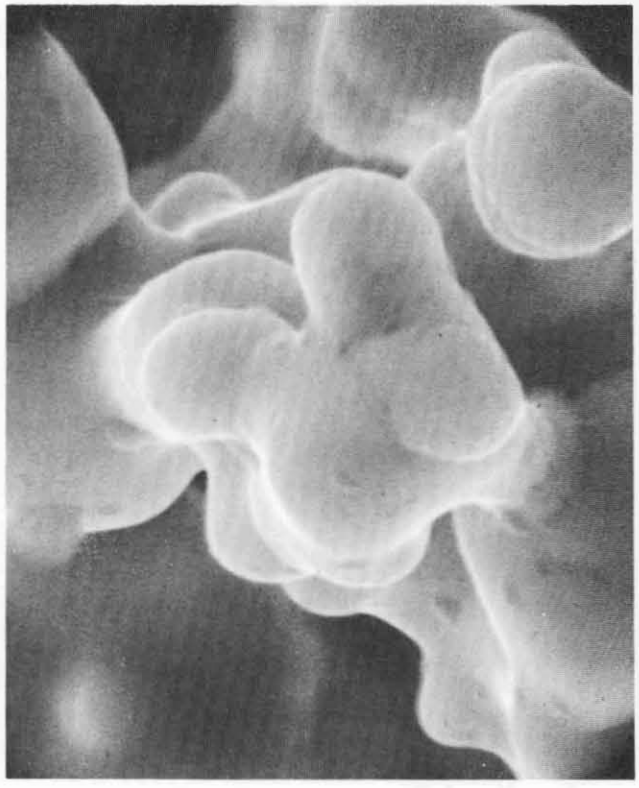

11,000X

FIGURE 33. SEM PHOTOMICROGRAPHS OF ISOSTATICALLY COMPACTED PLAQUES, INCO 287 POWDER 80% 15$\mu$

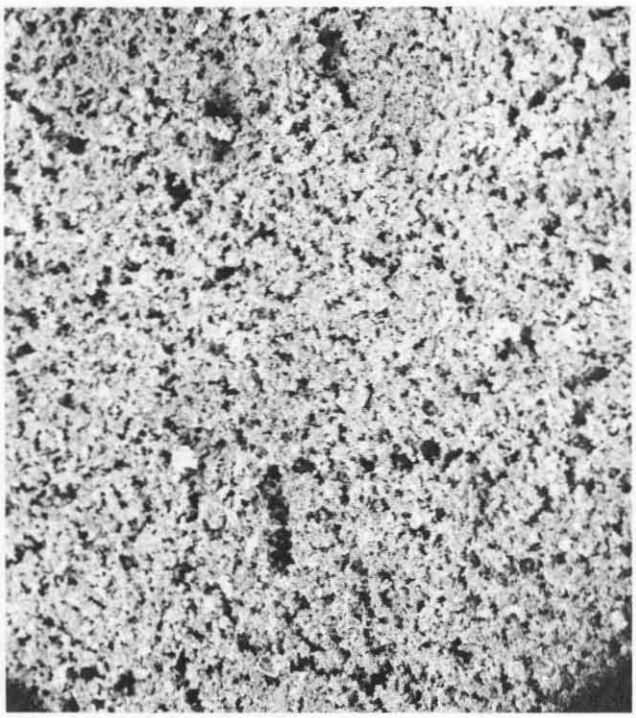

100X

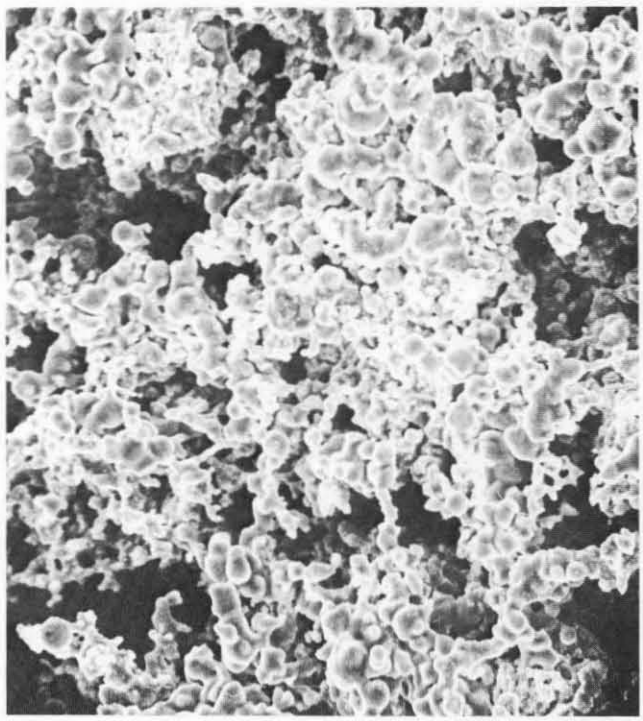

1000X

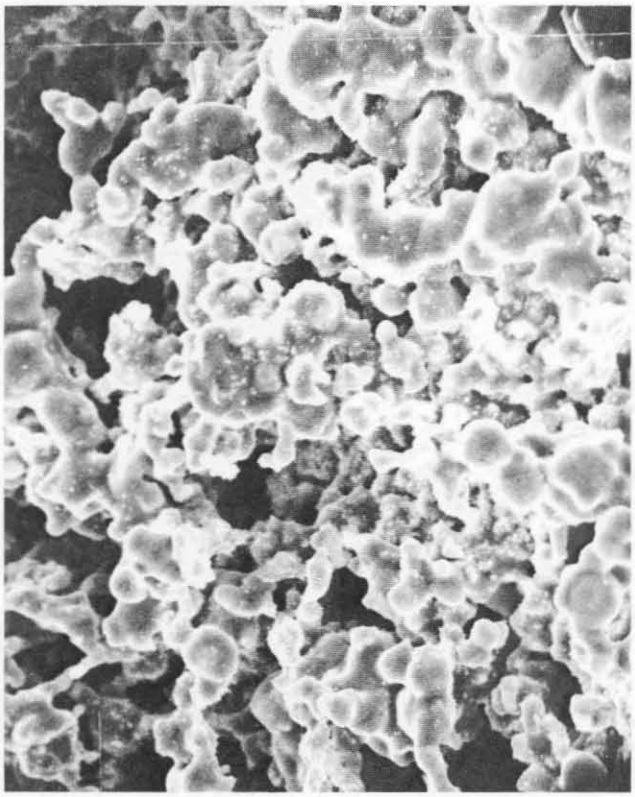

2000X

10,000X

FIGURE 34. SEM PHOTOMICROGRAPHS OF ISOSTATICALLY COMPACTED PLAQUE, BLENDED POWDER*, 80 % 25$\mu$

*INCO 287 and Sherrit-Gordon Powders

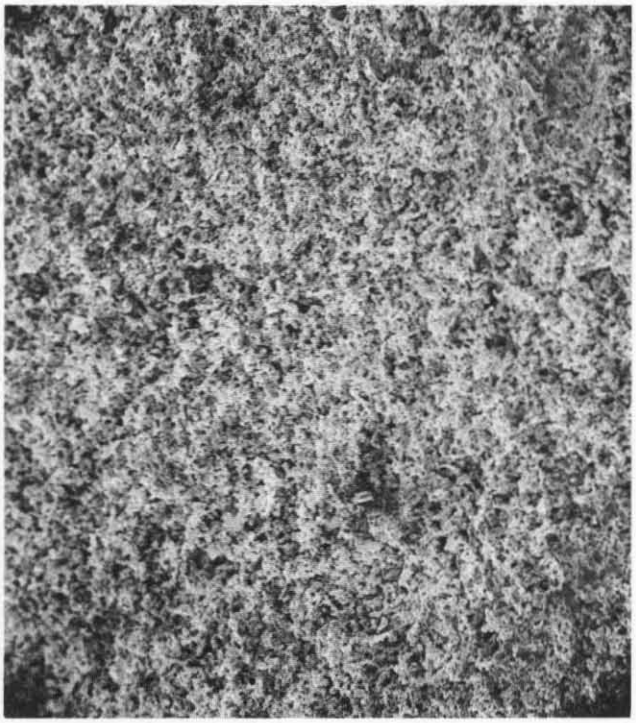

115X

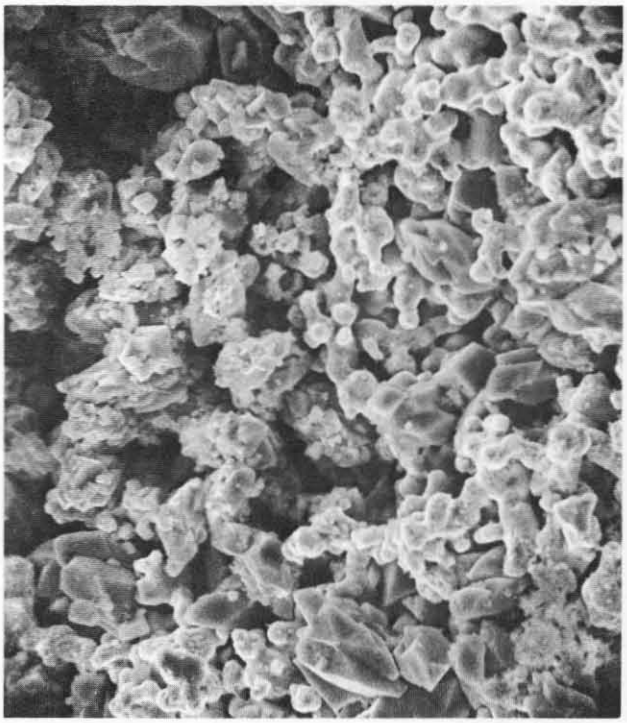

1150X

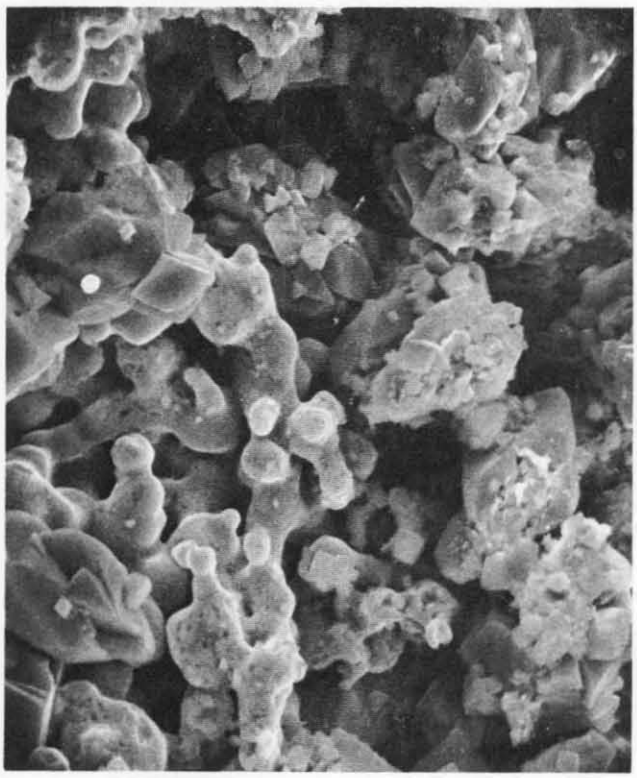

2300X

11,500X

FIGURE 35. SEM PHOTOMICROGRAPHS OF CYCLED ELECTRODE MADE FROM ISOSTATICALLY COMPACTED PLAQUE, INCO 287 POWDER, 80 % 25$\mu$

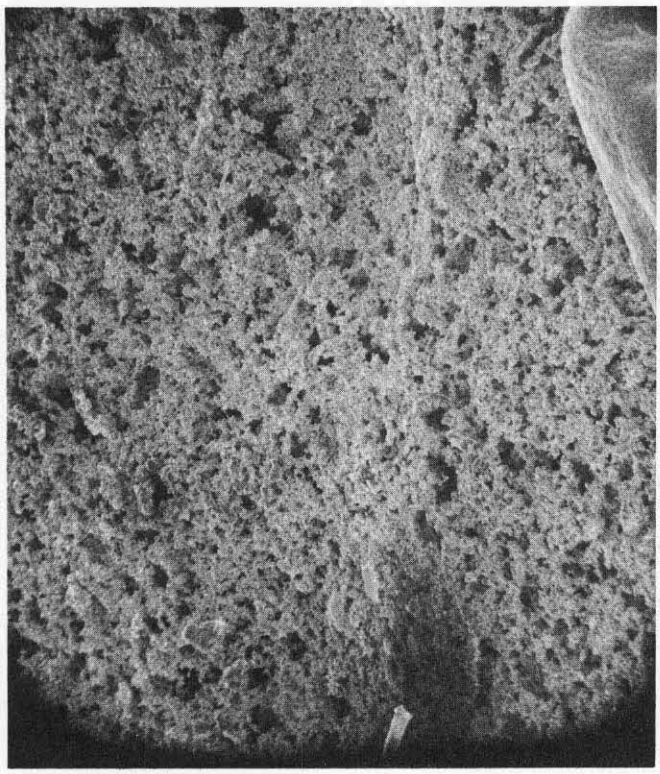

100X

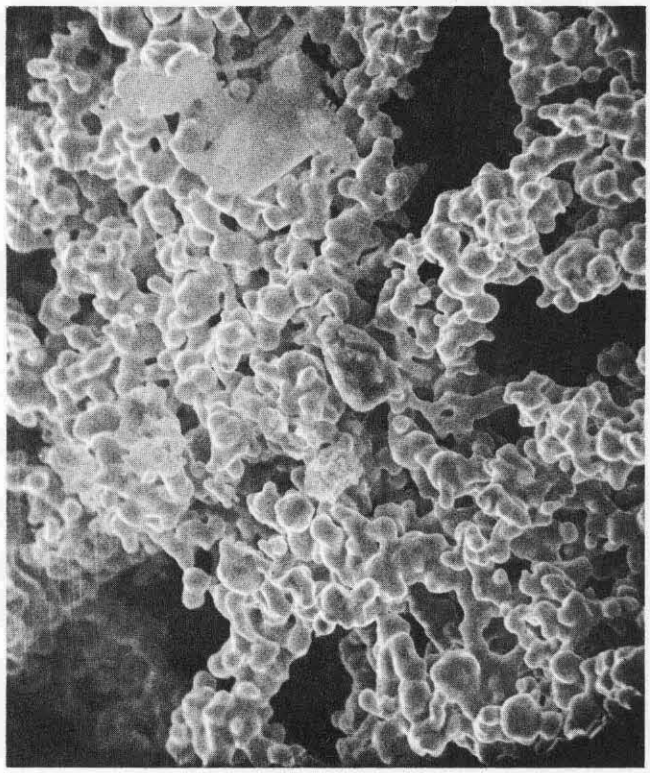

1000X

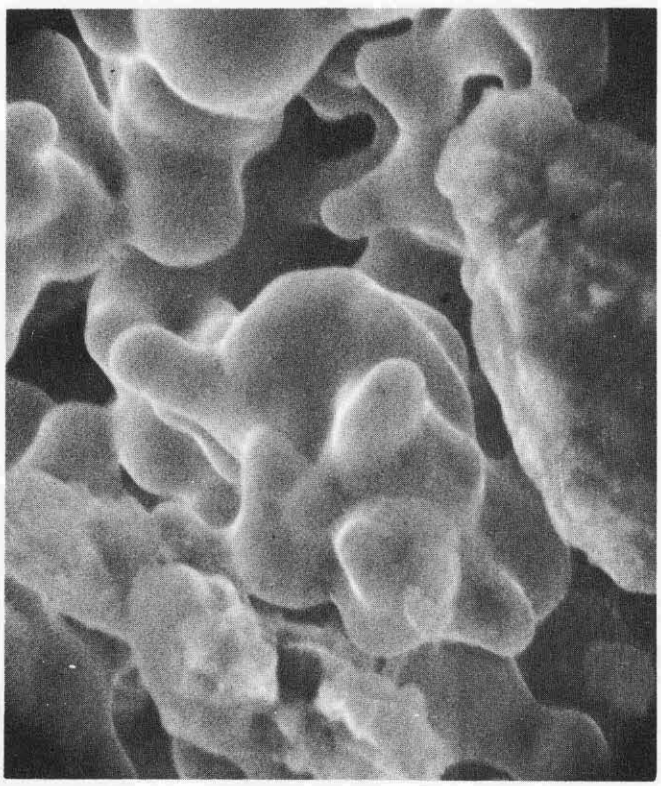

5000X

FIGURE 36. SEM PHOTOMICROGRAPHS OF ISOSTATICALLY COMPACTED PLAQUE, INCO 287 POWDER, 80 % 50$\mu$

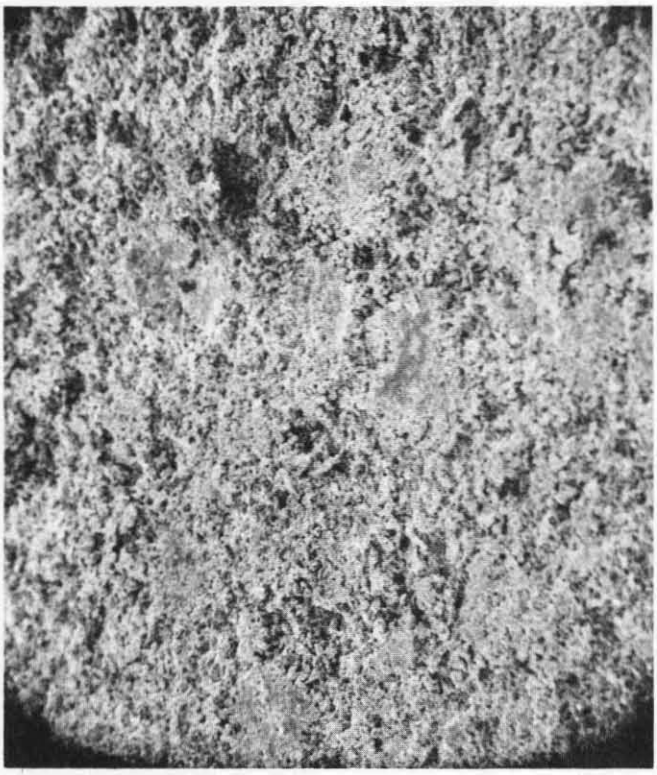

101X

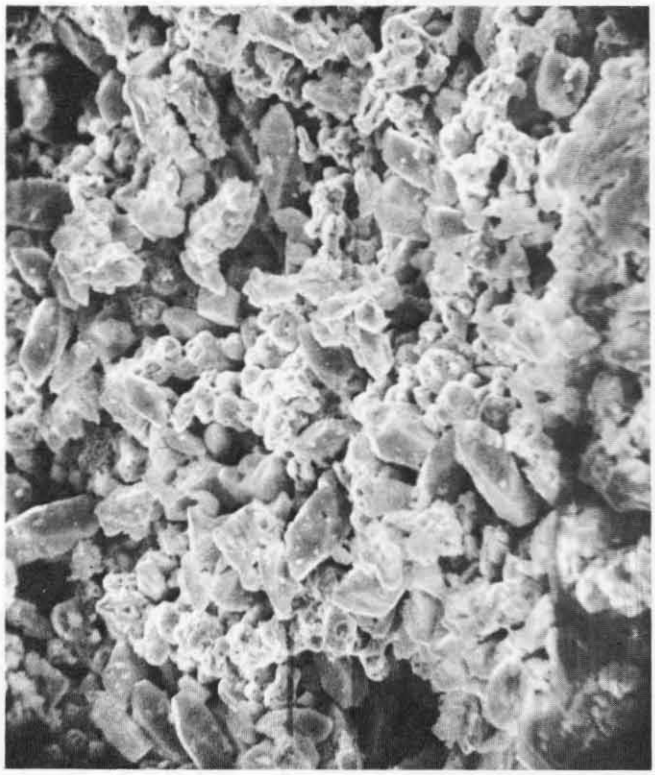

1010X

5050X

FIGURE 37. SEM PHOTOMICROGRAPHS OF CYCLED ELECTRODE MADE FROM ISOSTATICALLY COMPACTED PLAQUE, INCO 287 POWDER, 80 % 50$\mu$

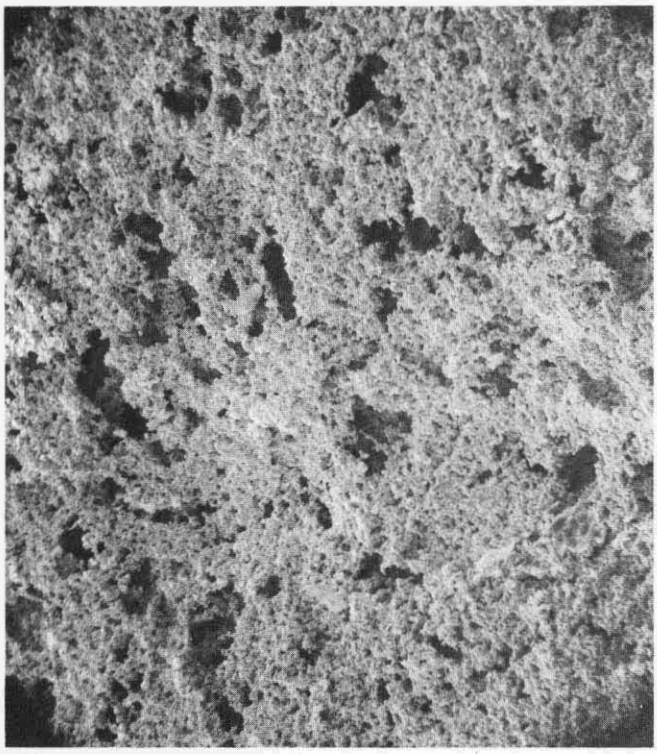

125X

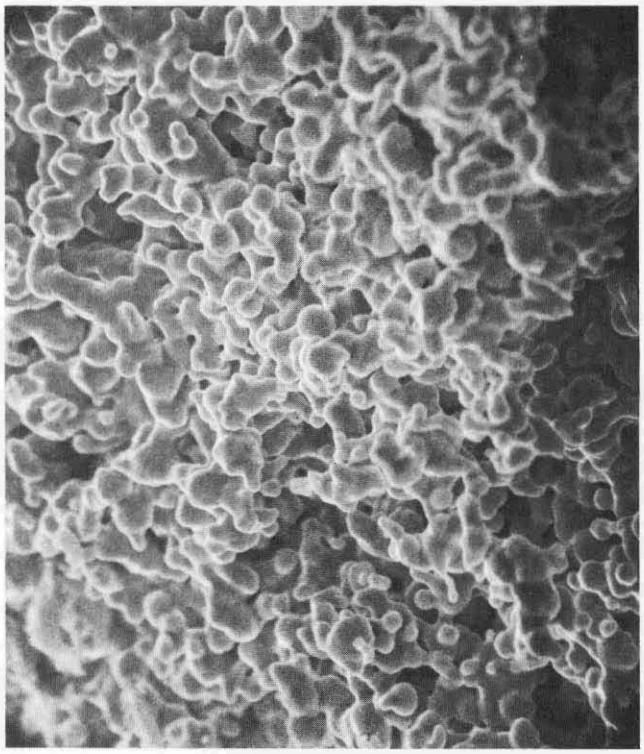

1250X

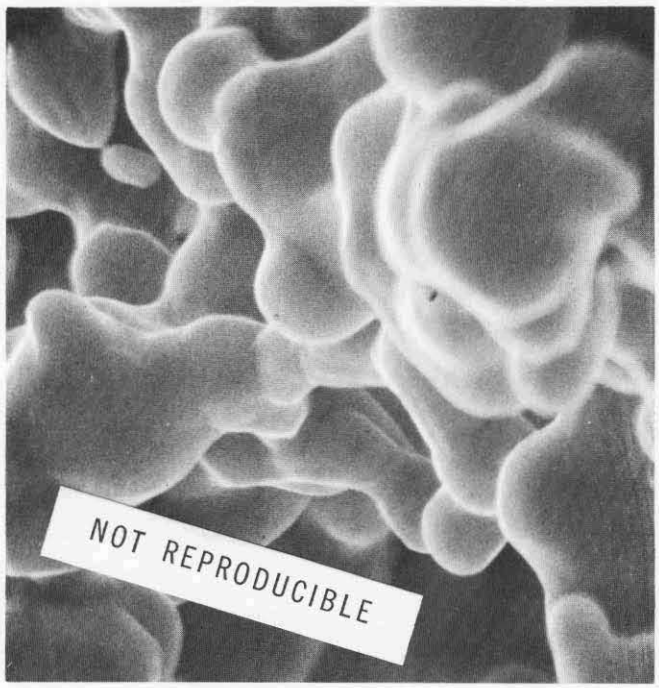


6100X

FIGURE 38. SEM PHOTOMICROGRAPHS OF ISOSTATICALLY COMPACTED PLAQUE, INCO 287 POWDER, 80 % 90$\mu$

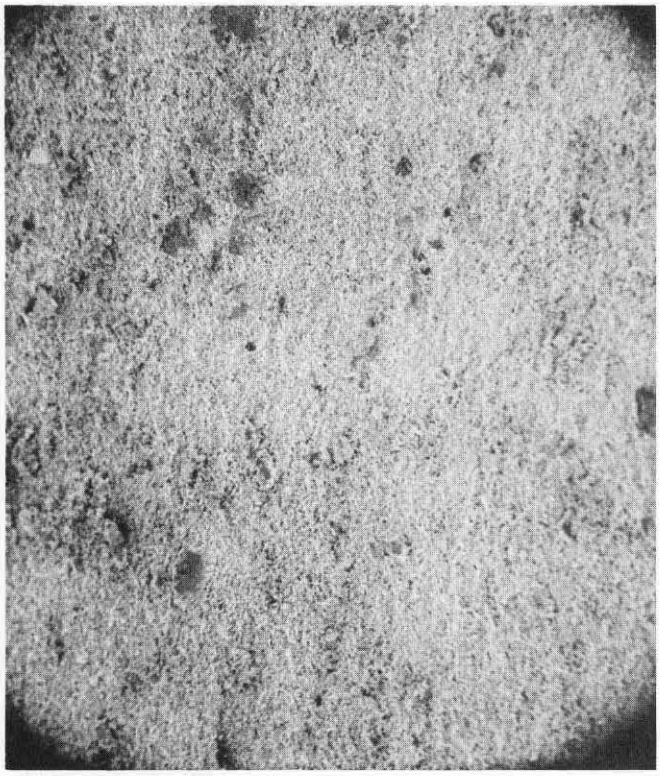

92X

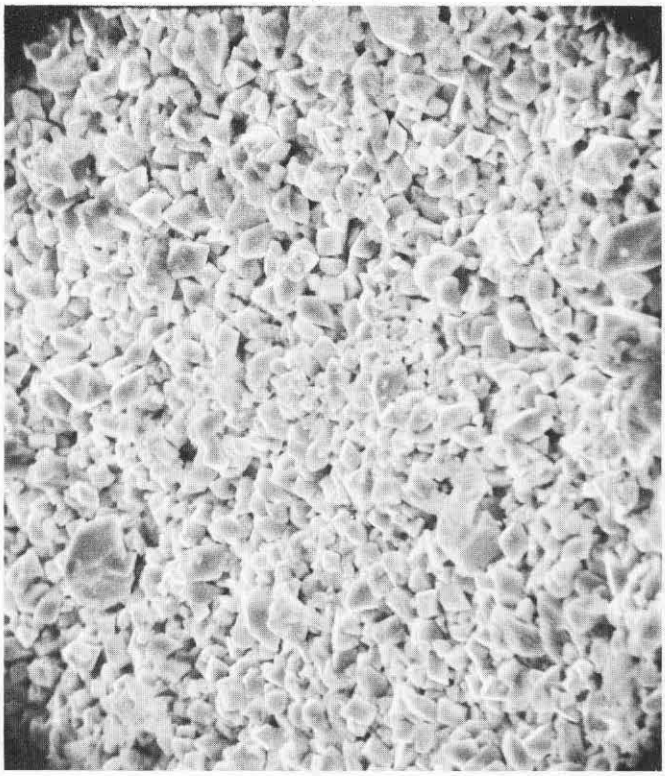

920X

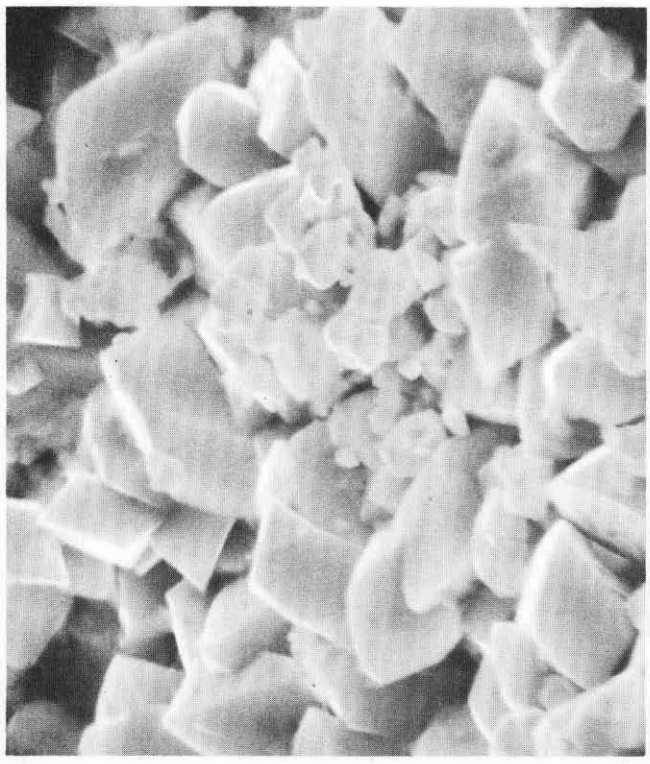

4600X

FIGURE 39. SEM PHOTOMICROGRAPHS OF FORMED ELECTRODE MADE FROM ISOSTATICALLY COMPACTED PLAQUE, INCO POWDER, 80 % 90$\mu$

# APPENDIX E

## ADDITIONAL SEM PHOTOMICROGRAPHS OF ISOSTATICALLY COMPACTED PLAQUES (60 % POROSITY 15 – 90$\mu$) AND ELECTRODES MADE FROM SAME

100X

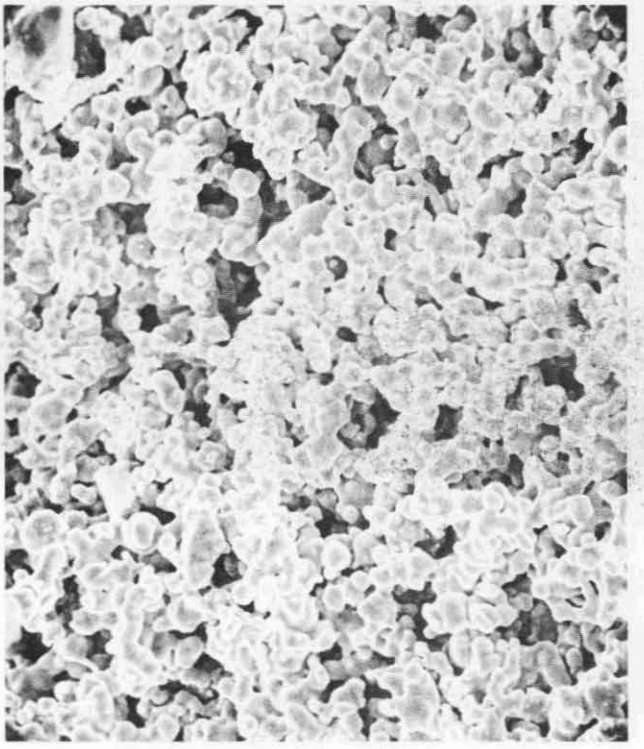

1000X



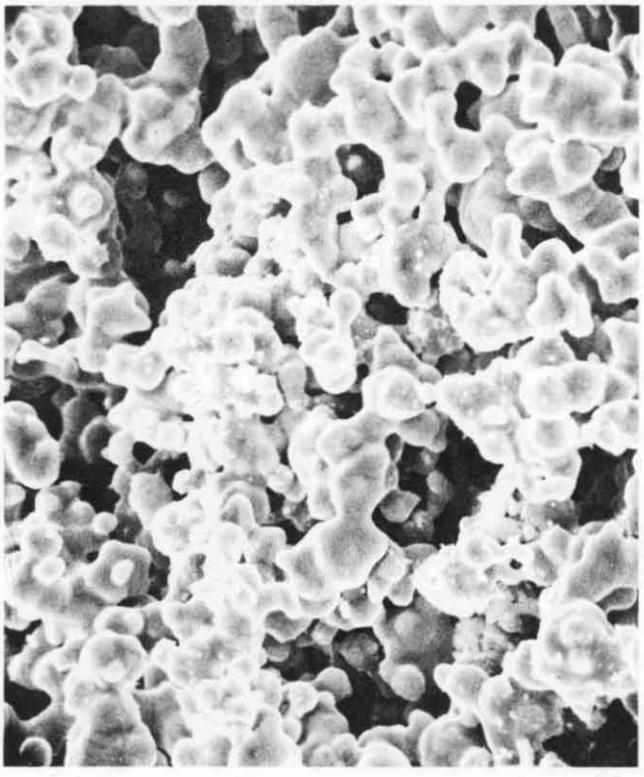

2000X

10000X

FIGURE 40. SEM PHOTOMICROGRAPHS OF ISOSTATICALLY COMPACTED PLAQUES, INCO 287 POWDER, 60 % 15$\mu$

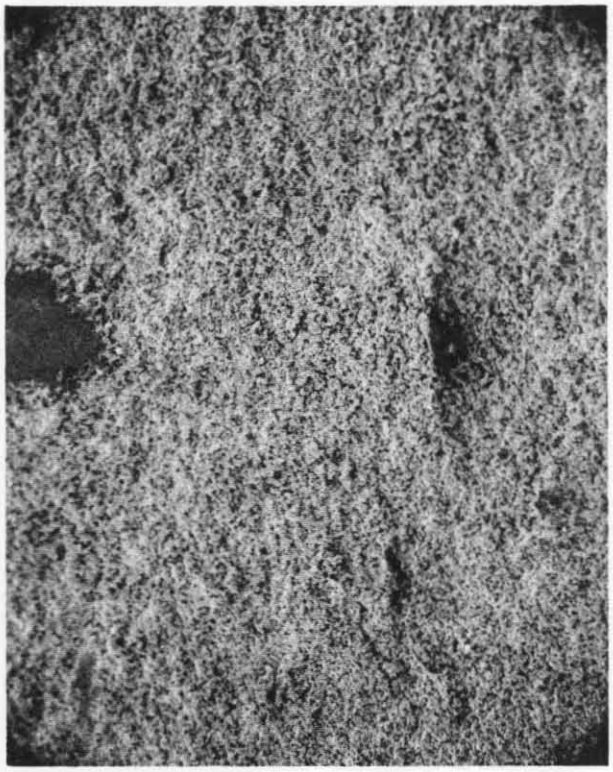

120X

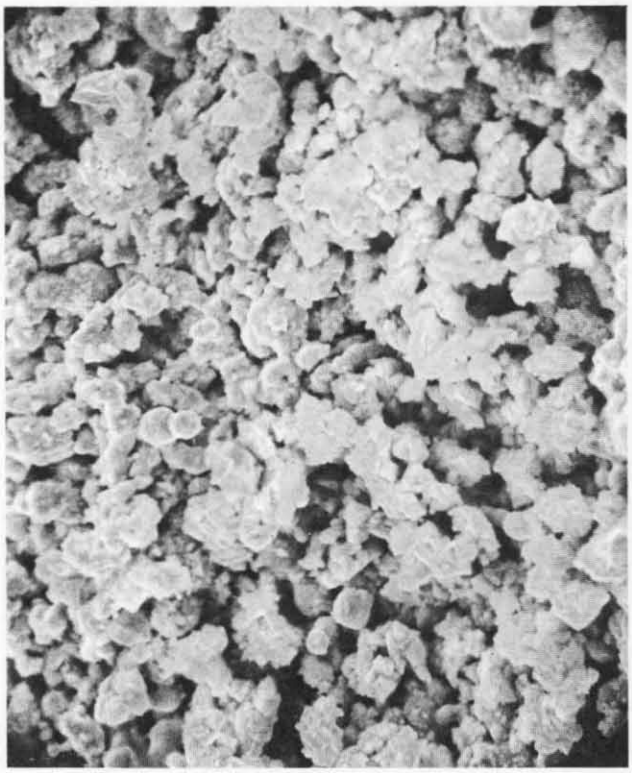

1200X

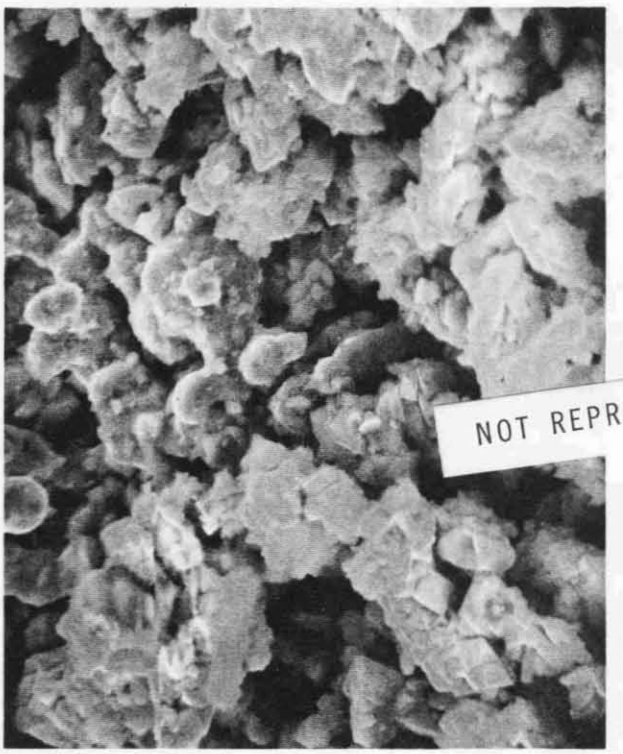

2400X

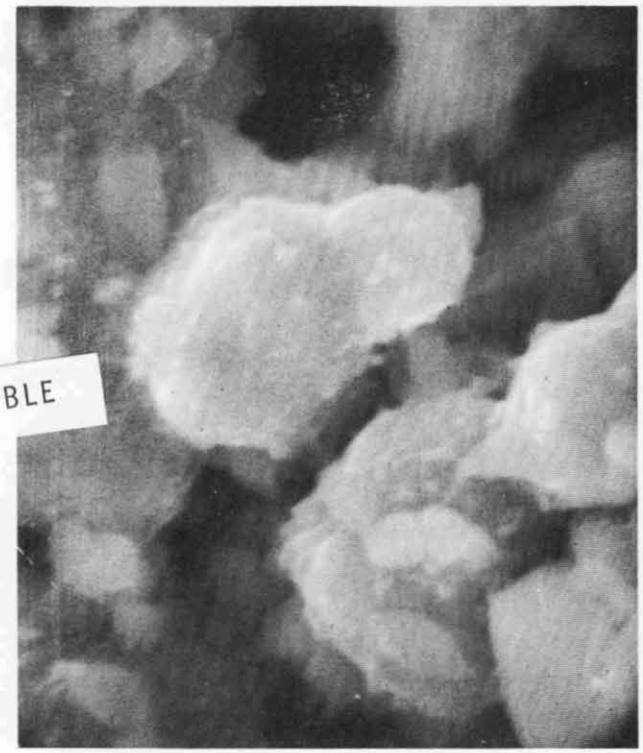

12000X



**FIGURE 41. SEM MICROGRAPH OF CYCLED ELECTRODE MADE FROM ISOSTATICALLY COMPACTED PLAQUE, INCO 287 POWDER, 60 % 15$\mu$**

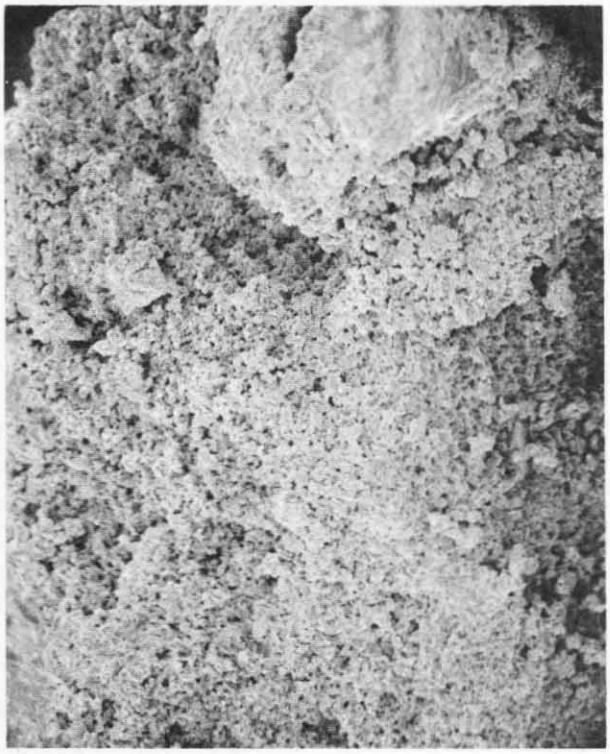

Cross Section 120X

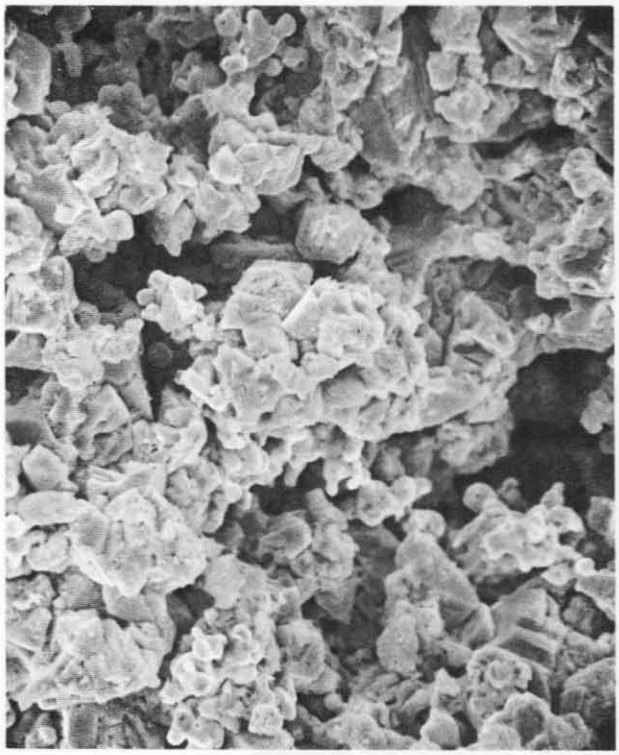

Cross Section 1200X

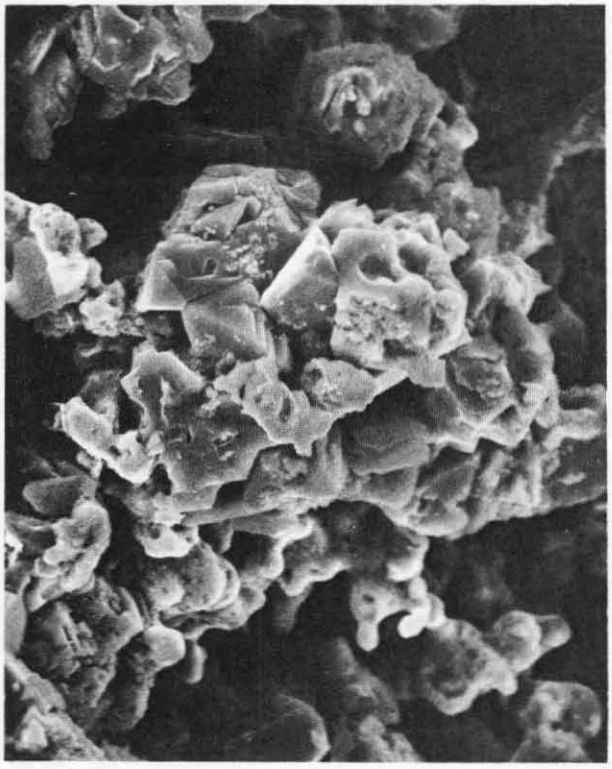

Cross Section 2400X

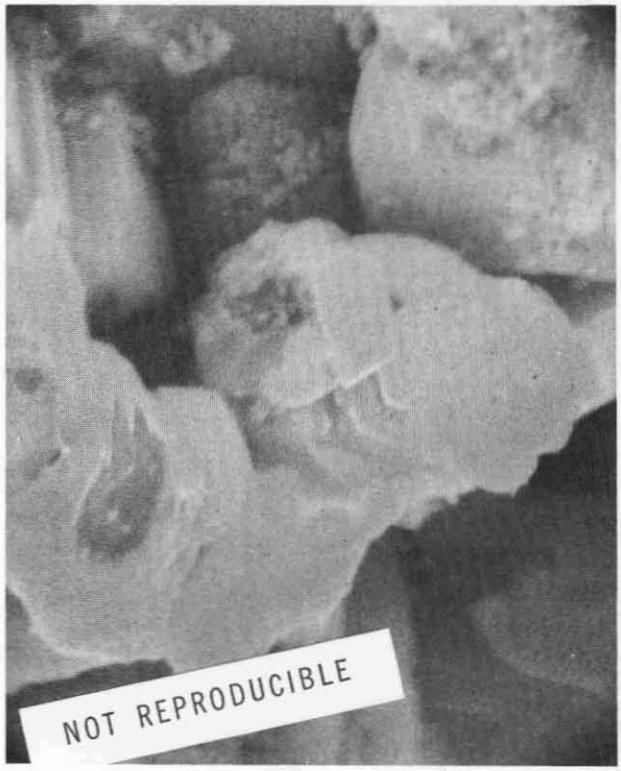


Cross Section 12000X

FIGURE 42. SEM PHOTOMICROGRAPHS OF CYCLE ELECTRODES MADE FROM ISOSTATICALLY COMPACTED PLAQUE, 60 % 25$\mu$

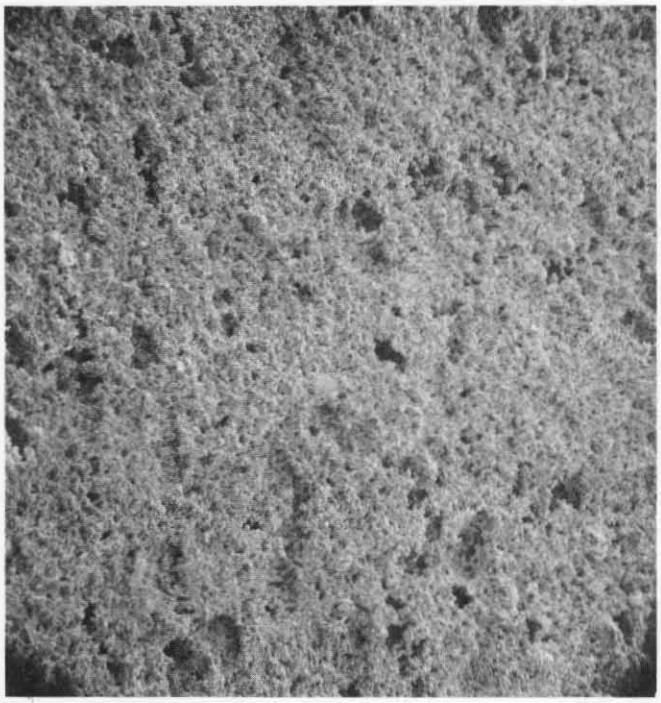

120X

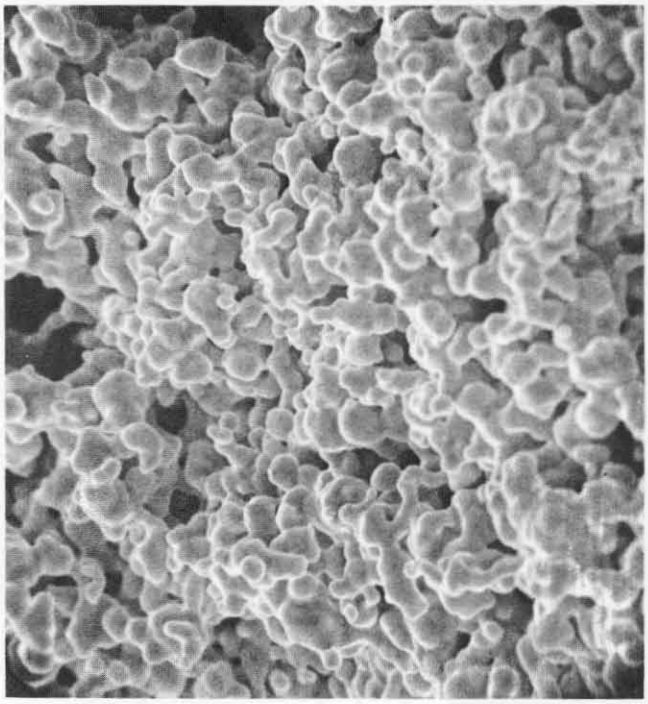

1200X

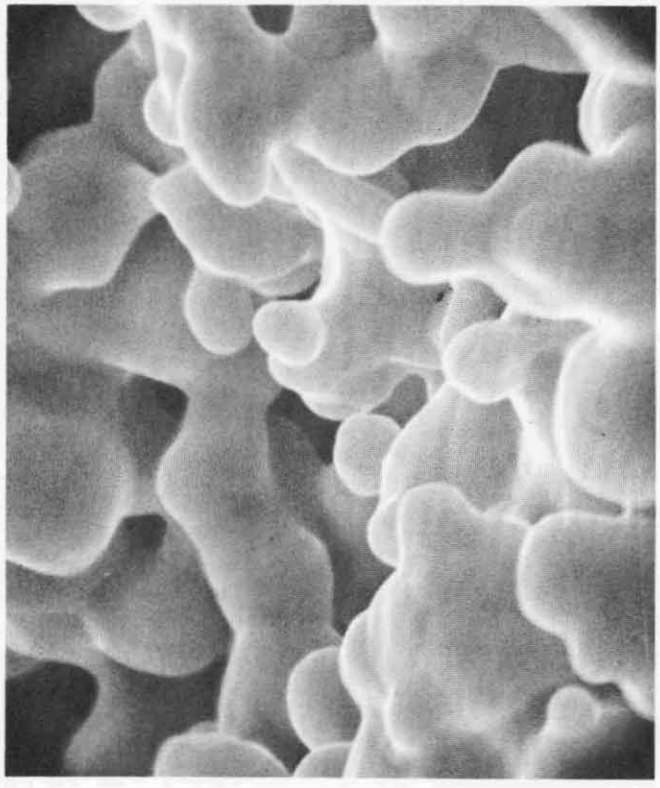

6000X

FIGURE 43. SEM PHOTOMICROGRAPHS OF ISOSTATICALLY COMPACTED PLAQUE, INCO 287 POWDER, 60 % 50 $\mu$

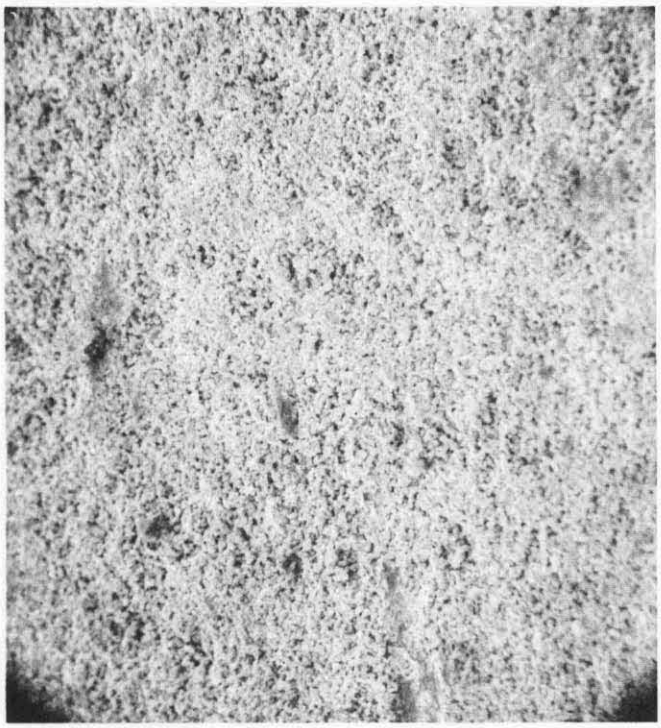

100X

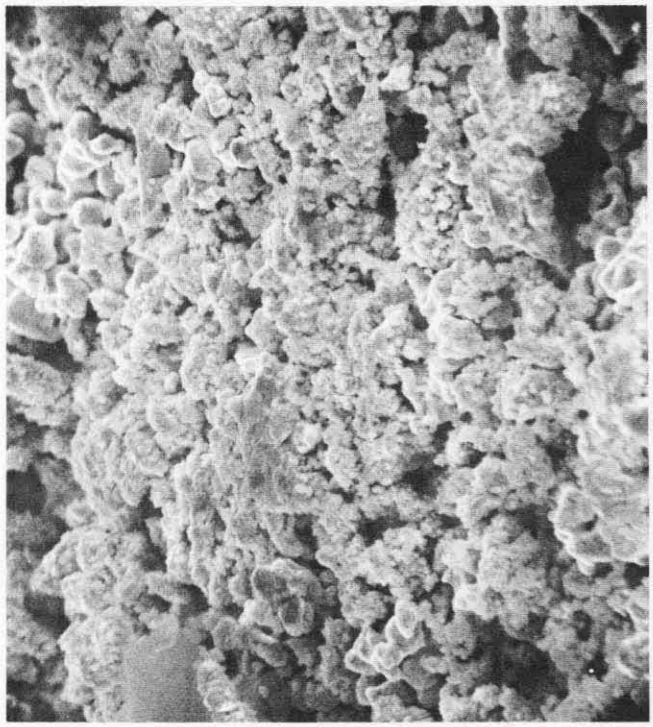

100X

5000X

FIGURE 44. SEM PHOTOMICROGRAPHS OF CYCLED ELECTRODE MADE FROM ISOSTATICALLY COMPACTED PLAQUE, INCO 287 POWDER, 60 % 50$\mu$

126X

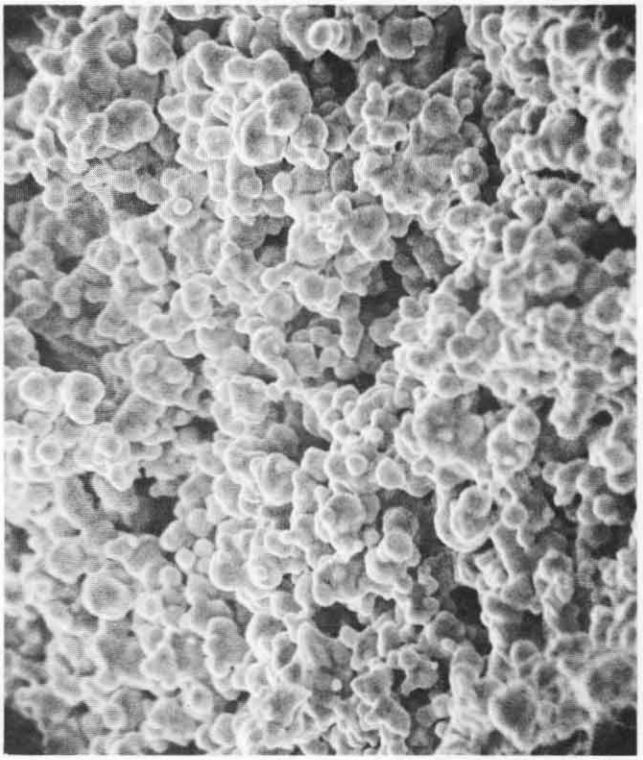

1206X

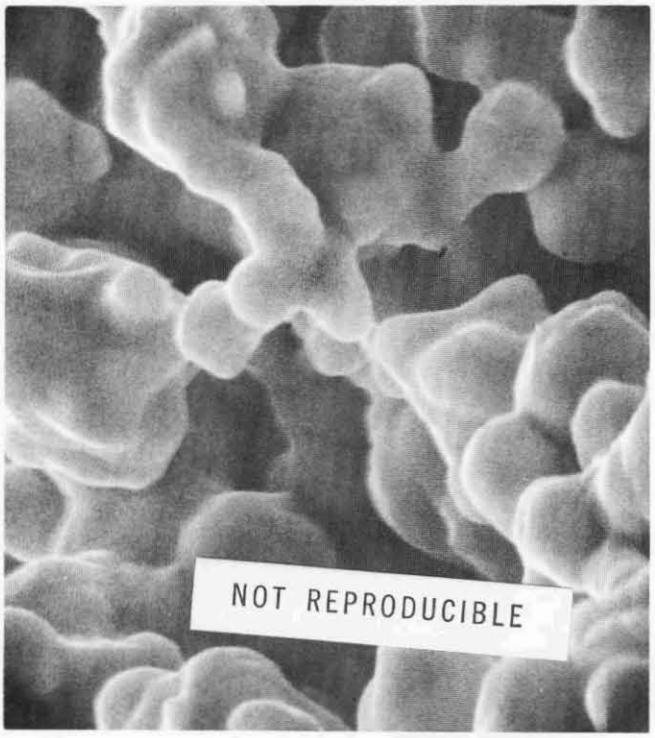


6300X

FIGURE 45. SEM PHOTOMICROGRAPHS OF ISOSTATICALLY COMPACTED PLAQUE, INCO 287 POWDER, 60 % 90$\mu$

110X

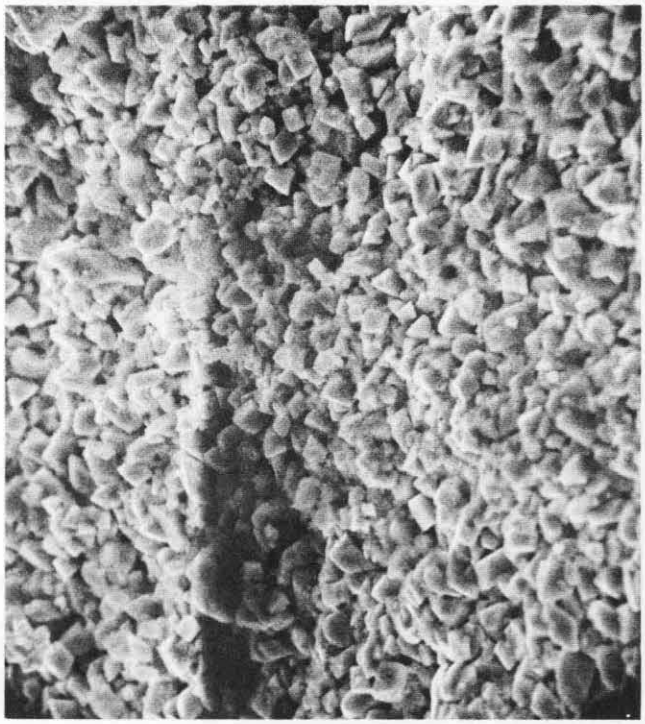

1100X

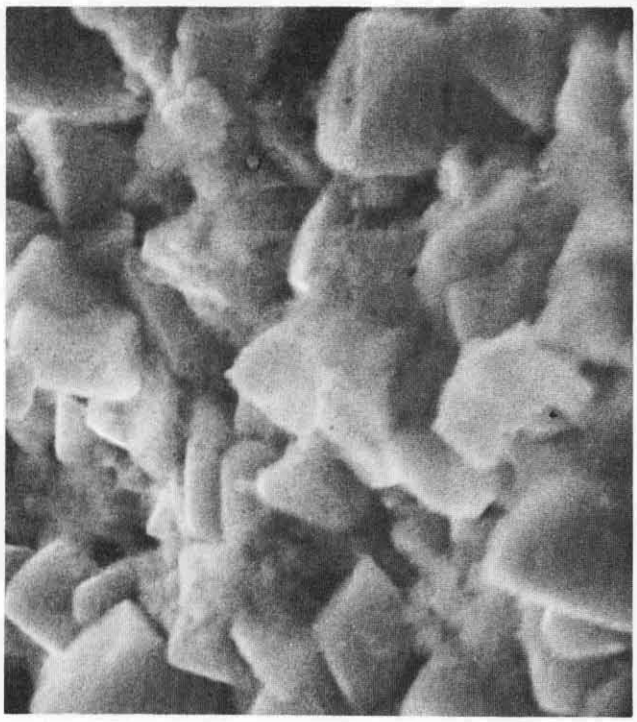

5500X

FIGURE 46. SEM PHOTOMICROGRAPHS OF FORMED ELECTRODE MADE FROM ISOSTATICALLY COMPACTED PLAQUE, INCO 287 POWDER, 60 % 90 $\mu$

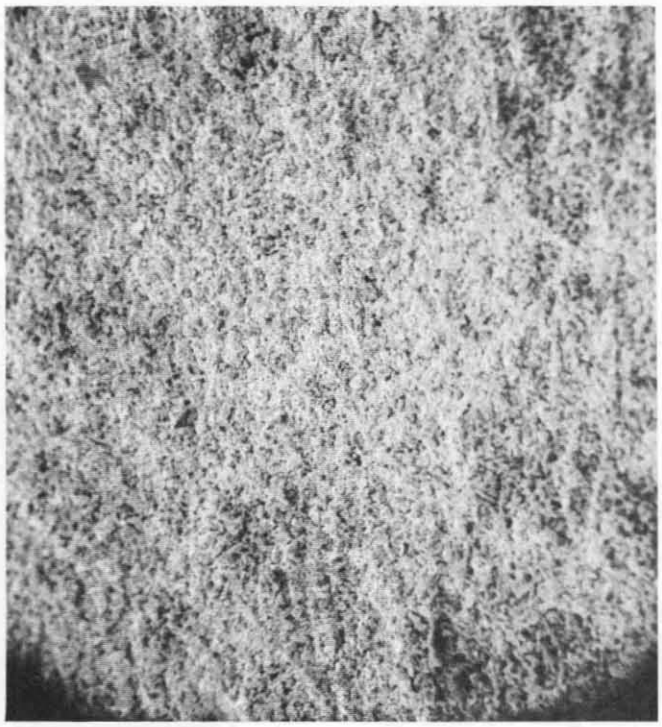

116X

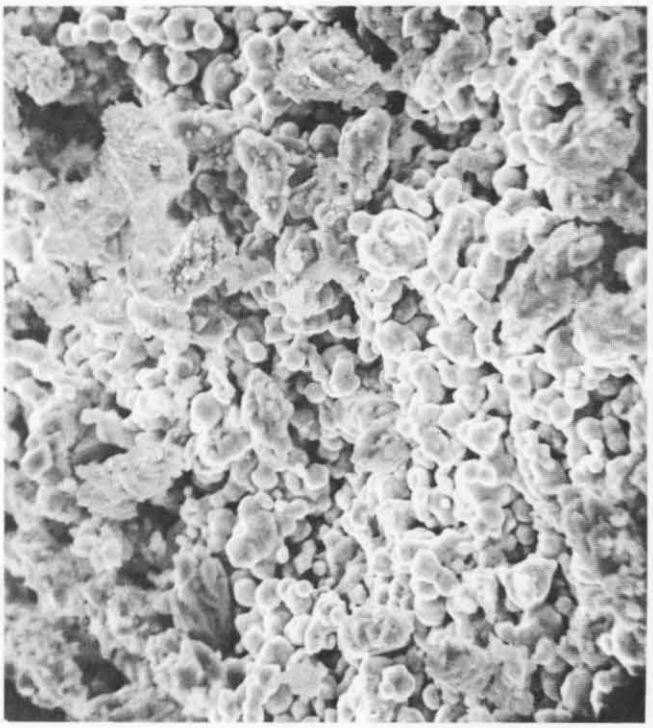

1160X

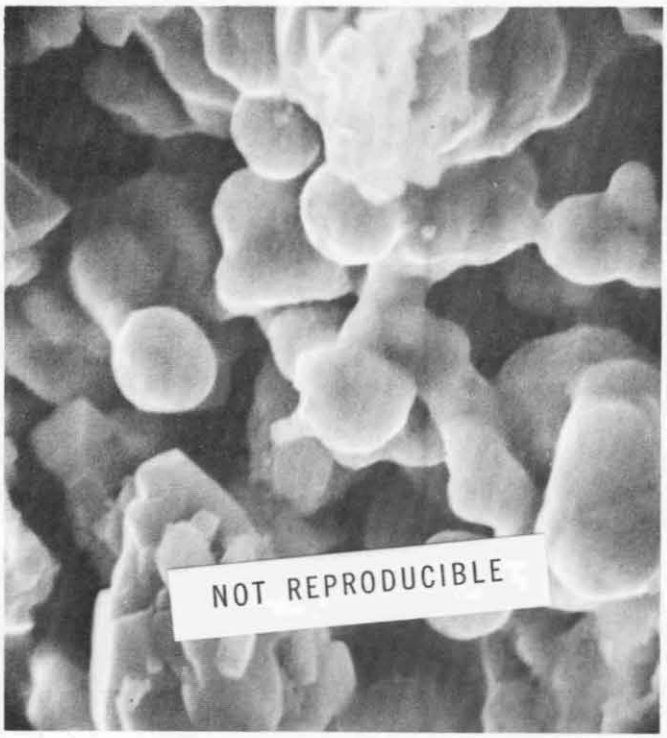


5800X

FIGURE 47. SEM PHOTOMICROGRAPHS OF CYCLED ELECTRODE MADE FROM ISOSTATICALLY COMPACTED PLAQUE, INCO 287 POWDER, 60 % 90$\mu$